Cape Peninsula University of Technology

# ENERGY POTENTIAL ASSESSMENT AND DESIGN OF A RUN-OF-RIVER HYDROPOWER PLANT

**by**

**GASSAN DARRIES**

**Dissertation submitted in partial fulfilment of the requirements for the degree**

**Master of Engineering in Energy**

**in the Faculty of Engineering and the Built Environment**

**at the Cape Peninsula University of Technology**

**Supervisor: Prof. A. Raji**
**Co-supervisor: Dr A. Ayeleso**

**Bellville**
**Date submitted: April 2022**

## DECLARATION

I, Gassan Darries, declare that the contents of this dissertation/thesis represent my own unaided work, and that the dissertation has not previously been submitted for academic examination towards any qualification. Furthermore, it represents my own opinions and not necessarily those of the Cape Peninsula University of Technology.

**20 April 2022**

**Signed** **Date**

# ABSTRACT

The global phenomenon of climate change has forced mankind to relook at its way of living. The subsequent worldwide effort to reduce harmful emissions has resulted in a search for using more renewable energy resources to replace the non-renewable energy types such as fossil fuels in energy production. In this intensified search for more renewable energy generating opportunities, South Africa amongst many countries, launched its own renewable energy independent power producer procurement programme (REIPPPP) to create more renewable energy projects. After five bidding windows for new tenders, the country had secured 105 new projects. Under the small projects segment, multiple small projects of under 5 MW capacity were already allocated. However, the minimum cut-off capacity of 1 MW, is excluding micro and pico hydropower options. Hence this research looked at the hydropower potential at wastewater treatment plants to supplement the electricity supply.

The Zandvliet Wastewater Treatment Works was selected for this research. The turbine options for hydropower at this site were evaluated and the Archimedes screw turbine was found to be the best candidate. A comparison of the energy yield was drawn between installing the hydropower scheme at the discharge point of the plant, against implementing it in the river in which the plant is discharging. The best turbine for the river was found to be the hydrostatic pressure machine.

The energy of the two sites was simulated in MATLAB and the resultant energy potential of the two sites was compared to indicate the maximum possible energy generation. The results show that the hydropower scheme at the wastewater plant generates considerably more power than the scheme at the river, even with additional water flow at the river. The turbine at the wastewater treatment plant generates 7.9 kW and 9.8 kW power for a low and high-efficiency turbine respectively, while the turbine at the river produces average power of 3 kW. The potential energy yield found in this study gives authorities and prospective owners an indication if there is merit in further investigations into hydropower projects at wastewater treatment plants. If only 20% of the more than 850 wastewater treatment plants in SA have a head of 1.5 m or more, they would have a collective annual energy potential of 10.4 GWh.

# ACKNOWLEDGEMENTS

Alhamdulillah, I firstly wish to thank Almighty Allah for granting me the strength, knowledge, and perseverance to complete this research.

My sincere appreciation to Dr Atanda Raji, my co-supervisor for his assistance and Dr Ayokunle Ayeleso, my co-supervisor for his passionate guidance, as well as my family for their unwavering support to help me achieve my goals.

The financial assistance of the National Research Foundation towards this research is also acknowledged. Opinions expressed in this thesis and the conclusions arrived at, are those of the author, and are not necessarily to be attributed to the National Research Foundation.

## DEDICATION

To my wife, Whaheeba, for her unconditional love and support throughout my life.

# TABLE OF CONTENTS

# LIST OF FIGURES

LIST OF TABLES

# GLOSSARY

| | |
|---|---|
| AST | Archimedes screw turbine |
| BW | Bid window |
| CF | Capacity factor |
| CHP | Combined heat and power |
| CSP | Concentrated solar power |
| D | Diameter |
| Di | Inside diameter |
| DMRE | Department of Mineral Resources and Energy |
| Do | Outside diameter |
| DOE | Department of Energy |
| EEZ | Exclusive economic zone |
| ESA | Ecological Society of America |
| ESHA | European Small Hydropower Association |
| ESKOM | Electricity Supply Commission |
| HK | Hydrokinetic |
| HPM | Hydrostatic pressure machine |
| HPW | Hydrostatic pressure wheel |
| IEA | International Energy Association |
| IHA | International Hydropower Association |
| IPP | Independent power producer |
| IRENA | International Renewable Energy Association |
| IRP | Integrated Resource Plan |
| Km | Kilometre |
| KPI | Key Performance Indicator |
| kW | Kilowatt |
| kWh | Kilowatt-hour |
| L | Length |
| l/s | litres per second |
| LHP | Large hydropower |
| Ml/d | Million litres per day |
| m/s | Meters per second |
| $m^2$ | Square meter |
| $m^3/s$ | Cubic meters per second |
| mm | Millimetre |
| MW | Megawatt |
| MWh | Mega-watt hour |

| | |
|---|---|
| P | Power |
| $P_{hyd}$ | Hydraulic power |
| $P_{mech}$ | Mechanical power |
| PV | Photovoltaic |
| $Q$ | Flow |
| $Q_{max}$ | Maximum flow |
| REIPPPP | Renewable energy independent power producer procurement programme |
| ROR | Run-of-river |
| RPM | Revolutions per minute |
| SHP | Small hydropower |
| $T$ | Torque |
| TWh | Terawatt hour |
| ULH | Ultra-low-head |
| UN | United Nations |
| UNIDO | United Nations Industrial Development Organization |
| VAHT | Vertical axis hydrokinetic turbine |
| W | Watt |
| WWTP | Wastewater treatment plant |
| ZWWTW | Zandvliet Wastewater Treatment Works |
| FIT | Feed-in tariff |

| | |
|---|---|
| $g$ | Gravity |
| $H$ | Head |
| $v$ | Velocity |
| $yr$ | Year |
| $\beta$ | Screw angle |
| $\eta$ | Efficiency |
| $\rho$ | Density |
| $\omega$ | Omega |

# CHAPTER ONE

# INTRODUCTION

## 1.1 Introduction

The current use of non-renewable energy sources has influenced the world climate to such a degree that, if the human race does not change its ways, it will have a severe negative impact on the entire globe and all living beings on it (Springmann et al., 2016). This concern prompted the intensified search and use of alternative and cleaner energy sources over the last decades. Many countries have signed international agreements, for example, the Kyoto Protocol, as a commitment to reduce emissions of greenhouse gasses that contribute to global warming and climate change (UNFCC, 2021). Furthermore, the reserves of non-renewable energy sources such as coal, oil, nuclear, and natural gas are limited and some of these reserves will be depleted within this century, at the current rate of exploitation (Covert et al., 2016).

These amongst other reasons gave rise to a universal drive to explore alternative and renewable energy sources such as solar, hydro, wind, biomass, and geothermal for increased usage and more effective utilization. Hydro electrical power plants are one of those alternative sources which are used successfully in many countries to generate thousands of megawatts of power. Many studies on small hydropower plants, especially in remote villages have shown that small hydropower is implemented successfully across the world (LIU, 2019)

## 1.2 Background to the research problem

Most cities and urbanised areas in the world have industries and water supply networks that transport megalitres of water with huge potential for power generation. Water treatment works, amongst other industrial plants have the potential to contribute to the ever-increasing demand for renewable energy. This renewable hydropower source is, however, underutilized and is not properly harnessed to achieve optimum benefit. Moreover, water flows come in different forms, but those that showed great promise for generating power are wastewater treatment effluents, inter-reservoir movement of water, cooling, and aquaculture farming plants. These sources often discharge into rivers and man-made canals with the pre-existing flow that can also be exploited for their hydropower potential. The impact of such a study may seem small in terms of the energy share in the overall hydropower basket, but it has the potential to contribute to the global need and bring some relief to many households the world over (Corcoran et al., 2015). South Africa for example has 853 wastewater treatment plants (SA Mitchell, MP de Wit, JN Blignaut, 2014). The thousands of litres of water that is discharged daily holds great hydropower potential that needs further investigation. In the last decade, there has been great emphasis by energy programs across the world to auction off renewable energy projects such as solar and wind technologies. However, the minimum capacity for these projects or bid requests, is much higher than what water treatment plants can deliver.

## 1.3 Statement of the research

The use of a wastewater treatment plant's effluent for the generation of electric power is still very low in South Africa (Van Vuuren et al., 2014). Hence, the present research assessed the hydropower potential of wastewater treatment plants to supplement the electricity supply.

## 1.4 Research Questions

- Which type of pico or small hydropower turbines are best suited for
- the considered sites to achieve optimum electric power?
- What is the potential energy that can be generated from the wastewater treatment plant sites?

## 1.5 Objectives of the research

The research objectives are as follows:

- To identify a suitable site for a case study to investigate its hydropower potential.
- To obtain the site data and find the best suited turbine.
- To determine the maximum potential energy generation of each site to find the best utilisation for the generated power.

## 1.6 Research design and methodology

The research methodology used in this paper is as follows:

- A comprehensive literature review is being done on renewable energy options and the various small hydropower systems and their components.
- A wastewater plant is selected and its discharge outflow conditions are obtained.
- The site conditions of the river in which the plant discharges are obtained.
- The most suitable hydropower turbines will be selected for both the wastewater treatment plant and the river.
- The respective turbines are modelled with a software program such as MATLAB and the generation capacity of each site is recorded.

- A comparison is drawn between the two systems at the plant and the river to evaluate which is the most desirable site in terms of power.
- Options for the hydropower usage are investigated.

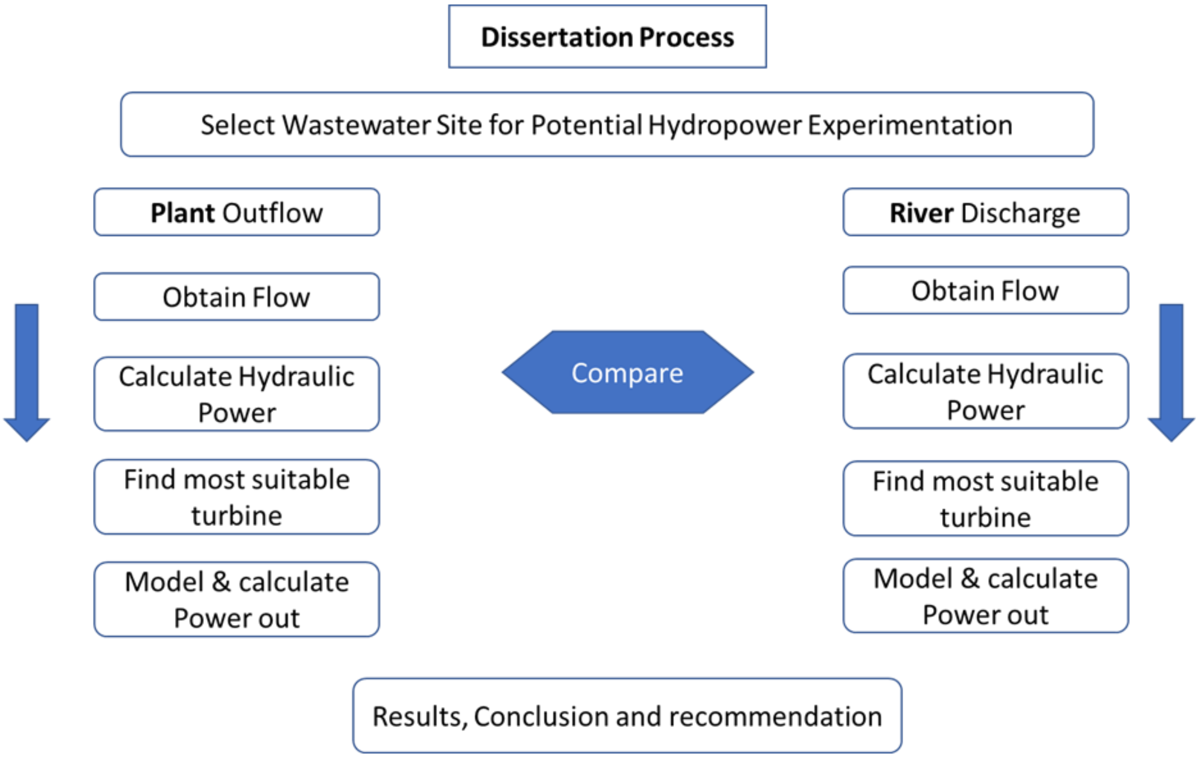


**Figure 1.1: Process of dissertation**

## 1.7 Delineations of the research.

In this research, an evaluation is done on the energy potential of a pico-hydropower system to be installed at the outlet of a chosen wastewater treatment plant. An accessible plant with usable data is selected. The requirement for the potential site is that the plant must discharge into a river, regardless of flow and head. In this study, the hydropower scheme is designed around the selected site's parameters. The river flow data is to be obtained; else it is to be measured at regular intervals to do monthly comparisons. A second hydropower system to be installed in the river in which the plant discharges, is also evaluated. The most suitable hydropower turbines are determined for the two sites and a comparison is drawn between the two sites' potential power.

## 1.8 Significance of research.

- This research contributes to the existing body of knowledge.

- The research outcomes give municipal authorities and other interested parties a quick view of the viability of a hydropower system on their wastewater plant.
- An optimum power generation capacity is achieved in the considered wastewater plant.
- This research gives ordinary people across the globe an early indication whether a hydropower system is feasible and practical to install in a river of a certain size.

## 1.9 Thesis organisation

This thesis consists of five chapters. Chapter one introduces the topic that this research is exploring, the objectives of the research, the methods that will be used, and the benefits of the research. Chapter two gives a comprehensive review of the literature on the renewable energy mix, with emphasis on South Africa. Small hydropower is further expounded upon in this chapter. The third chapter selects a wastewater treatment plant to do a case study on. The water outflow characteristics are obtained and the hydropower turbine options to be deployed are explored and the best one selected. The flow conditions of the river in which the wastewater plant discharges its water, are obtained. The hydropower turbine options to be installed at the river are evaluated and the most suitable one is selected. The theoretical model is finally designed in this chapter. Chapter four presents the modelling and simulation and discusses the results. Chapter five presents the research conclusions and recommendations. Figure 1 gives an illustration of the dissertation process.

# CHAPTER TWO

# LITERATURE REVIEW

2.1 Introduction

2.2 Background - need for renewable energy

2.3 Renewable energy types

2.4 Renewable energy in the South African context

- 2.4.1 Renewable Energy Independent Power Producer Procurement Programme
- 2.4.2 Integrated Resource Plan
- 2.4.3 Energy Mix
- 2.4.4 Electricity import and export
- 2.4.5 Wind Energy
- 2.4.6 Solar Energy
- 2.4.7 Biomass Energy
- 2.4.8 Geothermal
- 2.4.9 Hydropower energy in South Africa currently

2.5 Hydropower energy

2.6 Hydropower classification by type of system

- 2.6.1 Run-of-river (ROR) vs reservoir hydropower system
- 2.6.2 Hydropower classification by size of system

2.7 Hydropower turbine types

- 2.7.1 Impulse and reaction turbines
- 2.7.2 Other turbines
- 2.7.3 Archimedes screw turbine
- 2.7.4 Waterwheel
- 2.7.5 Modern waterwheels
- 2.7.6 Hydrokinetic turbines

2.8 Ultra-low-head technologies

2.9 Hydropower at the discharge of industrial plants

2.10 Combined heat and power at wastewater treatment plants

2.11 Summary

## 2.1 Introduction

In this chapter, a review of the relevant literature is done. The chapter presents an overview of the renewable energy types and its implementation in South Africa. Several classifications and different types of small hydropower schemes are also discussed. Thereafter, previous research on hydropower such as turbine types, ultra-low head technologies and discharge of industrial plants are explored.

## 2.2 Background - need for renewable energy

The United Nations (UN) has set seventeen universal goals for sustainable development across the world. One of these goals, Climate Action, says that carbon emissions need to be reduced by 45% by the year 2030 from the figures that were recorded in the year 2010 (IPCC, 2018). This goal has prompted many countries to embark on an intensive drive to find alternative cleaner energy sources. If this goal is reached, it will still only limit the global rise in temperature by 1.5 °C (IPCC, 2018). One of the main culprits of carbon emissions is the burning of fossil fuels such as coal and oil, especially to generate electricity. This practice should thus be minimised or substituted with a cleaner energy type.

In the last decade, many countries have started programmes to implement renewable energy projects (Apostoleris et al., 2018). South Africa is no exception and has started its own renewable energy independent power producer programme (REIPPPP), which will be discussed in the next section.

## 2.3 Renewable energy types

Before getting into hydropower, which is the primary energy type considered in this research, it is important to have an overview of how this energy type fits into the bigger basket of energy sources, especially renewable energy. This give us an idea of the future relevance of hydropower and how it fits into the renewable energy basket. Renewable energy comes from sources that do not get depleted when used.

Figure 2.1 shows a world renewable energy forecast for the year 2050. Wind energy stands out as the highest utilised source for power generation, followed by solar energy and then hydropower, with an 8% share of the total world energy production. This gives us an understanding that hydropower will still be very vital as an energy source in the world energy market in the next few decades (Gielen et al., 2019).

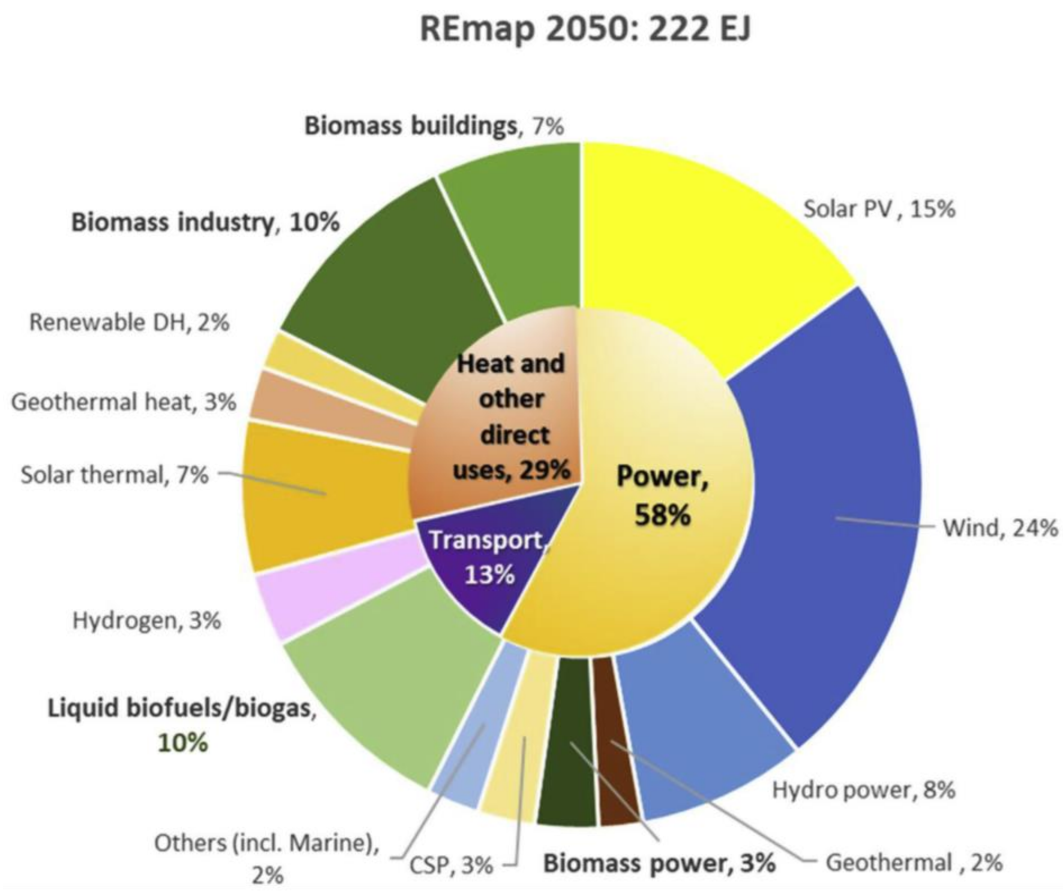


**Figure 2.1: World renewable energy map with the share of various sources (From Gielen et al., 2019)**

## 2.4 Renewable energy in the South African context

South Africa, like many other countries, has adopted various cleaner energy policies over the years. Significant amongst those is the Paris Agreement that was signed in 2015 at the COP21 conference. This is a legally binding international treaty to limit global warming to below two degrees Celcius (UNFCC, 2021).

### 2.4.1 Renewable Energy Independent Power Producers Procurement Programme

South Africa first introduced feed-in tariffs (FIT) for renewable energy projects more than two decades ago, but this FIT system was replaced soon after (Eberhard, 2014). The Renewable Energy Independent Power Producers Procurement Programme (REIPPPP) was launched in 2011 (DOE, 2013), (IPP, 2021). The independent power producers (IPP) office was established by the Department of Mineral Resources and Energy (DMRE), the Development Bank of Southern Africa (DBSA), and the National Treasury (NT), to facilitate the IPP projects. The REIPPPP can be seen as an auction instrument that created scope for various renewable energy projects. These projects are created and proposed by prospective suppliers, the IPPs. Various stakeholders including consortiums of investors, engineers, creditors, communities, amongst others, were brought together in this competitive bidding process (Müller & Claar, 2021). Eberhard and Naude (2017) show a timeline in Figure 2.2, on how the first four bidding windows and their respective components panned out in a Gantt chart layout. The progress of the various stages of the tender windows is tracked according to the date. Bidding window five was opened after the end date on the chart.

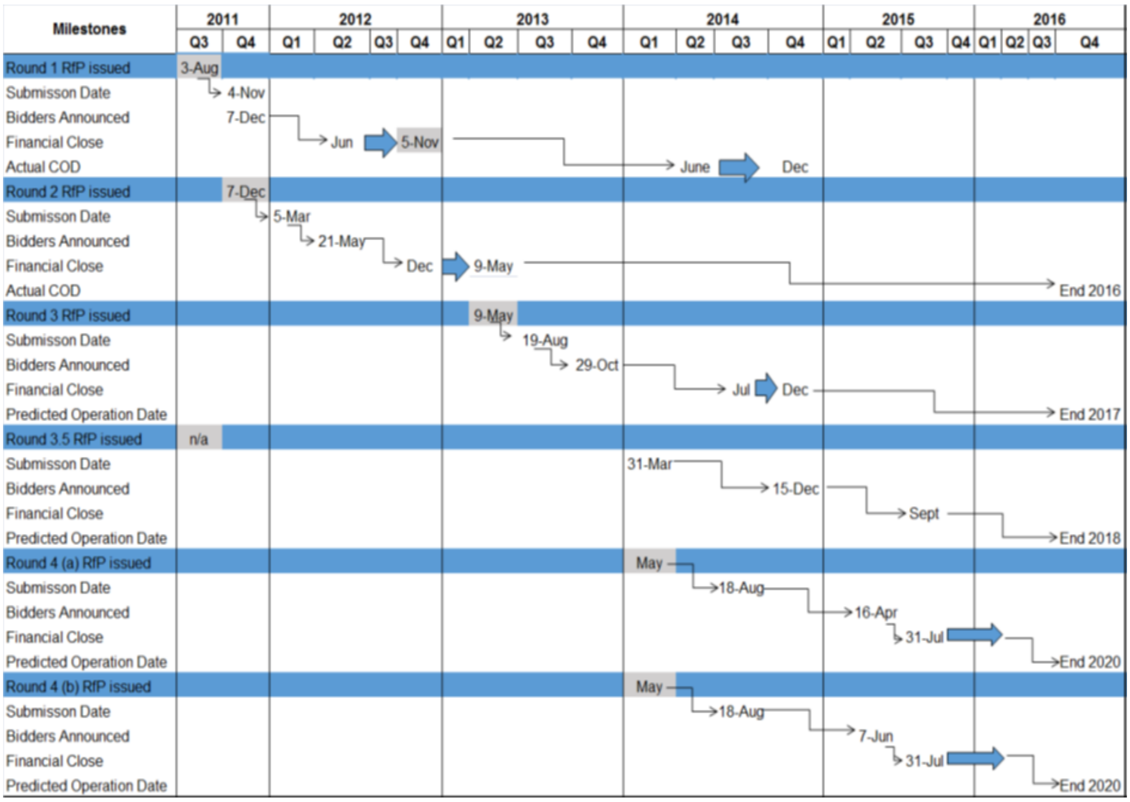


**Figure 2.2: SA REIPPPP Tender Process Timeline (From Eberhard & Naude, 2017)**

The South African REIPPPP programme enjoys prominent attention on the world stage with a keen interest in its successes in terms of the energy transition. Aspects such as socio-economic impact, financial investment, ownership, and transitional involvement, are some of the notable features of the program that are debated (Swilling & Annecke, 2012). The most anticipated outcome is probably the way this programme will shape the energy future of the country.

The REIPPPP has thus far opened a few bid windows (BW). The first round attracted mostly European firms. By the fifth bidding round, 92 projects have been closed financially. The REIPPPP have awarded 112 tenders of renewable energy projects by June 2021 (Müller & Claar, 2021). Table 2.1 gives a summary of the REIPPPP projects that were awarded up to bid window three. It shows that wind and solar are almost equal in capacity and together are far ahead of other project types.

**Table 2.1: Renewable energy allocation of REIPPPP up to August 2015 (From Eberhard, 2014)**

| Technology | First Allocation (Aug 2011) | Second Allocation (Oct 2012) | Third Allocation (Aug 2015) | Total | % Share of Total |
|---|---|---|---|---|---|
| Onshore wind | 1850 | 1470 | 3040 | 6360 | 48 |
| Solar PV | 1450 | 1075 | 2200 | 4725 | 36 |
| CSP | 200 | 400 | 600 | 1200 | 9 |
| Biomass | 13 | 48 | 150 | 210 | 2 |
| Biogas | 13 | 48 | 50 | 110 | 1 |
| Small Hydro | 75 | 60 | 60 | 195 | 1 |
| Small projects | 100 | 100 | 200 | 400 | 3 |
| Landfill Gas | 25 | 0 | 0 | 25 | 0 |
| **Total** | **3275** | **3200** | **6300** | **13225** | **100** |

Table 2.2 shows the list of projects that were awarded in 2021 for bidding window five (BW 5). The BW 5 projects consist only of wind and solar projects, which are similar in size. The wind projects have a total capacity of 1.6 GW and the total capacity of the solar projects is 975 MW (DMRE, 2021). Table 2.2 shows a complete list of all the renewable energy projects that were awarded up to bidding window five and Table 2.3 summarises all the projects from bid window one to five.

**Table 2.2: Preferred bidders for bidding window five (Adapted from DMRE, 2021)**

| No | **Wind** Project | **Capacity** (MW) | No | **Solar** Project | **Capacity** (MW) |
|---|---|---|---|---|---|
| 1 | Coleskop Wind Energy Facility; | 140 | 13 | Grootfontein PV 1; | 75 |
| 2 | San Kraal Wind Energy Facility; | 140 | 14 | Grootfontein PV 2; | 75 |
| 3 | Phezukomoya Wind Energy Facility; | 140 | 15 | Grootfontein PV 3; | 75 |
| 4 | Brandvalley Wind Farm; | 140 | 16 | Grootspruit Solar PV Project; | 75 |
| 5 | Rietkloof Wind Farm; | 140 | 17 | Graspan Solar PV Project; | 75 |
| 6 | Wolf Wind Farm; | 84 | 18 | Sannaspos Solar PV Project; | 75 |
| 7 | Beaufort West Wind Facility; | 140 | 19 | Du Plessis Dam Solar PV 1; | 75 |
| 8 | Trakas Wind Facility; | 140 | 20 | Kentani Solar Facility; | 75 |
| 9 | Sutherland Wind Facility; | 140 | 21 | Klipfontein Solar Facility; | 75 |
| 10 | Rietrug Wind Facility; | 140 | 22 | Klipfontein 2 Solar Facility; | 75 |
| 11 | Waaihoek Wind Facility; | 140 | 23 | Leliehoek Solar Facility; | 75 |
| 12 | Dwarsrug Wind Facility; | 124 | 24 | Braklaagte Solar Facility; and | 75 |
| | | | 25 | Sonoblomo Solar Facility. | 75 |
| | Total | **1608** | | | **975** |

**Table 2.3: South African renewable energy IPP procurement programme, bidding windows 1 - 5**
Adapted from (DMRE, 2021), (IPP, 2021)

| | | | | | |
|---|---|---|---|---|---|
| | | **BIDDING WINDOW 1** | | | |
| **SOLAR** | **MW** | **ONSHORE WIND** | MW | | |
| RustMo1 | 6,93 | Hopefield | 65,4 | | |
| Konkoonsies Solar | 9,65 | Dassiesklip Wind Energy Facility | 27 | | |
| Kalkbult Solar Park | 72,4 | MetroWind (Van Standens ) | 27 | | |
| Droogfontein Solar Power | 45,4 | Jeffreys Bay Wind Farm | 135,1 | | |
| Aries Solar | 9,65 | | | | |
| De Aar Solar Power | 45,6 | | | | |
| Herbert PV Power Plant | 19,6 | | | | |
| Greefspan PV Power Plant | 9,9 | | | | |
| Lesedi | 64 | | | | |
| Letsatsi | 64 | | | | |
| Kathu Solar Energy Facility | 50 | | | | |
| | 397,13 | | 254,5 | | |
| | | **BIDDING WINDOW 2** | | | |
| Sishen Solar Facility | 74 | Amakhala Emoyeni | 133,7 | **Hydro** | |
| Aurora-Rietvlei Solar Power | 9 | Tsitsikamma Community Wind Farm (“TC” | 94,8 | Stortemelk Hydro (Pty) Ltd | 4,4 |
| Vredendal Solar Park | 8,82 | Wind Farm West Coast 1 | 90,82 | Neusberg Hydro Electric Project | 10 |
| Linde | 36,8 | Waainek | 23,28 | | |
| Dreunberg | 69,6 | Grassridge | 59,8 | | |
| Jasper Power Company | 75 | Chaba | 21 | | |
| Boshoff Solar Park [Jacaranda Energy (P | 60 | Gouda Wind Project | 135,5 | | |
| Upington Airport | 8,9 | | | | |
| Solar De Aar 3 Proprietary Limited | 75 | | | | |
| CSP | | | | | |
| Bokpoort CSP Project | 50 | | | | |
| | 467,12 | | 558,9 | | 14,4 |
| | | **BIDDING WINDOW 3** | | | |
| Adams Solar PV 2 | 75 | Red Cap - Gibson Bay | 110 | **Landfill Gas** | |
| Tom Burke Solar Park | 60 | Longyuan Mulilo De Aar 2 North Wind En | 139 | Johannesburg Landfill Gas to Elect | 18 |
| Mulilo Sonnedix Prieska PV | 75 | Nojoli Wind Farm | 87 | | |
| Electra Capital | 75 | Longyuan Mulilo De Aar Maanhaarberg W | 96 | **Biomass** | |
| Pulida Solar Park | 75 | Khobab Wind Farm | 138 | Mkuze | 16 |
| Mulilo Prieska PV | 75 | Noupoort Mainstream Wind | 79 | | |
| CSP | | Loeriesfontein 2 Wind Farm | 138 | | |
| Xina CSP South Africa | 100 | | | | |
| Karoshoek Consortium | 100 | | | | |
| | 635 | | 787 | | |
| | | **BIDDING WINDOW 4** | | | |
| Aggeneys Solar Project | 40 | Copperton Windfarm | 102 | **Hydro** | |
| Bokamoso 67.90 | 67,9 | Excelsior Wind Energy Facility | 31,9 | Kruisvallei Hydro | 4,7 |
| De Wildt | 50 | Garob Wind Farm | 135,9 | TOT | 19,1 |
| Droogfontein 2 Solar | 75 | Golden Valley Wind | 117,7 | | |
| Dyason's Klip 1 | 75 | Kangnas | 136,7 | | |
| Dyason's Klip 2 | 75 | Oyster Bay Wind Farm 1 | 140 | | |
| Greefspan PV Power Plant No. 2 | 55 | Perdekraal East | 107,8 | | |
| Konkoonsies II Solar Facility | 75 | Roggeveld Wind Farm | 140 | | |
| Sirius Solar PV Project One | 75 | The Karusa Wind Farm | 139,8 | | |
| Solar Capital Orange | 75 | The Nxuba Wind Farm | 138,9 | | |
| Waterloo Solar Park | 75 | The Soetwater Wind Farm | 139,4 | | |
| Zeerust | 75 | Wesley-Ciskei | 32,7 | | |
| | 812,9 | | 1363 | | |
| | | **BIDDING WINDOW 5** | | | |
| Grootfontein PV 1; | 75 | Coleskop Wind Energy Facility; | 140 | | |
| Grootfontein PV 2; | 75 | San Kraal Wind Energy Facility; | 140 | | |
| Grootfontein PV 3; | 75 | Phezukomoya Wind Energy Facility; | 140 | | |
| Grootspruit Solar PV Project; | 75 | Brandvalley Wind Farm; | 140 | | |
| Graspan Solar PV Project; | 75 | Rietkloof Wind Farm; | 140 | | |
| Sannaspos Solar PV Project; | 75 | Wolf Wind Farm; | 84 | | |
| Du Plessis Dam Solar PV 1; | 75 | Beaufort West Wind Facility; | 140 | | |
| Kentani Solar Facility; | 75 | Trakas Wind Facility; | 140 | | |
| Klipfontein Solar Facility; | 75 | Sutherland Wind Facility; | 140 | | |
| Klipfontein 2 Solar Facility; | 75 | Rietrug Wind Facility; | 140 | | |
| Leliehoek Solar Facility; | 75 | Waaihoek Wind Facility; | 140 | | |
| Braklaagte Solar Facility; and | 75 | Dwarsrug Wind Facility; | 124 | | |
| Sonoblomo Solar Facility. | 75 | | | | |
| | 975 | | 1608 | | |
| | **3287,2** | | **4571** | | |

- **Renewable energy pricing**

Renewable energy has become cheaper since the first REIPPPP auction started. Electricity supply quotes have decreased significantly since the first bidding window. Figure 2.3 shows that the average tendered price across all technologies has decreased significantly from R2.02 per kWh in BW1 to 70 cents per kWh in the fourth round. (Department of Energy, 2016).

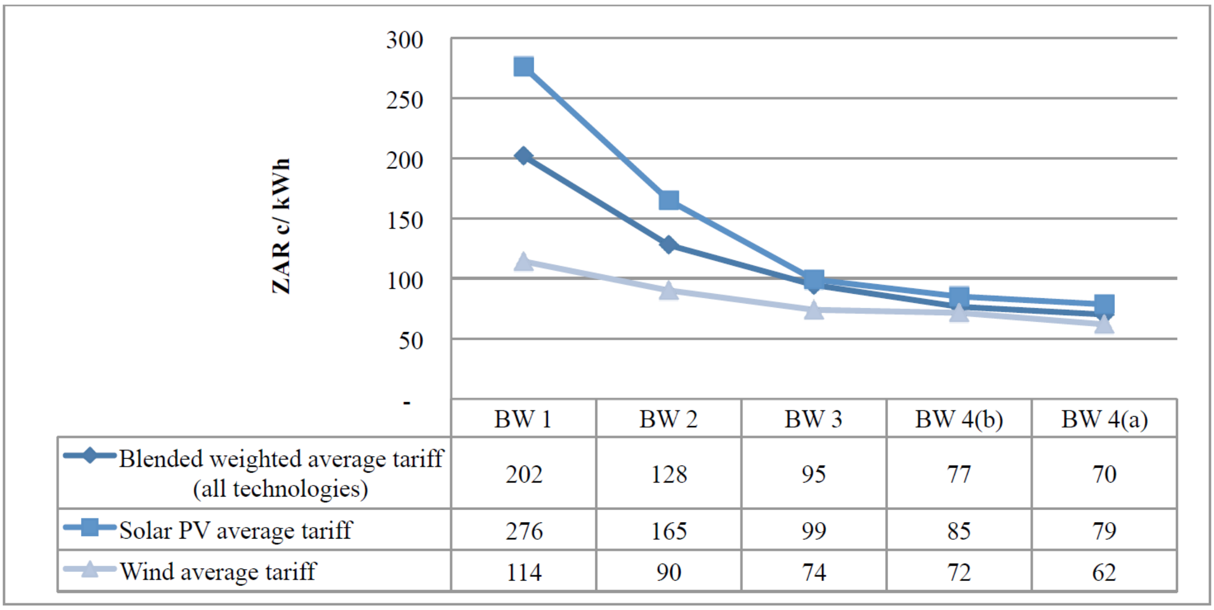


| | BW 1 | BW 2 | BW 3 | BW 4(b) | BW 4(a) |
|---|---|---|---|---|---|
| Blended weighted average tariff (all technologies) | 202 | 128 | 95 | 77 | 70 |
| Solar PV average tariff | 276 | 165 | 99 | 85 | 79 |
| Wind average tariff | 114 | 90 | 74 | 72 | 62 |

**Figure 2.3: Comparative price per kWh for wind, solar, and all technologies from bidding window 1 -4 (From Eberhard & Naude, 2016)**

The decline in renewable energy prices is not just a South African phenomenon. We can see in Figure 2.4 that in all the countries in which renewable electricity projects were auctioned off, the price decreased consistently. The reduction in hardware prices is the biggest factor that influenced this decline. The decline in hardware cost was mostly influenced by the growth in the market, which will continue for some time.

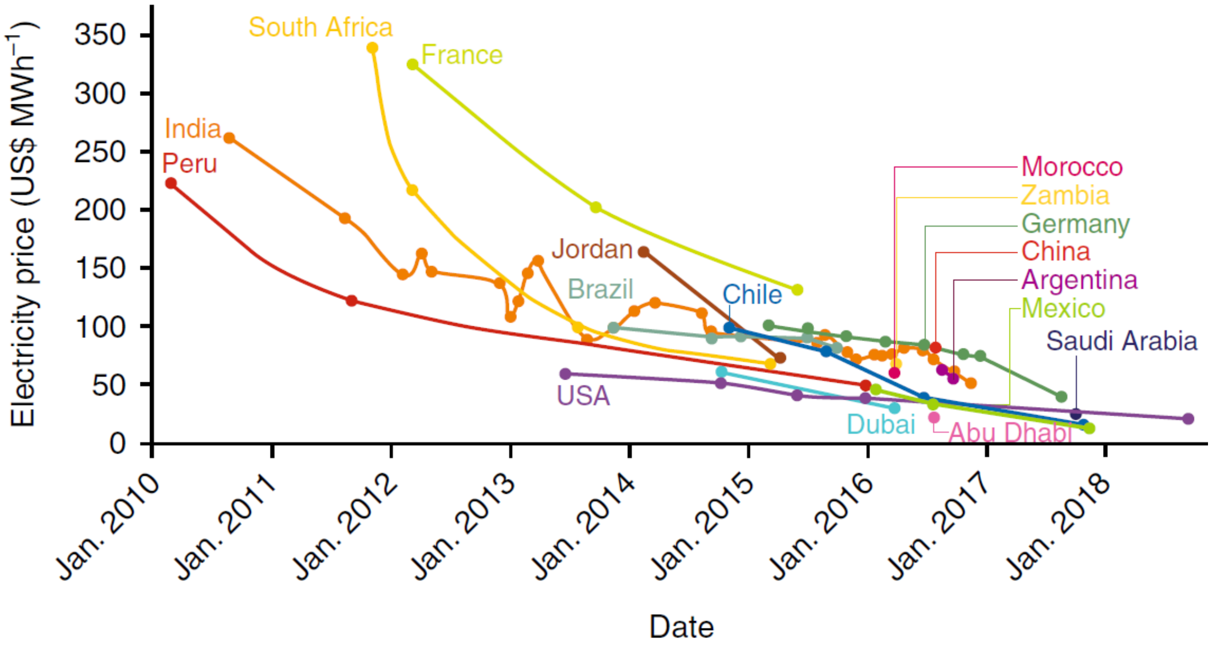


**Figure 2.4: Electricity supply price of various countries over eight years (From Apostoleris et al., 2018)**

- **Small Projects Renewable Energy Programme**

The South African renewable energy IPP procurement programme has also launched the small projects section under its REIPPPP. This programme gives smaller businesses that may not have international partners or certification, the opportunity to tender for projects. Under the small projects division, projects of not less than 1 MW and not bigger than 5 MW are entertained. Table 2.4 shows a list of the small projects that were allocated since the beginning of the programme. The initial total target for small projects was 100 MW, but it was later increased to 400 MW (IPP, 2021).

**Table 2.4: List of small projects allocated by the REIPPPP (IPP, 2021)**

| Project | Type | MW | Province | Area/City |
|---|---|---|---|---|
| Adams Solar PV Project (Pty) Ltd | Photovoltaic (Other) | 5 | Northern Cape | Hotazel |
| Augrabies Solar PV1 | Photovoltaic (Other) | 5 | Northern Cape | Kakamas |
| Bellatrix Solar PV Project | Photovoltaic (Other) | 5 | Northern Cape | Victoria-West |
| Busby Renewables Biomass Project | Biomass | 5 | Mpumalanga | Wakkerstroom |
| Capella Solar PV Project | Photovoltaic (Other) | 5 | North West | Piet Plessis |
| Castor Solar PV Project | Photovoltaic (Other) | 5 | Free State | Boshof |
| Du Plessis Solar PV4 | Photovoltaic (Other) | 5 | Northern Cape | De Aar |
| George Biomass to Energy Project | Biomass | 5 | Western Cape | George |
| Heuningspruit PV1 | Photovoltaic (Other) | 5 | Free State | Kroonstad |

| | | | | |
|---|---|---|---|---|
| Hopefield Community Wind Farm | Onshore Wind | 5 | Western Cape | Hopefield |
| Keren Energy Disselfontein | Photovoltaic (Other) | 5 | Northern Cape | Disselfontein |
| Keren Energy Kakamas | Photovoltaic (Other) | 5 | Northern Cape | Kakamas |
| Keren Energy Keimoes | Photovoltaic (Other) | 5 | Northern Cape | Keimoes |
| Klawer Wind Farm | Onshore Wind | 5 | Western Cape | Klawer |
| Roma Energy Danielskuil | Photovoltaic (Other) | 5 | Northern Cape | Danielskuil |
| Roma Energy Mount Roper | Photovoltaic (Other) | 5 | Northern Cape | Kuruman |
| Skuitdrift 1 | Photovoltaic (Other) | 5 | Northern Cape | Augrabies |
| Skuitdrift 2 | Photovoltaic (Other) | 5 | Northern Cape | Augrabies |
| Steynsrus PV1 | Photovoltaic (Other) | 5 | Free State | Steynsrus |
| Steynsrus PV2 | Photovoltaic (Other) | 5 | Free State | Steynsrus |

### 2.4.2 Integrated Resource Plan (IRP2019)

The Integrated Resource Plan (DMRE, 2019) is another landmark in the South African renewable energy landscape. The IRP 2019 that was signed by the minister of Energy in October 2019, is a follow-up on the original IRP 2010-2030 document. The plan gives an overview of how electricity will be generated in SA going forward. The plan looks at the background of the energy situation in SA, aspects impacting the plan (environmental, economic, social, international agreements), and the energy mix available to the country.

The draft version of this "living document", IRP 2018, invited comments from the public. The public submissions and responses to that request are incorporated into the final issue of the IRP 2019. After analysing the results of modelling and simulation of the different energy sources, plants, and their capacities, nine main decisions were taken and published in the plan. In the first decision, Decision 1, the government undertakes to establish a power purchase program that will assist with additional capacity that will help with Eskom's shortfall in supply. This medium-term power purchase programme is similar to the plan that was adopted in the IRP 2010. Table 2.5 shows the existing energy sources, the current contracted, and the future additional capacity that will be filled (DMRE, 2019).

**Table 2.5: Proposed Updated Plan for the Period Ending 2030 (From DMRE, 2019)**

| | Coal | Nuclear | Hydro | Storage (Pumped Storage) | PV | Wind | CSP | Gas / Diesel | Other (CoGen, Biomass, Landfill) | Embedded Generation |
|---|---|---|---|---|---|---|---|---|---|---|
| 2018 | 39 126 | 1 860 | 2 196 | 2 912 | 1 474 | 1 980 | 300 | 3 830 | 499 | Unknown |
| 2019 | 2 155 | | | | | 244 | 300 | | | 200 |
| 2020 | 1 433 | | | | 114 | 300 | | | | 200 |
| 2021 | 1 433 | | | | 300 | 818 | | | | 200 |
| 2022 | 711 | | | | 400 | | | | | 200 |
| 2023 | 500 | | | | | | | | | 200 |
| 2024 | 500 | | | | | | | | | 200 |
| 2025 | | | | | 670 | 200 | | | | 200 |
| 2026 | | | | | 1 000 | 1 500 | | 2 250 | | 200 |
| 2027 | | | | | 1 000 | 1 600 | | 1 200 | | 200 |
| 2028 | | | | | 1 000 | 1 600 | | 1 800 | | 200 |
| 2029 | | | | | 1 000 | 1 600 | | 2 850 | | 200 |
| 2030 | | | 2 500 | | 1 000 | 1 600 | | | | 200 |
| TOTAL INSTALLED | 33 847 | 1 860 | 4 696 | 2 912 | 7 958 | 11 442 | 600 | 11 930 | 499 | 2600 |
| Installed Capacity Mix (%) | 44.6 | 2.5 | 6.2 | 3.8 | 10.5 | 15.1 | 0.9 | 15.7 | 0.7 | |

Installed Capacity
Committed / Already Contracted Capacity
New Additional Capacity (IRP Update)

One of the highlighted issues in the IRP2019 report is the evident decline in the electricity energy sent-out. It can be seen in Figure 2.5, between 2010 and 2018, there is a stark contrast between the expected electricity delivery, compared to the actual electricity sent out. The promulgated IRP 2010–2030 promised a 3% growth rate but we only saw an average compounded rate of -0.6% over the period. In 2016 this was equivalent to an 18% drop in expected supply from 244 TWh to 296 TWh (DMRE, 2019).

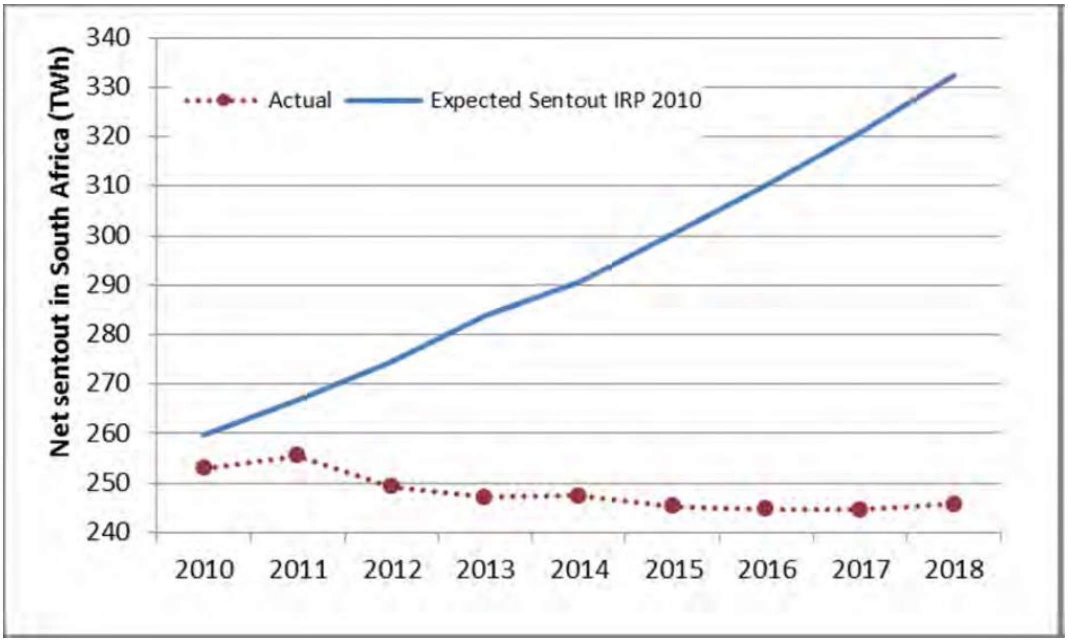


**Figure 2.5:: Expected Electricity Sent-out from IRP 2010–2030 vs Actual (From DMRE, 2019)**

### 2.4.3 Energy Mix

The forecasted renewable energy mix that resulted from the REIPPPP consists predominantly of solar, wind, and to a lesser extent bioenergy and hydropower. We will expound on these types in the next sections. Before we get into the renewable energy mix of South Africa, it is important to have a look at the overall electricity supply mix. With the current focus on renewable energy projects in the country and abroad, it is easy to get distracted from the fact that coal is still the predominant source of electricity. Figure 2.6a shows that non-renewable energy sources had an 83% share in 2018. The 17% renewable energy is discussed in the following section. In the renewable energy capacity chart, geothermal has a zero percent share.

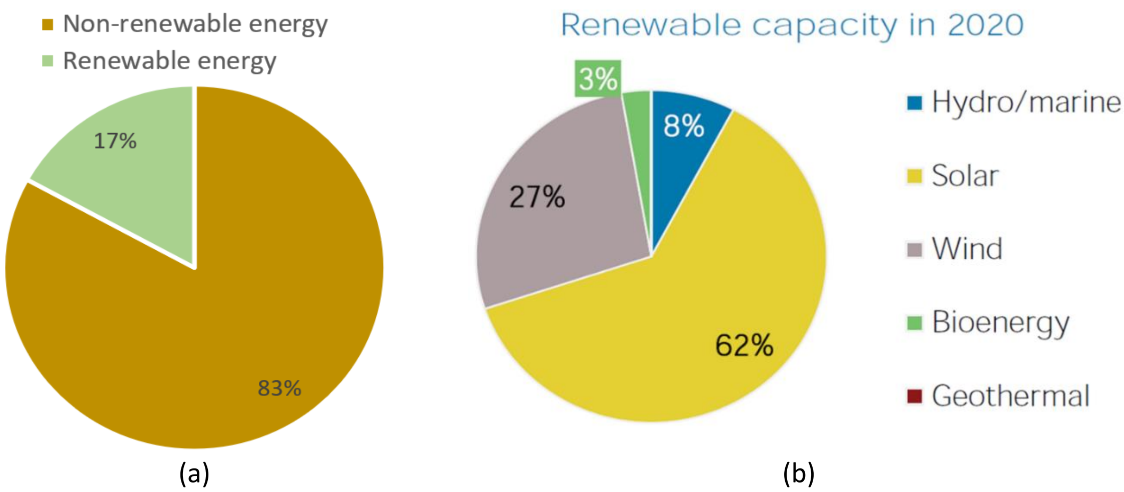


**Figure 2.6: (a) Total electrical energy sources in South Africa in 2018. (b) The capacity of Renewable energy sources in South Africa in 2020**

**(From IRENA, 2020).**

### 2.4.4 Electricity import and export

South Africa imported about 3% of its total electricity in 2016 (DOE, 2019). The bulk of this comes from the Cahora Bassa hydropower scheme in Mozambique (Figure 2.7). Eskom, the main utility also exports 6% of its total electricity to neighbouring counties, Botswana, eSwatini, Lesotho, Mozambique, Namibia, Zambia, and Zimbabwe.

**Figure 2.7: The Cahora Bassa hydropower scheme (From Wikimedia, 2007)**

### 2.4.5 Wind Energy

Wind energy is the renewable energy type that has shown the most potential for the future of South Africa. Wind energy projects received the biggest total bid allocation of the REIPPPP. From the first to the fifth bidding window allocations, 12 onshore wind projects have been awarded a total share of 7968 MW. The most common capacity per wind farm project is 140 MW. Figure 2.8 shows the Wesley-Ciskei Wind Farm near Hamburg in the Eastern Cape. This is one of the bidding window 4 projects that are due to reach the operation stage. The BW 5 awarded projects are only expected to produce power in 2024 (DMRE, 2021).

**Figure 2.8: The Wesley-Ciskei wind farm near Hamburg in the Eastern Cape was allocated under the fourth bidding window (From Smith, 2021)**

- **Offshore wind**

No offshore wind power projects have yet been allocated in SA. However, Rae and Erfort (2020) showed in their research that South Africa has an annual offshore wind potential of 44.52 TWh at shallow depths of less than 50 m. It also has 2 387.08 TWh at depths up to one kilometer. They identified three initial regions that are suitable for offshore wind farms. Figure 2.9(a) shows the location of the regions namely, Struisbaai, KwaDukuza, and Richards Bay. Figure 2.9(b) shows the coastline of South Africa has a promising wind capacity factor (CF) in the country's exclusive economic zone (EEZ) (Rae & Erfort, 2020).

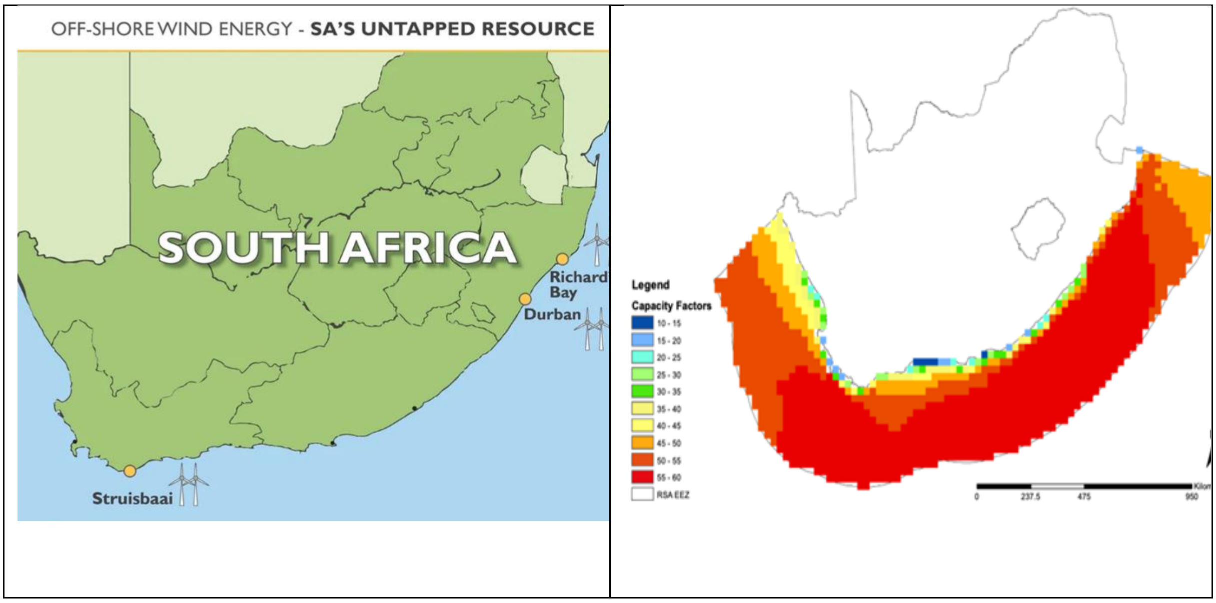


a b

**Figure 2.9: Offshore wind potential in South Africa: (a) three proposed sites for offshore wind farming. (b) the wind capacity factor in the exclusive economic zone of the country**

**(Rae & Erfort, 2020)**

The image in Figure 2.10 shows three different floating options for offshore wind turbines that are being explored. Most of the current wind turbines however, are fixed to the sea bottom. The European countries, in particular the United Kingdom, has the largest offshore wind capacity in the world, powering 7.5 million homes, and a third of the country's electricity will come from offshore wind, projects one of the largest installers (Orsted, 2021).

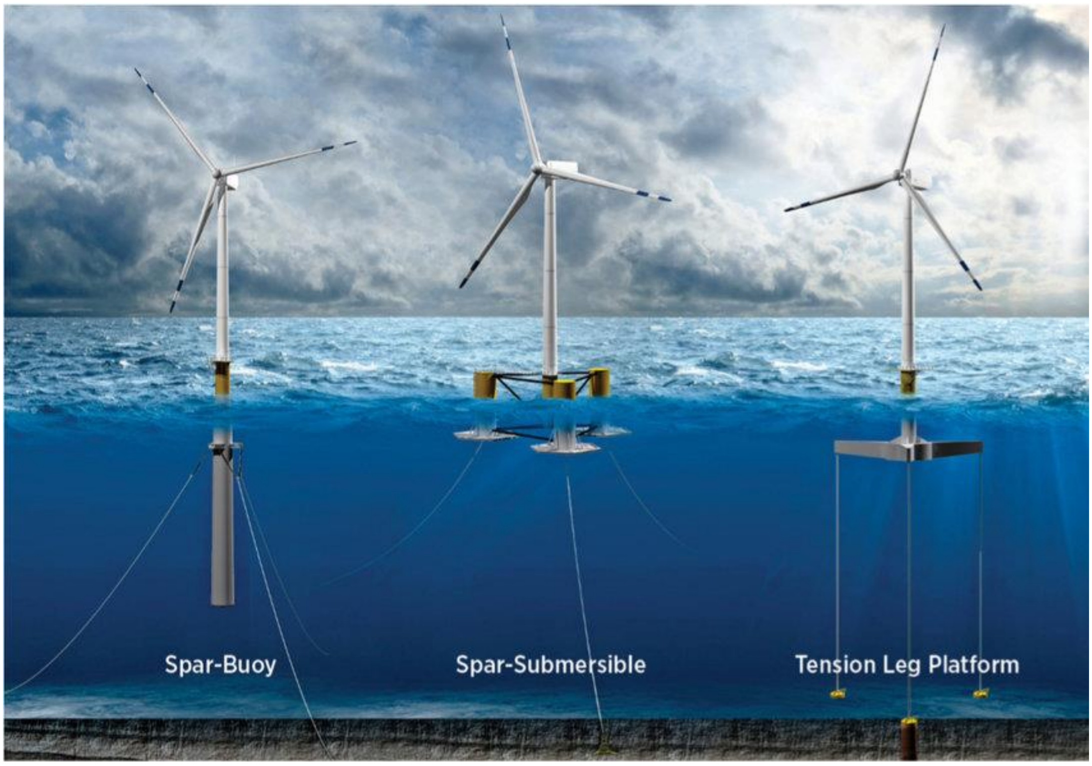


**Figure 2.10: Three different floating options for offshore turbines (From Wisatesajja et al., 2019)**

### 2.4.6 Solar Energy

In the last decade, the solar energy industry has experienced fast growth across the globe. Since the REIPPPP first awarded solar project tenders, South Africa has also seen fast growth in this industry (Letcher, 2018). Solar power has received the majority share of the REIPPPP awarded projects. Solar energy consists of two technologies: photovoltaics (PV) and concentrated solar power (CSP). Figure 2.11 shows the installed capacity of solar energy in SA. From no capacity in 2011, the technology grew steadily to 6 MW in 2020.

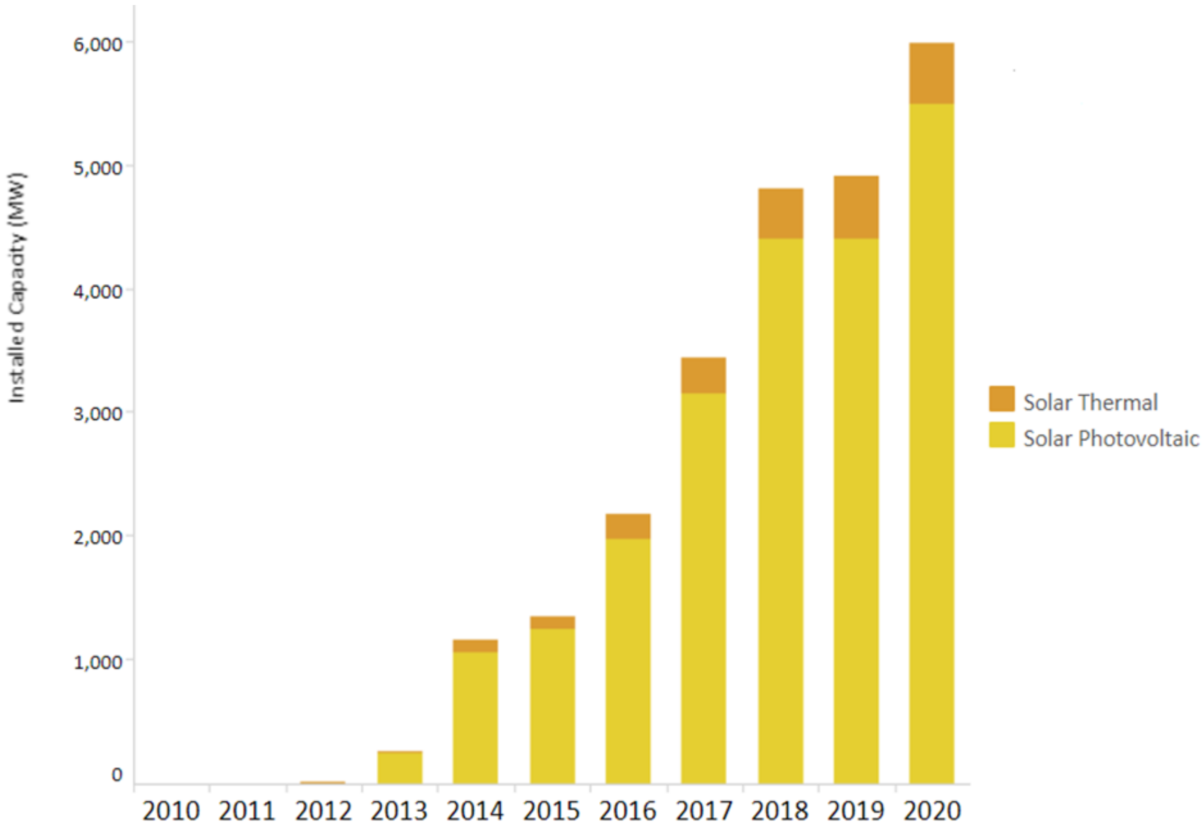


**Figure 2.11: Solar power capacity in South Africa over the last decade (From IRENA, 2021)**

- **Photovoltaics**

Photovoltaics (PV) or solar cells are electronic devices that convert the sun rays into an electrical potential. The cells are grouped on a board to form a solid flat usable panel. The connected cells produce a higher collective voltage and the panels are connected together to form a big electricity generating plant. Amongst the renewable energy projects that were awarded by the REIPPPP up to bidding window five, 51 projects were for PV, with a total capacity of 3037 MW (IPP, 2021). Multiple projects have reached the grid connection stage already. The Jasper solar plant in Figure 2.12 is an example of a modern commercial plant of 96 MW capacity. The plant is expected to generate 180 GWh of electricity per year, with a lifespan of 25 years (Renewable-technology, 2016).

**Figure 2.12: The Jasper solar power plant in the Northern Cape, South Africa (From Renewable-technology, 2016)**

- **Solar CSP**

Concentrated solar power (CSP), differs from PV in that it uses the thermal energy of the sun to generate power. It uses numerous mirrors to reflect the sun's rays onto a central point. This point consists of a liquid that is heated to create steam, which in turn drives a turbine to create electricity. The advantage of CSP over PV is that the specialised heated liquid that is used, can store heat and thereby still generate power after the sun has set.

Three CSP projects have been allocated through the REIPPPP programme by bid window 5, with a combined capacity of 250 MW. The Redstone concentrated solar thermal power (CSP) plant in Figure 2.13, is in the Northern Cape in South Africa. This 100 MW CSP project that was awarded in 2015 via the SA REIPPPP programme, is the first of its kind in Africa. The plant started producing power in 2018 and is expected to deliver 480 GWh per year. The plant can store heat for 12 hours, thereby delivering power during the night time (NS ENERGY, 2018).

**Figure 2.13: The Redstone concentrated solar power plant in the Northern Cape, South Africa (From NS ENERGY, 2018)**

### 2.4.7 Biomass Energy

Biomass energy is derived from organic biomass material. This type of energy is derived from either plant or animal residue to produce heat or electricity. Examples of biomass are domestic waste, wood or forest material, food crops or their waste, or even aquatic organisms.

The Mkuze project in KwaZulu-Natal, South Africa, (Figure 2.14) is one of the first projects that was given the go-ahead by the IPP procurement programme. This 16 MW plant uses mainly sugar cane residue (Piccinini, 2018).

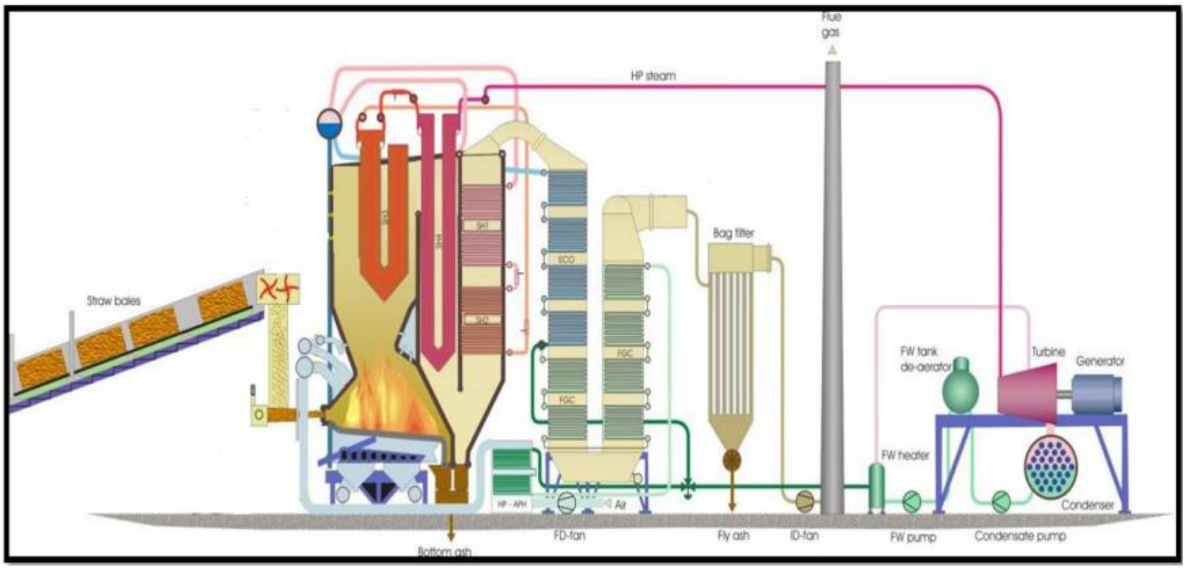


**Figure 2.14: Diagram of the power plant of the Mkuze biomass project (From Piccinini, 2018)**

- **Biomass fuel in IPP projects**

Figure 2.15 shows typical wood chips, the kind that is used at the Sappi plant sawmill in Mpumalanga in South Africa. Theron (2015) reported that the biomass project of Ngodwana Energy has signed a power purchase agreement with the SA government as part of the IPP procurement programme, to deliver 25 MW of energy.

(a) (b)

**Figure 2.15: Biomass fuel: (a) wood chips from the Sappi mill (Theron, 2015) . (b) sugar cane from the KwaZulu-Natal region to be used in the Mkuze biomass plant (Piccinini, 2018)**

- **Potential benefits of biomass in South Africa**

The woody residues from forests, mills, and gardens offer good biomass potential. The Coega Biomass Centre in the Eastern Cape in South Africa (Figure 2.16), is a biomass beneficiation plant that takes in this woody residues and make biomass pallets that supply other energy generation plants (Roodbol, 2020).

**Figure 2.16: The Coega Biomass Centre in South Africa is a beneficiation plant (From Roodbol, 2020)**

### 2.4.8 Geothermal

Geothermal energy is the heat from below the earth's surface that is used to generate electric power. The depth and temperature of this heat vary and are accessed through various methods to generate electricity. Figure 2.17 shows an illustration of geothermal energy plant. South Africa does not have major geothermal reserves and there are no known future projects planned.

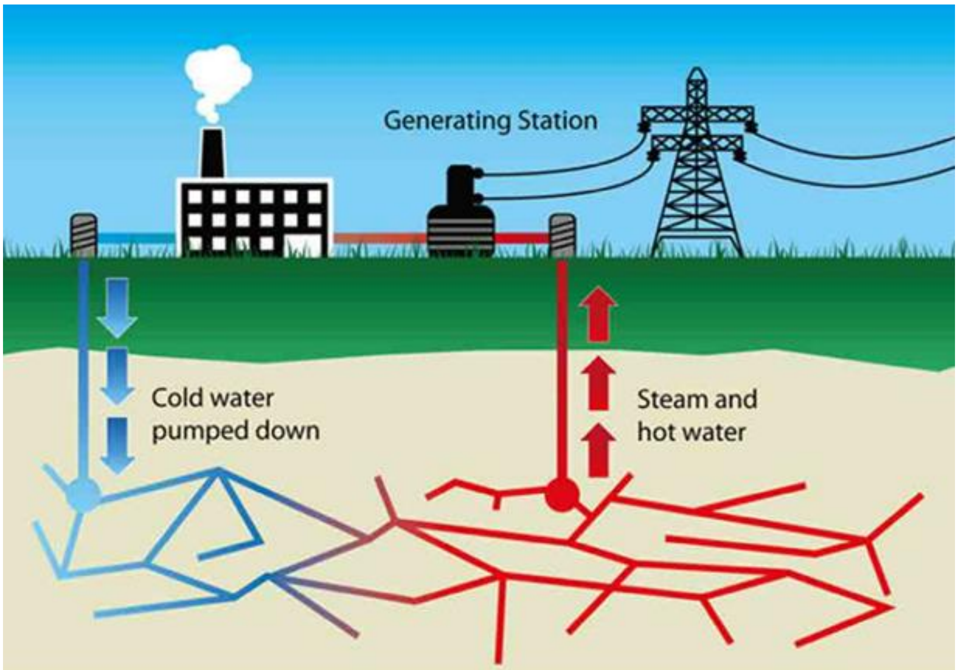


**Figure 2.17: Illustration of a typical geothermal energy plant (From Wikimedia, 2015)**

### 2.4.9 Hydropower energy in South Africa currently

South Africa is forecasted to use 8% hydropower by the year 2050 (DOE, 2013). Currently, there is a mix of small run-of-river plants, pumped hydro, and multiple conduit hydropower schemes. A major share of hydropower is imported from a neighbouring country.

Since the launch of the REIPPPP, the South African government has given three small hydropower projects preferred bidders status for implementation.

The Neusberg hydropower project in Figure 2.18 was allocated during bidding window 2 and the project was completed in January 2015. This run-of-river project sits on the Orange river in the Northern Cape and it has a capacity of 10 MW. The project is contracted to deliver power for 20 years (Green, 2012).


**Figure 2.18: Location of the Neusberg small hydropower station on the Orange river in the Northern Cape in South Africa (Adapted Google Maps, 2021b)**

The Stortemelk hydropower project (Figure 2.19) was allocated in the second bidding window of the REIPPPP and was commissioned in 2016. This project is operated as a run-of-river scheme and it sits on the Botterkloof dam in the Free State province. The project with its vertical Kaplan turbine has a capacity of 4.3 MW and is expected to deliver 28 GWh of electricity per year over its 20-year contractual period (REH, 2016).

**Figure 2.19: Stortemelk hydropower plant on the Botterkloof Dam in the Free State in South Africa (From REH, 2016).**

The Kruisvallei Hydro project in Figure 2.20 was allocated during the fourth bidding window. The run-of-river project sits on the Ash River in the Free State province and it started operation in February 2021. The hydropower scheme with its twin run-of-river turbines has a total capacity of 4 MW and an annual electric-generation potential of 24 GWh (Smith, 2021).

(a) (b)

**Figure 2.20: Kruisvallei Hydropower project on the Ash River in South Africa: (a) first hydropower turbine (b) turbine two of the hydropower scheme (From Red Rocket, 2021)**

## 2.5 Hydropower energy

Hydropower is one of the most reliable forms of renewable energy sources, with 62% of the total share of renewable sources in the world (World Bank, 2020). Small hydropower is the fastest expanding form of hydropower, with 4,4GWh supplied globally in 2018 (IHA, 2019). However even with the growth in this sector, there were still one billion people in the world without electricity in 2018 (IEA, 2018). In developing countries, there is a great potential to expand the small hydropower sector (Lahimer et al., 2012). Even in developed countries with a good national electricity grid, there are still good opportunities to further develop the sector of small hydropower to positively contribute to the goal of producing cleaner energy (IEA, 2018). Previous studies of hydropower on run-of-river systems concentrated predominantly on systems that incorporate a penstock. This type of hydropower system is used in applications with medium to high head, leaving a gap for further research in the area of ultra-low head hydropower applications (Singh & Singal, 2017). Figure 2.21 shows typical examples of run-of-river schemes.

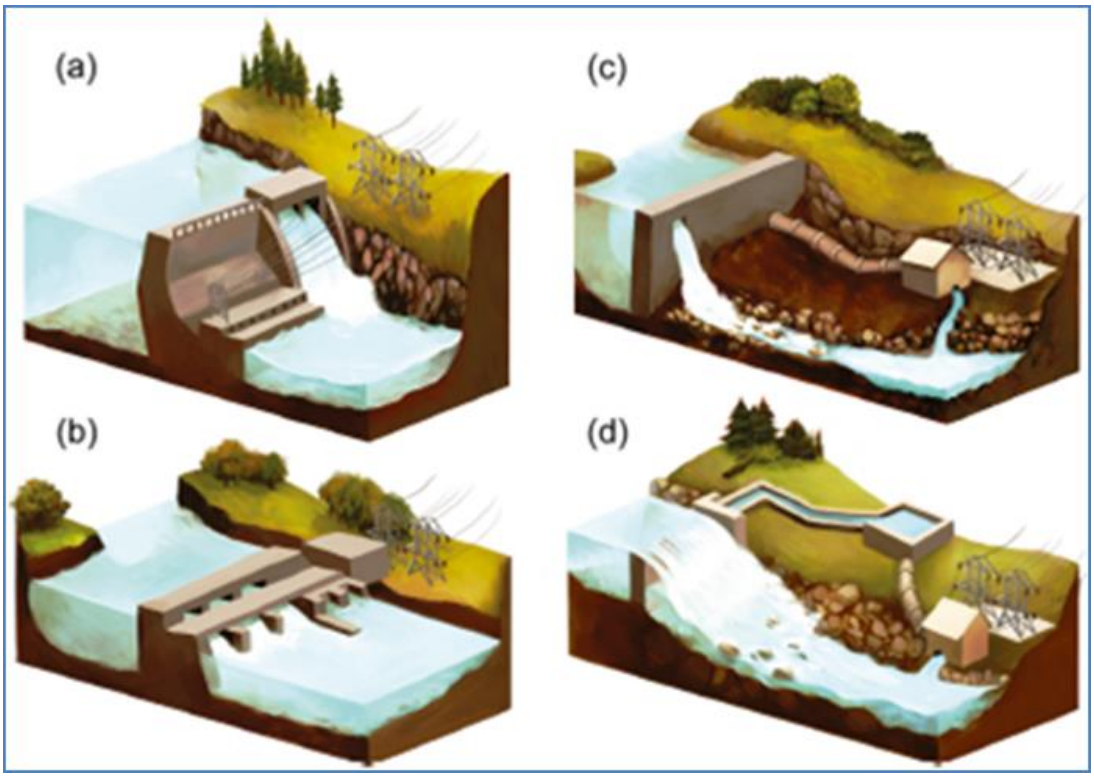


**Figure 2.21: Schematic on primary small hydropower classification a) At reservoir b) no storage c)storage with diversion d) diversion without storage (From Couto & Olden, 2018)**

## 2.6 Hydropower classification by type of system

In a research review of hydropower plants, Singh and Singal (2017) have listed over 50 different research papers in a table form, summarising the columns according to the author, components, operation, and optimising techniques. This chart shows to what extent research has been done in this area. The types of Hydropower are classified into different schemes depending on the approach taken.

LIU et al., (2019) classify hydropower by looking at the purpose of the system (whether single or multipurpose) or the type of system (run-of-river or reservoir) or the size of the system (large, medium, or small) or the head (high, low, or ultra-low) or the connection system (grid or off-grid) or the regulation performance (peaking run-of-river or seasonal storage). Some of these systems are described in more detail below.

### 2.6.1 Run-of-river (ROR) vs reservoir hydropower system

In run-of-river (ROR), a portion of the river water is diverted and channelled through a penstock onto the turbine lower down to generate electricity as illustrated in Figure 2.22 (Davis & Graham, 2004). In low head applications which are typically pico- and micro hydropower, the turbines are placed directly in the diverted part. They can also be placed in the river or the canal itself (Singh & Singal, 2017). Run-of-river hydropower does not have a dam or storage reservoir (Figure 2.23) and is thus solely dependent on the availability of water flow in the river or canal. However, pondage is usually implemented when water is dammed up before the penstock or behind a weir in a very low head river or canal to increase the level and flow rate of the river. Kumar & Katoch (2014) has summarised various indicators for the sustainability of hydropower into two main groups. In the analytical model that was developed for run-of-river hydropower models, Basso and Botter (2012) found that plants in water with variable flow are less energy-efficient than plants with more constant water flow. Other aspects of a small run-of-river hydropower installation are the hydrological conditions of the river such as the riverbed width, flow and head.

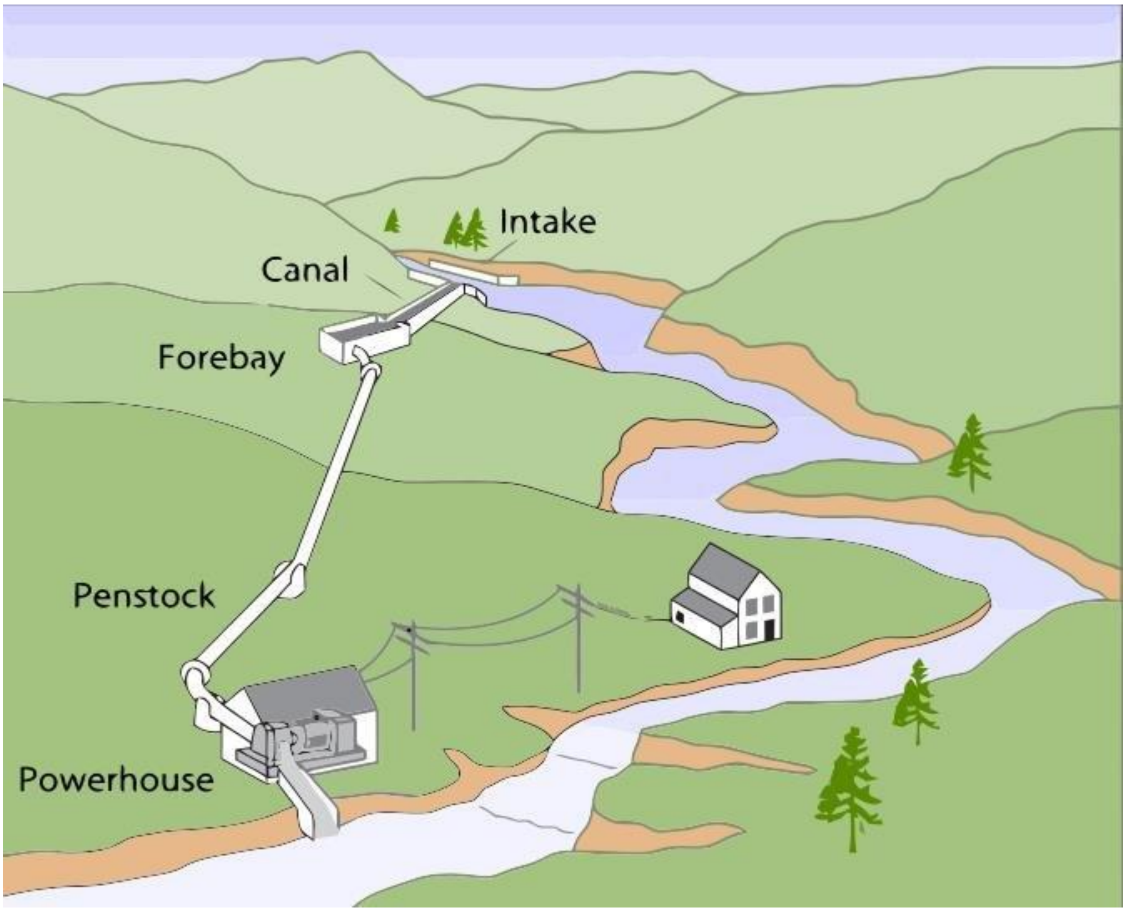


**Figure 2.22: Typical run-of-river illustration (From Ali et al., 2018)**

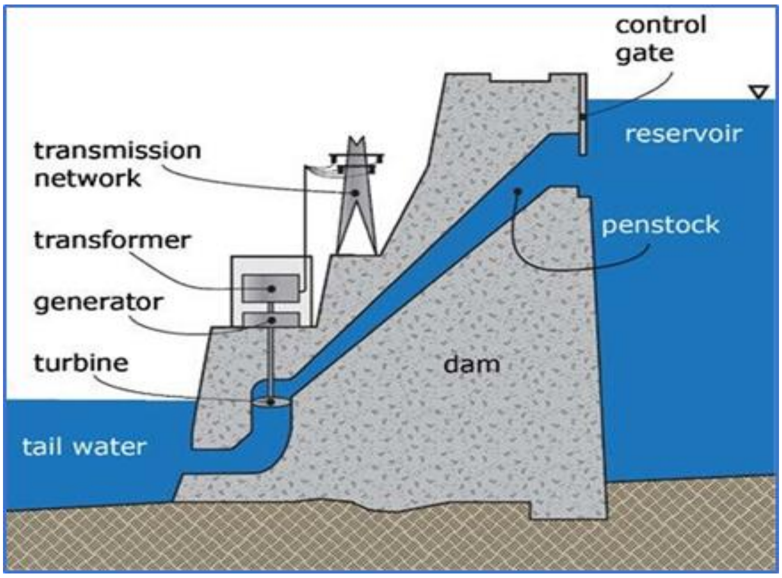


**Figure 2.23: Example of hydropower system at a reservoir (From Viadero et al., 2017)**

- **Pumped hydropower**

Pumped storage hydropower schemes consist of two reservoirs with about one to a few hundred meters height difference between them. The scheme acts as a storage system where water is pumped during an off-peak time from the lower to higher reservoir. During peak time or when needed, the water flows down to the lower level reservoir, through the turbines to generate electricity. The pumped hydropower scheme that is connected to the main electricity grid thus acts as a backup system for electricity that can be switched on within a few minutes (Barta, 2018). South Africa has various pumped hydropower systems as listed in Table 2.6

**Table 2.6: Hydropower installations in South Africa (Barta, 2018)**

| Hydroelectric plant | Location, river or town (province) | Owner/administrator/ operator | Installed capacity (MW) |
|---|---|---|---|
| Ncora | Ncora River (E. Cape) | Eskom | 2 |
| First Falls | Umtata River (E. Cape) | Eskom | 6 |
| Second Falls | Umtata River (E.Cape) | Eskom | 11 |
| Colley Wobbles | Mbashe River (E. Cape) | Eskom | 42 |
| Vanderkloof | Orange River (N. Cape) | DWS/Eskom | 240 |
| Gariep | Orange River (N. Cape) | DWS/Eskom | 360 |
| Steenbras PSS | Cape Town (W. Cape) | City of Cape Town | 180 |
| Drakensberg PSS | Bergville (KZulu-Natal) | DWS/Eskom | 1000 |
| Palmiet PSS | Grabow (W. Cape) | DWS/Eskom | 400 |
| Ingula PSS | Van Reenen (KZulu-Natal) | DWS/Escom | 1332 |

### 2.6.2 Hydropower classification by size of system

Hydropower is more commonly categorised according to its size or capacity. The various sizes are listed in Table 2.7 and described in the following sections.

**Table 2.7: Hydropower classification per size (Barta and Grøn, 2002)**

| Category | Power Output |
|---|---|
| Pico | Up to 20 kW |
| Micro | 20 kW to 100 kW |
| Mini | 100 kW to 1 MW |
| Small | 1 MW to 10 MW |
| Macro (large) | > 10 MW |

- **Large hydropower**

Large hydropower (LHP) is generally classified as plants that produce more than 10 MW of electricity (Breeze, 2019). Large hydropower (Figure 2.24) is characterized by big dams that involve major civil work initially with potentially high environmental impacts. They are typically connected to a national electricity grid. These major installations are usually only undertaken by governments and big businesses to absorb the big upfront investment and it can take years to implement (Ansar et al., 2014). Large hydropower schemes, however, form the backbone of many countries' electricity supply. Pumped hydropower is a large hydropower type with the additional benefit that it is flexible and has a fast response to adapt to load changes (Rehman et al., 2015).

**Figure 2.24: Chief Joseph Dam hydropower scheme in Washington, USA is an example of large hydropower (From NWS, 2016)**

- **Small hydropower (SHP)**

Small hydropower (SHP) is generally accepted as hydropower plants with a capacity of up to 10 MW. Small hydropower is grouped in different sizes according to the capacity of projected output power. The International Energy Association categorizes them as mini-, micro-and pico-hydropower (IEA, 2018). The output power capacity of each plant ranged from 100 kW to 1 MW, 5 kW to 100 kW, and 0 kW to 5 kW, respectively.

Family hydropower falls under pico-hydropower but is classified in certain countries as hydropower schemes producing power under 1 kW. Countries differ on the exact size of the respective classification of sub sizes of SHP. Micro hydropower, for example, is classified as < 100 kW in China, 5 - 500 kW in Austria, 1 – 200 kW in Indonesia, and < 150kW in Pakistan (World Bank, 2020). Small hydropower is quicker and more cost-effective to implement than LHP. This is one of the distinct features of SHP that enables it to be installed in remote areas and off-grid areas. These features have caused SHP to be implemented at a fast pace in China, India, and Brazil amongst others, in the last decade. However, SHP has not been fully utilized in the rest of the world. The reason for the underutilization of SHP can be ascribed to the fact that LHP was favoured historically by governments for the low per-unit cost and the limited knowledge of SHP (IRENA, 2018). In research by Couto and Olden (2018), they claim that the environmental impacts of SHP are substantial, but it is undermined by legislation. They strongly recommend that an environmental impact assessment (EIA) or at least a basic assessment (BA) should be done before the deployment of each hydropower scheme.

- **Ultra-low head hydropower**

Ultra-low head hydropower (ULH) has ahead of between 0 and 3m. It can also be seen as pico- hydropower under 5 kW (IEA 2018). In low head applications of less than 1m, the turbines make use of the flow of water or the kinetic energy of the water, as opposed to the potential energy of water in higher head applications. In a study on ultra-low-head hydroelectric technology, Zhou and Deng (2017) found that the typical turbine selection chart for hydropower is not comprehensive when it comes to ultra-low head applications. Further modifications are needed on existing turbines to improve efficiency and cost in ultra-low head applications. Hydrostatic pressure wheels (HPW) and hydrostatic pressure machines (HPM) are the latest upgrade to the waterwheel to make it more efficient. Hydrostatic pressure machines generate a head and utilise the potential energy as well.

## 2.7 Hydropower turbine types

Hydropower turbines come in various shapes and sizes and the various types are categorised for the conditions or purpose that they are best suited for. Prior researches have produced multiple selection charts for different turbines and the conditions or hydropower systems that they are best suited for. The following sections discuss the main groups of turbines.

### 2.7.1 Impulse and reaction turbines

Turbines are generally classified as the impulse or reaction type, as depicted in Figure 2.25. The main difference between the two turbines is that in the impulse turbine, all the water is jetted through a nozzle onto the cups of the runner. The kinetic energy causes the wheel to turn. In the reaction turbine, the water is guided under pressure over the blades by the frame of the unit. The pressure and kinetic energy of the water turns the blades (Paish, 2002).

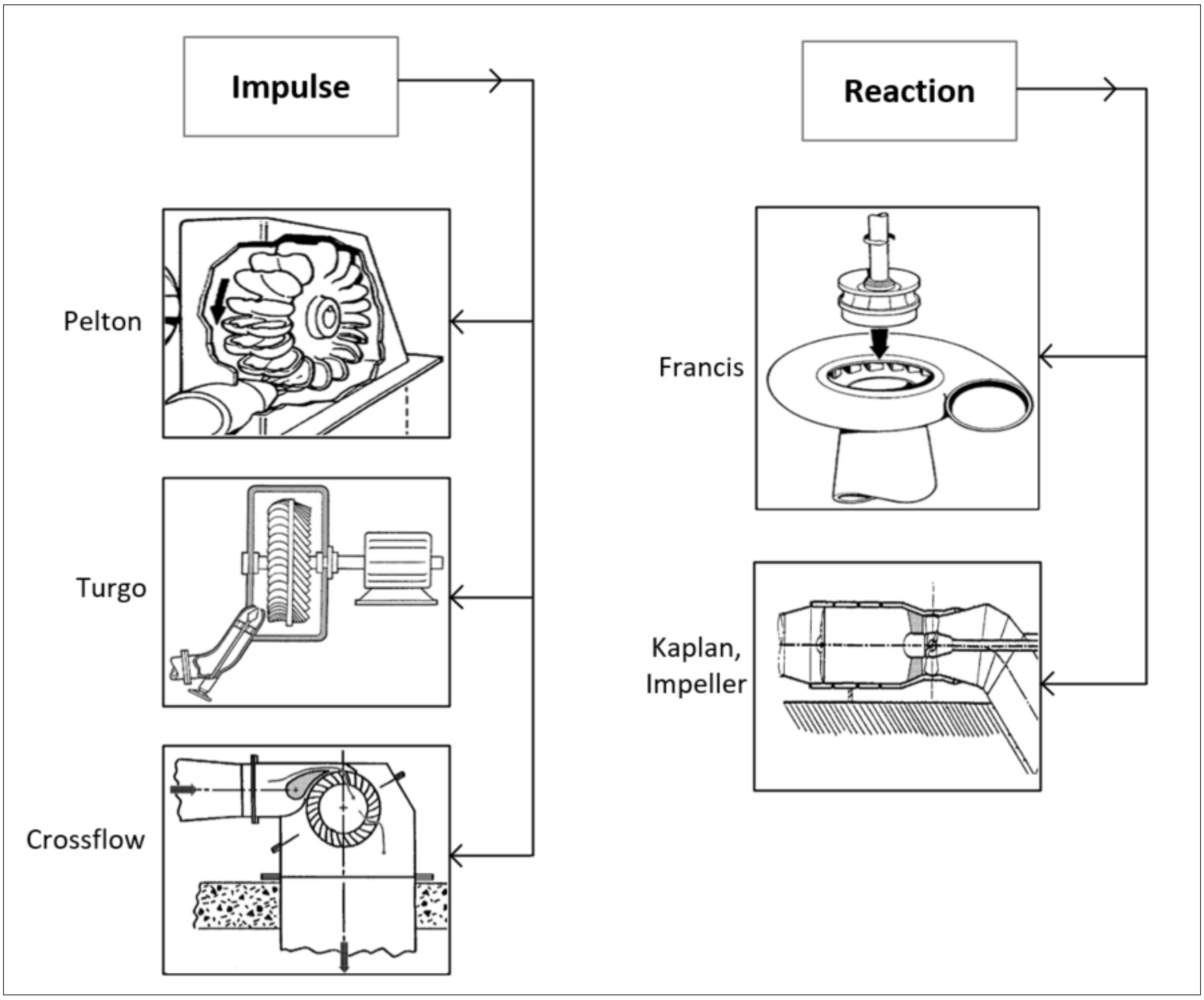


**Figure 2.25: Diagram of the impulse and reaction type turbines (Adapted From Paish, 2002)**

### 2.7.2 Other turbines

Table 2.8 shows an extended list of the 15 different turbine types with their respective head and flow ranges (Basar *et al.*, 2014). Waterwheels and the Archimedes screw do not fit into the impulse and reaction categories but they are groups on their own.

**Table 2.8: Comparison of fifteen types of pico- hydro turbines (Basar et al., 2014)**

| Category | Turbine | Head (m) | | Flow (L/s) | |
|---|---|---|---|---|---|
| | | Max | Min | Max | Min |
| Impulse turbine | Peltric set | 50 | 20 | 20 | 10 |
| | Pico power pack | 100 | 25 | 15 | 3 |
| | Low-cost DC | 60 | 20 | 10 | 5 |
| | MDFH | 30 | 20 | 2 | 1 |
| | Stream engine | 100 | 2 | 1,5 | 0,04 |
| | Turgo | 20 | 5 | 8 | 2 |
| | Cross-flow | 20 | 5 | 50 | 5 |

| | | | | | |
|---|---|---|---|---|---|
| Reaction turbine | Power pal | 5 | 1 | 130 | 35 |
| | Open flume | 6 | 3 | 100 | 10 |
| | Split reaction | 10 | 2 | 16 | 8 |
| Wheel | Overshot | 10 | 2,5 | 4 | 2 |
| | Undershot | 2,5 | 0,5 | 10 | 7 |
| | Pump as turbine | 20 | 5 | 50 | 5 |
| | Submersible Pico hydro | In-stream | | 4 | |
| | Archimedes screw | 5 | 2 | 8 | 0,5 |

### 2.7.3 Archimedes screw turbine

Figure 2.26 shows an illustration of the operation of the Archimedes screw turbine. The screw of the turbine is installed at an incline. Water running down the trough, exerts a force on the blades, causing the screw to turn. The slow turning screw is linked through a reduction gearbox to a generator. This mechanical power is used to generate electricity.

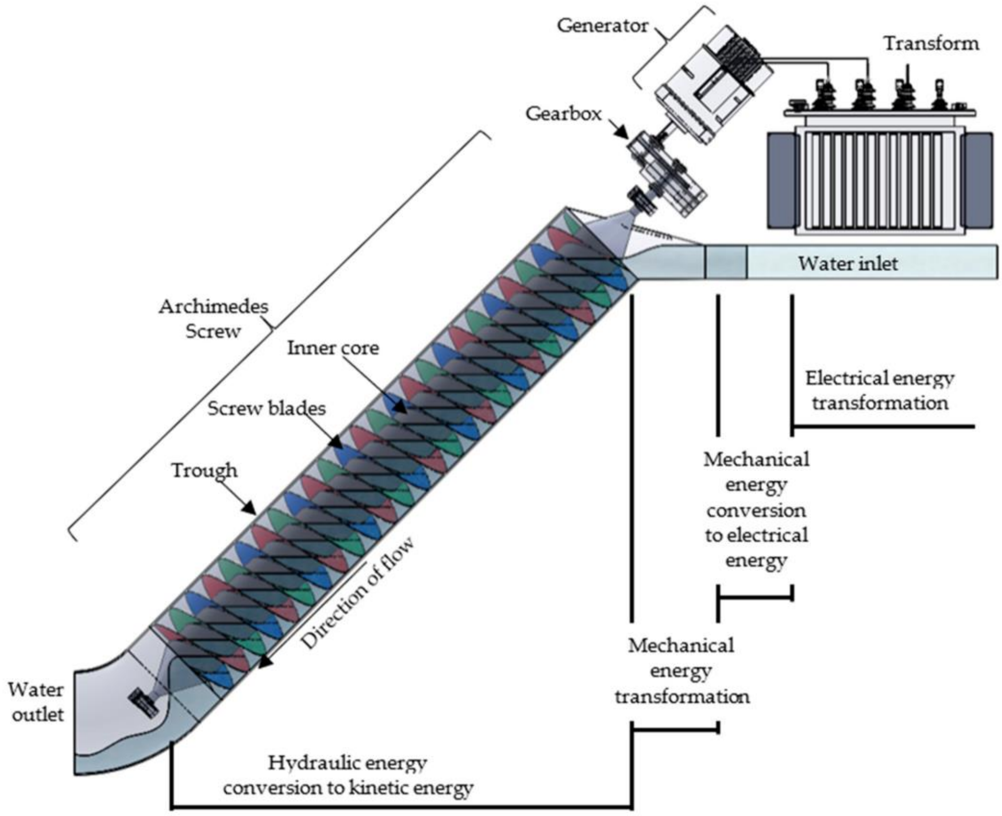


**Figure 2.26: Illustration of the Archimedean screw turbine (From Edirisinghe et al., 2021)**

### 2.7.4 Waterwheel

Waterwheels are termed according to the height and application of the water in which they are installed. The undershot waterwheel is used in water, with an extremely low head and only the bottom blades of the wheel submerged in the water. The middle shot or breastshot waterwheel is similar to the undershot. However, the water enters the wheel blades at a higher point about halfway up on the upstream side (Figure 2.27). At an overshot waterwheel, the steam of water is applied to the top of the wheel and runs over the wheel, causing it to turn in a clockwise direction.

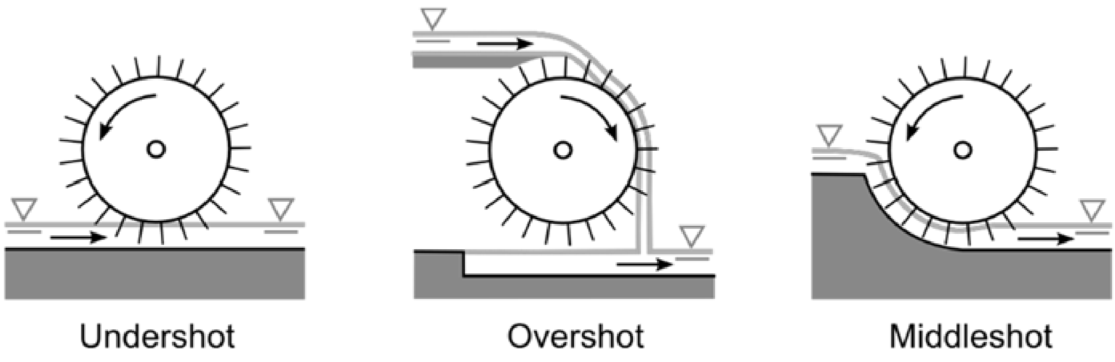


**Figure 2.27: Types of waterwheels (From Fajar et al., 2018).**

### 2.7.5 Modern waterwheels

The conventional waterwheel in the previous section has undergone a revamp. A new design has emerged in the form of a hydrostatic pressure wheel. This wheel does not only make use of the kinetic energy of the water, but it uses the force of the potential difference of the upstream and downstream water to push the wheel blades. The upstream and downstream difference in height is established by the wheel that seals the water off in a water passage. This backs up the water on the upstream side to a level that is governed by the hub height and some leakage. Figure 2.28 shows a three-dimensional image of the hydrostatic pressure wheel.

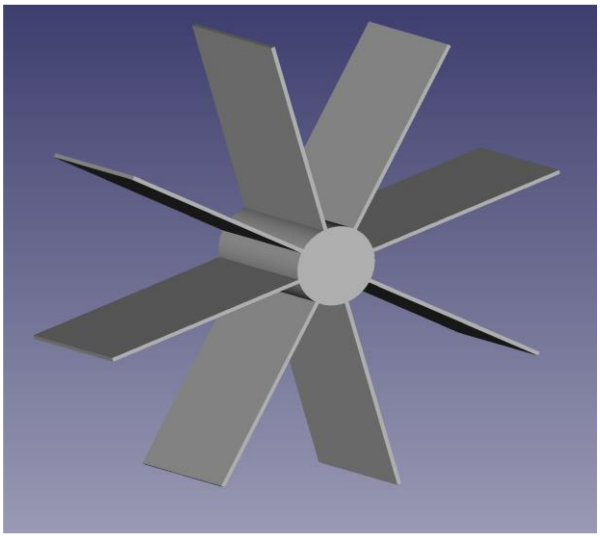

**Figure 2.28: 3D view of a hydrostatic pressure wheel (From Cassan et al., 2021)**

### 2.7.6 Hydrokinetic turbines

Hydrokinetic (HK) turbines are used to convert hydrokinetic energy in streams, tidal currents, and canals. It is considered ideal for use in man-made canals. A comprehensive list of the various types of hydropower turbines and their uses is depicted in Figure 2.29 (Khan et al., 2009). The main classification is whether the axis is horizontal or vertical. Hydrokinetic turbines require limited alteration to the water pathways, thereby increasing the feasibility of the unit. In a study conducted by Niebuhr (2019), a hydrokinetic turbine was installed in an existing irrigation canal in the Northern Cape, South Africa. The results have shown that the small-scale HK systems can be integrated into existing water infrastructure in South Africa and optimized to prove as a practical renewable energy generation option.

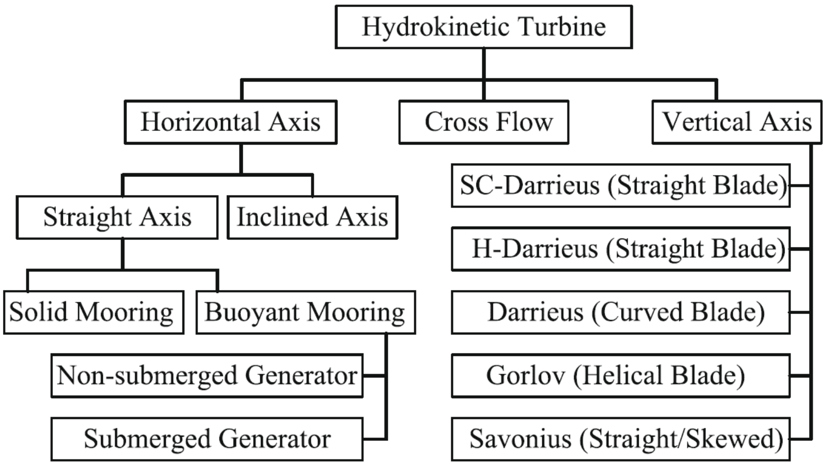


**Figure 2.29: Hydrokinetic types (From Khan et al., 2009)**

## 2.8 Ultra-low-head technologies

Ultra-low-head hydropower systems differ considerably from the rest of the hydropower schemes. The European Small Hydropower Association report (ESHA, 2004) shows the performance characteristics of the various turbines with different variations of its runner designs for different applications. The results show that there are not many designs that are suitable for ultra-low head run-of-river applications (ESHA, 2004). In a study by Jawahar and Michael (2017), it was found that large turbines are often used to generate power for small loads, which is not ideal. This means that further research needs to be done to optimize turbine suitability for ultra-low head hydropower applications. An example of a turbine design, specifically for ULH deployment is the one that is patented by a company called JAG Seabell Co., Ltd in the UNIDO report (UNIDO, 2015). This unit comprises two vertical mounted cross-flow turbines. Hydrokinetic turbines are another type that is well suited for ultra-low head hydropower schemes, which comes in axial and vertical variations (Eme et al., 2019). In a study on the optimization of the hydrokinetic turbine, a specific case was researched on the canals in South Africa. It is shown in a practical example that this type of turbine is capable of producing over 1000 W in a canal, with an average flow rate of $7m^3/s$ (Niebuhr et al., 2019). However, these hydrokinetic turbines require water of more than 1.5m deep. This is not always possible in canals and at the lower course of rivers. However, hydrostatic pressure converters that are a redesign of the waterwheel are showing great promise in terms of power and efficiency (Senior et al., 2008).

Sari *et al.*, (2018) found that in the last decade, turbine technologies have evolved such that it warrants a relook at the conventional way of operating small hydropower. Recent innovations in conduit hydropower technologies are depicted in Figure 2.30.

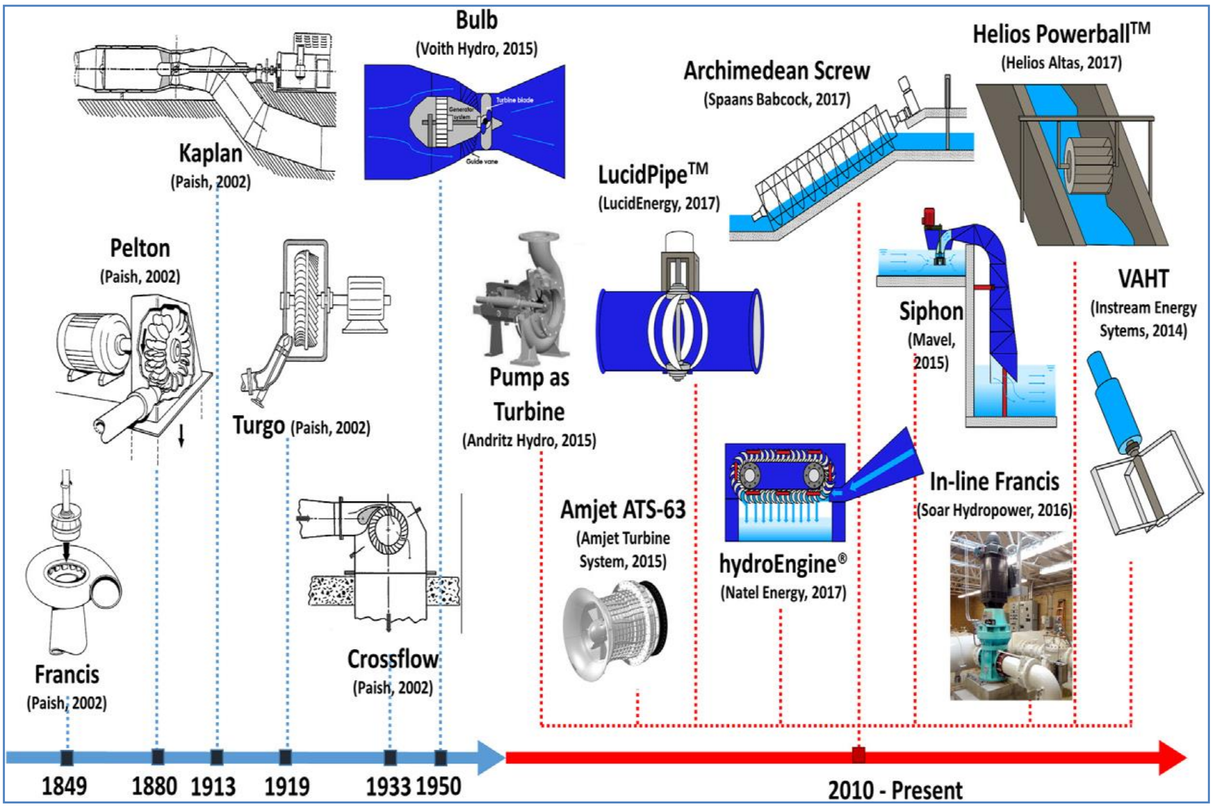


**Figure 2.30: In-conduit hydropower technology evolution (From Sari et al., 2018a)**

In a study by Zhou and Deng, (2017), they have found that the abundant ultra-low head (ULH) available sources across the world have a high potential for generating hydropower sustainably. The potential hydropower that can be generated from various sources is summarised in Table 2.9. The study recommends further research in high-efficient turbines, to reduce the cost of components, improve feasibility, and improve material properties of components to prolong its service lives.

**Table 2.9: Summary of water sources with ULH hydropower potential (From Zhou & Deng, 2017)**

| AREA | DESCRIPTION |
|---|---|
| Rivers and Streams | 119.9 TWh/yr technically recoverable from HK in the USA<br>1 MW of electrical power can be generated in the New York East river with minimal environmental impact.<br>Multiple 200 W low-head, pico-hydro units were installed in Vietnam using locally sourced wood and bamboo |
| Canals | Britain to exploit waterways and build 25 small-scale hydroelectric schemes to produce 40 MW |
| Piping Systems | Surplus pressures such as pressure relief valves can be used to generate electricity |

| | |
|---|---|
| Wastewater | Wastewater plants discharge at a flow of 0.05 to 15.99 $m^3$/s in a Massachusetts study, with 1.2 to 5.18 m head.<br>The hydropower generators at the Deer Island plant produce over 6m kWh/yr.<br>The Millbury wastewater plant in Massachusetts produces about 20 kW of power from an available head of 1.7 m and an average flow volume of 1.4 $m^3$/s. |
| Other | Tailrace from power stations<br>Tidal energy<br>Desalination plants |

## 2.9 Hydropower at the discharge of industrial plants

Industrial outflows have become common and continuous in modern societies. This occurrence, where recycled water is discharged happens in multiple industries. Water treatment plants and the supply networks of modern cities possess a high potential for hydropower (Van Vuuren et al., 2014). Figure 2.31 shows an example of the discharge outflow of the Rooiwal wastewater treatment plant in South Africa.

**Figure 2.31 Rooiwal Wastewater Treatment Works outlet in South Africa (From Loots et al., 2015)**

Stormwater run-off, wastewater treatment works (WWTW), and industrial manufacturing and cooling plants all discharge into a waterway of sorts (Hijdra et al., 2014). Many of these artificial waterways have a flow that is controllable and thus potentially good characteristics for ULH hydropower deployment (Zhou & Deng, 2017).

Figure 2.32 shows a diagram of a typical wastewater treatment scheme and the potential position for a WWTP hydropower site.

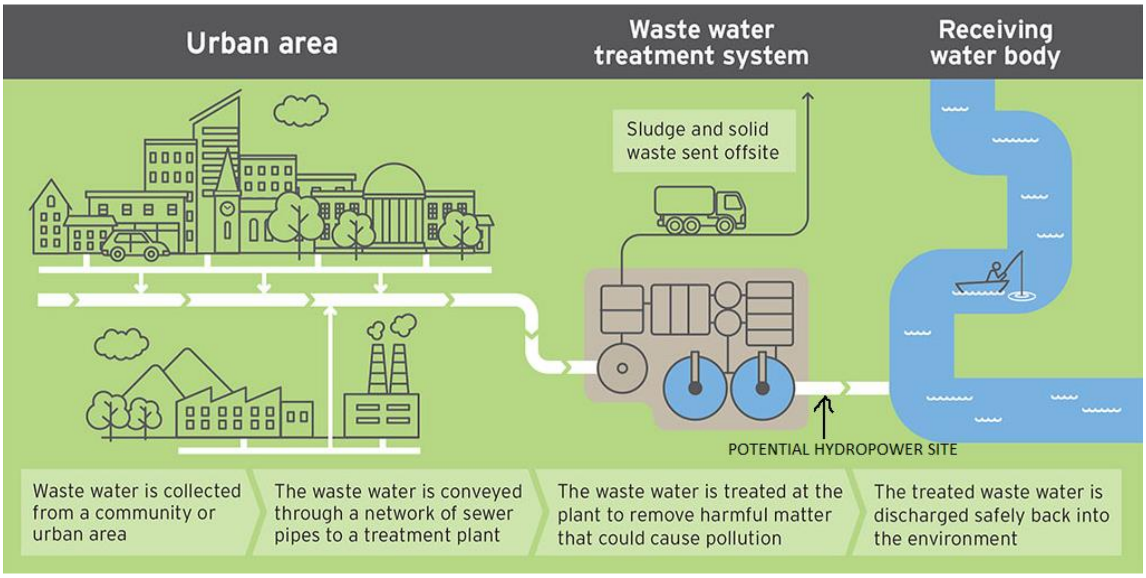


**Figure 2.32: Typical wastewater treatment scheme with potential site indicated (Adapted from EPA, 2020).**

Mümtaz et al., (2017) has developed a fuzzy logic tool to evaluate low-head hydropower technologies at the outlet of a wastewater treatment plant. The real-time application of an AST at the Tatlar plant in Turkey proved successful Figure 2.33.

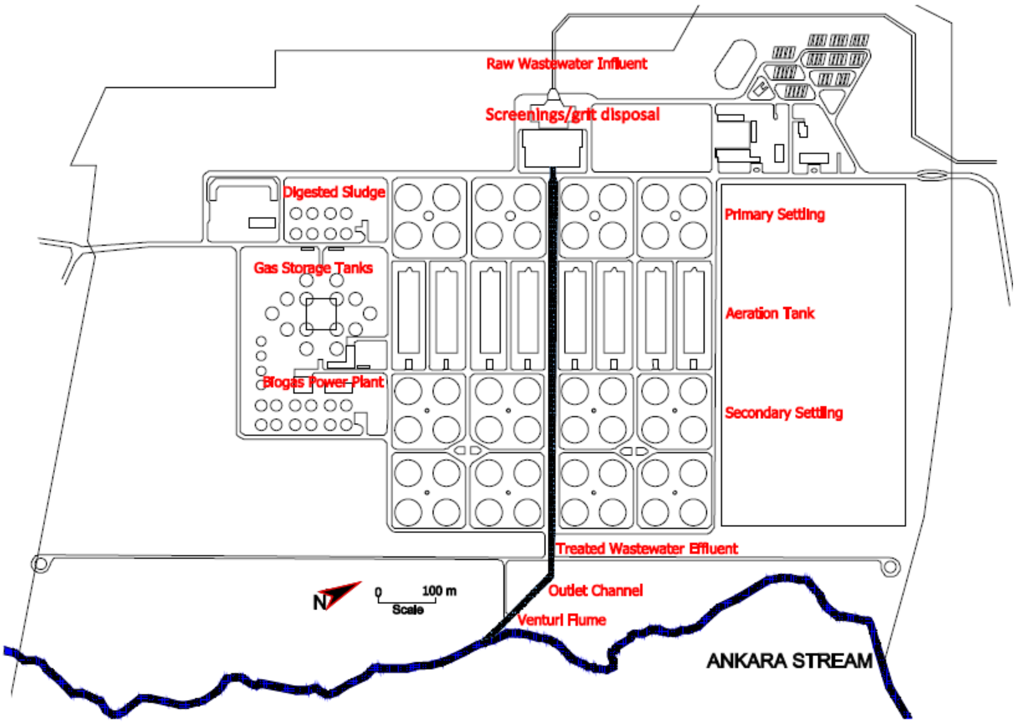


**Figure 2.33: Wastewater treatment plant layout in Ankara where AST was installed (From Mümtaz et al., 2017)**

Power et al. (2014) has developed a method to evaluate energy recovery at a wastewater treatment plant (Figure 2.34). A list of the energy recovery potential and economic viability of all the plants in Ireland and UK was developed using this method. Bousquet et al (2017) developed a similar tool as Power et al (2014) and created a list of the hydropower potential for plants in Switzerland.

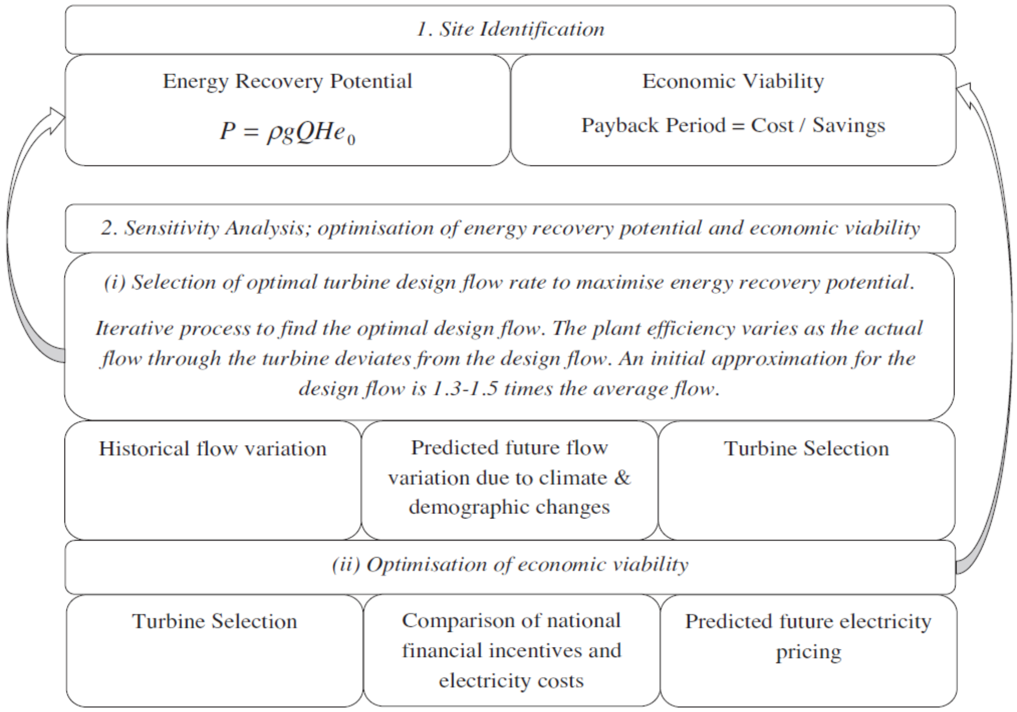


**Figure 2.34: Procedure to evaluate energy recovery at a wastewater treatment plant (From Power et al, 2014)**

Hatata et al.,(2019) investigated the small hydropower potential on eight different sites in Egypt. The MATLAB results show the most efficient schemes in Table 2.10 and that the project is feasible.

**Table 2.10: Annual energy output of eight small hydropower sites in Egypt (Hatata et al., 2019)**

| No. | Locations | Annual turbine electrical energy generation(kWh) | |
|---|---|---|---|
| | | Kaplan | Cross-flow |
| 1 | DA | 3804785 | 3300537 |
| 2 | RT | 2646949 | 2418200 |
| 3 | RB | 2336340 | 2260485 |
| 4 | MA | 1755313 | 1597785 |
| 5 | RA | 1691449 | 1506927 |
| 6 | RM | 1634950 | 1540626 |
| 7 | ZE | 1146397 | 1046087 |
| 8 | RN | 633389 | 669582 |

## 2.10 Combined heat and power at wastewater treatment plants

Combined heat and power (CHP) is a technology that is preferred over hydropower at treatment plants under certain circumstances (Llácer-Iglesias et al., 2021b). CHP is not dealt with in this paper but it is worth mentioning for the fact that the two technologies could be seen as competing energy generation options at water treatment plants. Hydropower at wastewater treatment plants is however only viable if there is a minimum usable head. Table 2.11 lists a few hydropower sites in South Africa that uses combined heat and power systems. The CHP in the Northern and Driefontein wastewater treatment works generate biogas by using cogeneration. The biogas is cleaned on-site and used to run CHP engines to generate electricity.

**Table 2.11: Proposed installation of combined heat and power equipment at plants in South Africa. (Franks et al., 2013)**

| Waste Water Treatment Plant | Plant Power Requirements | Planned CHP (Units) | Planned CHP (total) |
|---|---|---|---|
| Northern | 6.75 MW | 4 x 380 kW<br>6 x 880 kW | 6.80 MW |
| Olifantsvlei | 3.75 MW | 3 x 380 kW<br>3 x 880 kW | 3.78 MW |
| Bushkoppie | 3.75 MW | 3 x 380 kW<br>3 x 880 kW | 3.78 MW |
| Goudkoppies | 2.03 MW | 1 x 380 kW<br>3 x 560 kW | 2.06 MW |
| Driefontein | 0.90 MW | 1 x 380 kW<br>1 x 560 kW | 0.94 MW |

In one of the latest surveys of real cases of hydropower schemes that are running at wastewater treatment plants, Llácer-Iglesias et al. (2021) found 49 small, mini and micro hydropower plants across various countries and recorded their data in a table form. Table 2.12

lists only the micro hydropower sites, that use treated effluent to generate energy. The output capacity factor is varying to such a degree that it cannot be used to draw any reliable conclusions.

**Table 2.12: Micro hydropower sites at wastewater treatment plants (Llácer-Iglesias et al., 2021)**

| Name | Country | Year | Head (m) | Available Flow (m3/s) | Installed Capacity (kW) | Output capacity factor (%) |
|---|---|---|---|---|---|---|
| La Douve 2 | Switzerland | 2001 | 79 | 0,108 | 75 | 90 |
| Iseltwald | Switzerland | 2014 | 120 | 0,0095 | 6,6 | 59 |
| Engelberg | Switzerland | 2010 | 50 | 0,139 | 55 | 81 |
| La Saunerie | Switzerland | 2014 | 4,5 | 0,127 | 15 | 268 |
| Schwyz | Switzerland | 2011 | 7 | 0,242 | 15,5 | 93 |
| Emmerich (TWE) | Germany | 2000 | 3,8 | 0,185 | 13 | 189 |
| Böhmenkirch | Germany | 2001 | 100 | 0,017 | 40 | 240 |
| Asan | South Korea | 2000 | 6,9 | 0,521 | 36 | 102 |
| Seobu | South Korea | 2010 | 2 | 6,019 | 74 | 63 |
| Tan Chun | South Korea | < 2017 | 2 | 10,417 | 60 | 29 |
| Joong Rang | South Korea | 2015 | 1,5 | 18,4 | 60 | 22 |
| Seo Nam | South Korea | 2015 | 1,5 | 18,86 | 100 | 36 |

Table 2.13 shows 17 of the wastewater treatment plants that Bousquet et al., (2017) found where hydropower technology is used to generate electrical energy. With the exception of a few cases, the ratio of installed capacity compared to the available flow and head at a site are realistic figures.

**Table 2.13: Actual cases of hydropower schemes at wastewater treatment plants (Bousquet et al., 2017)**

| Name | Country | Equipment | Head | Design Flow (m³/s) | Installed Capacity (kW) | Output capacity factor (%) |
|---|---|---|---|---|---|---|
| Aire, Geneva | Switzerland | Kaplan | 5 | 3,2 | 200 | 127 |
| As Samra | Jordan | Pelton | 104 | 3,2 | 1600 | 49 |
| As Samra | Jordan | Francis | 41 | 3,2 | 1680 | 131 |
| Deer Island, Boston | USA | Kaplan | 8,8 | 26,2 | 2000 | 88 |
| Elsholt | England | AST | | 2,6 | 180 | |
| Emmerich | Germany | AST | 3,8 | 0,4 | 13 | 87 |
| Engelberg | Switzerland | Pelton | 54,4 | 0,16 | 50 | 59 |
| Grachen | Switzerland | Pelton | 365 | 0,09 | 262 | 81 |
| Hsinchu | Taiwan | | | | 11 | |
| La Asse, Nyon | Switzerland | Pump | 94,25 | 0,293 | 220 | 81 |
| La Douve I, Leysin | Switzerland | Pelton | 545 | 0,08 | 430 | 101 |
| La Douve II, Leysin | Switzerland | Pelton | 83 | 0,108 | 75 | 85 |
| Morgental, St Gallen | Switzerland | Pelton | 190 | 0,84 | 1350 | 86 |
| North Head, Sydney | Australia | Kaplan | 60 | 3,5 | 4500 | 218 |
| Point Loma, San Diego | USA | Francis | 27 | 7,6 | 1350 | 67 |
| Profay, Le Cheble | Switzerland | Pelton | 449 | 0,1 | 350 | 79 |
| Taichung | Taiwan | | | | 68 | |

## 2.11 Summary

This chapter presented an overview on renewable energy and the energy mix in the South African context. It further gives the background to hydropower and its overall standing in the renewable energy basket. A summary of the different types of hydropower schemes are discussed. These schemes are grouped according to their types and sizes, with emphasis on small and low head hydropower systems. The chapter also looked at hydropower turbine types and different options for the outflow of water treatment plants are explored. The next chapter focuses on site selection and evaluation of its potential hydropower. Thereafter, the considered turbine for the selected site is modelled and the output energy is determined.

# CHAPTER THREE

# SITE SELECTION AND TURBINE OPTIONS AND DESIGN



## 3.1 Introduction

In this chapter, a wastewater plant is chosen to evaluate the hydropower potential. The specific site conditions and the turbine options are also explored. The most suitable turbine in terms of site and water flow conditions, as well as power generation capability, is selected. The parameters for the selected turbine type are modelled based on the real site specifications and wastewater treatment works' discharge outflow.

## 3.2 Site selection and background

The Zandvliet wastewater treatment works (ZWWTW) in Cape Town, South Africa, was selected to investigate the potential hydropower that can be generated at this site. The plant has no known special or superior features over other plants, but it does discharge into a river via a 200 m canal. Like most major cities and developing urban areas, this plant is a necessity for the healthy existence of dense residential areas (Angelakis et al., 2018). The plant was initially built in 1999 and serves the surrounding communities of about 15km in radius. The plant can treat about 72 million litres of effluent per day and is in the process of being expanded (IOL, 2019). Moreover, the plant is in the process of being upgraded to a treatment capacity of 90 million litres per day (Steffanutti Stocks, 2020).

The ZWWTW pumps recycled water into a canal that transports the water over about 200 m to discharge it into the Kuilsriver where it travels for about seven kilometers to the sea.

## 3.3 Hydropower potential factors at the plant outlet

The ZWWTW is one of hundreds of wastewater treatment plants across the country and the world. The plant is currently treating an average of 72000 $m^3$ litres of effluent per day. According to the topographical map in Figure 3.1, the lowest point of the plant, where it discharges is about 13 m above mean sea level and the highest point at the entrance of the canal (linking the river) is about 15 m above mean sea level. This gives a conservative height difference of at least 2 m between the two sites. With the road intersecting between the points, it is estimated that a head of 1.5 m can be established on this site for a hydropower scheme.

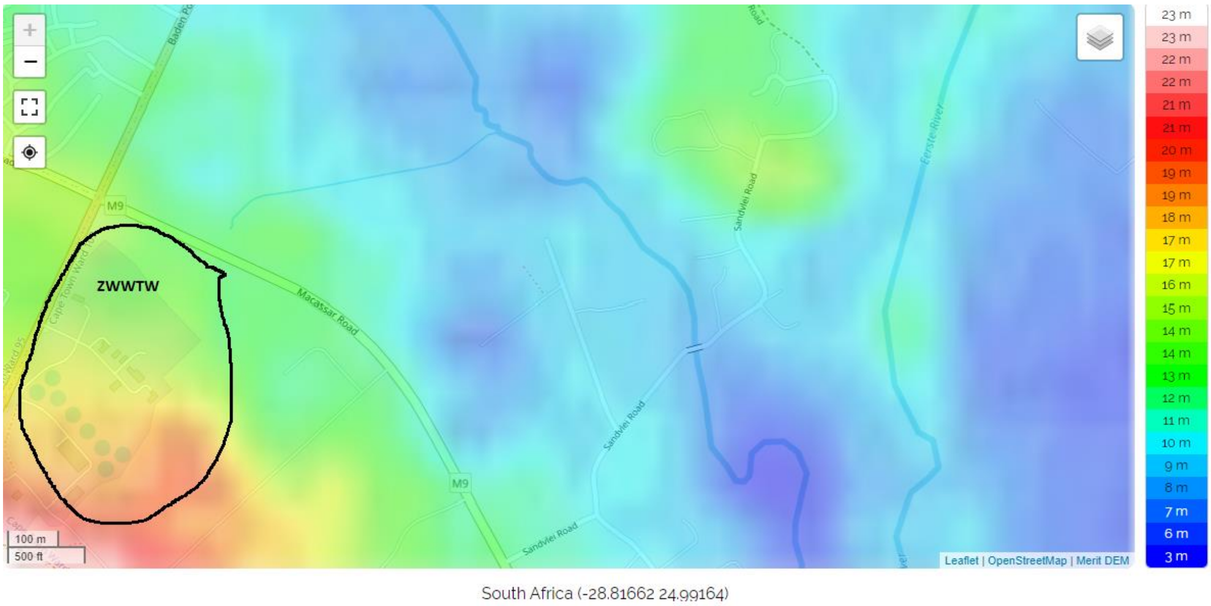


**Figure 3.1: Topographical layout of the Zandvliet wastewater treatment works area (topographicmap.com, 2021)**

### 3.3.1 Discharge characteristics

The discharge outflow data of the ZWWTW that was obtained from the city's municipal authority is shown in Figure 3.2. The recycled water discharge shows hourly and monthly varying flow patterns that will be considered when calculating potential power. The water density is assumed to be similar to regular potable water. The toxicity and chemical and pathogen concentration levels of the water fall outside the scope of this research and are not considered.

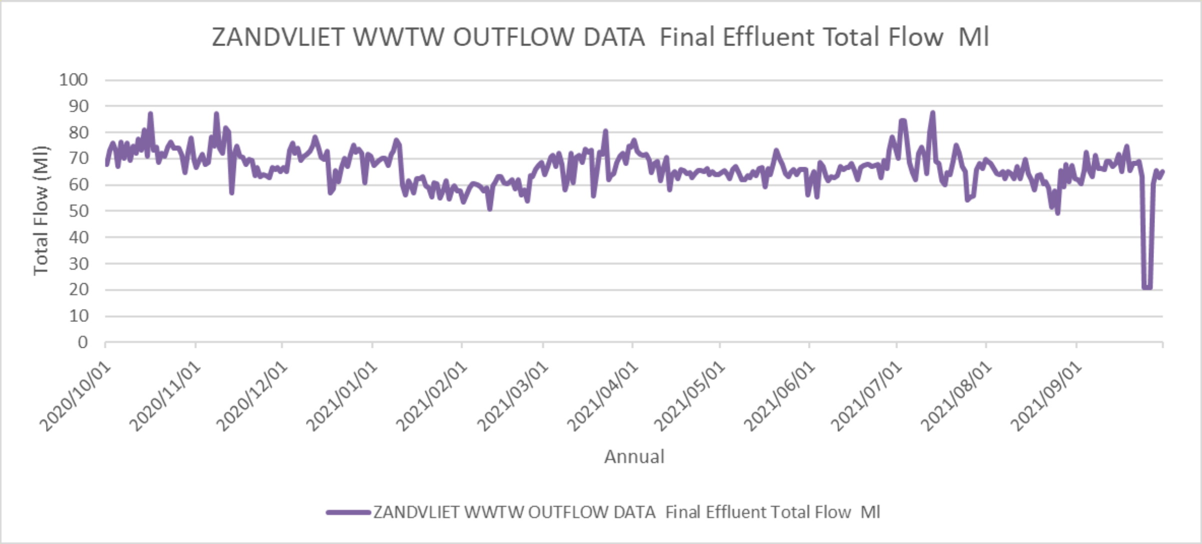


**Figure 3.2: Outflow of the Zandvliet Wastewater Treatment Works**

## 3.4 Turbine options for the ZWWTW

The ultra-low head condition of the ZWWTW limits the turbine options to a few. Boys *et al.* (2018) found that there are few viable turbine technologies available in the range of under 5 m head and under 10 $m^3/s$ flow. The Archimedes screw turbine is one of the most suitable for low head sites.

Overshot and undershot waterwheels are also usable but their maximum mechanical efficiencies are only 71%, and 30% respectively (Denny, 2004).

In a study by Sari *et al.*, (2018), different turbines are matched to the most suitable conditions. Table 3.1 shows a list of prospective turbines with the applications they are best suited for. Only AST and the Kaplan turbine are singled out for use at a wastewater treatment plant.

**Table 3.1: Low-head turbine types and their application (Sari *et al.*, 2018)**

| Type | Application |
|---|---|
| **Archimedean screw** | Canal, WWTP, |
| **Kaplan** | WWTP, |
| **Hydroengine** | Run-of-river |
| **Vertical hydrokinetic (Vaht)** | Canal |
| **Modular waterwheel** | Canal |

The Kaplan turbine however is not suitable for heads lower than 1.5 m. The Andritz turbine chart in Figure 3.3 shows that only the Kaplan turbine can work under a 7 m head, but this turbine is specified to only work from 2 m and up, making it unsuitable for this research.

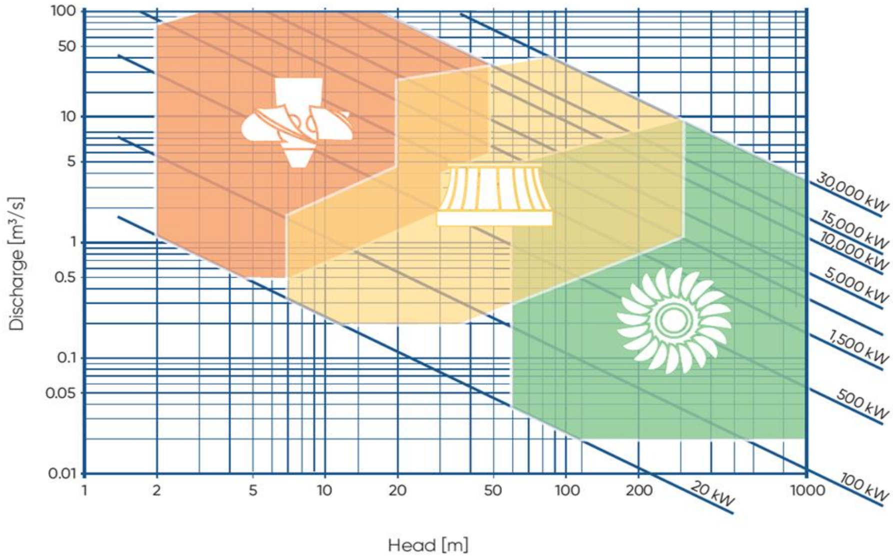


**Figure 3.3: Andritz's turbine chart according to head and flow (ANDRITZ, 2021)**

## 3.5 Archimedes screw turbine selection motivation

By inspecting the turbine head graph in Figure 3.4, the AST stands out as the only suitable turbine in terms of its head and flow characteristics.

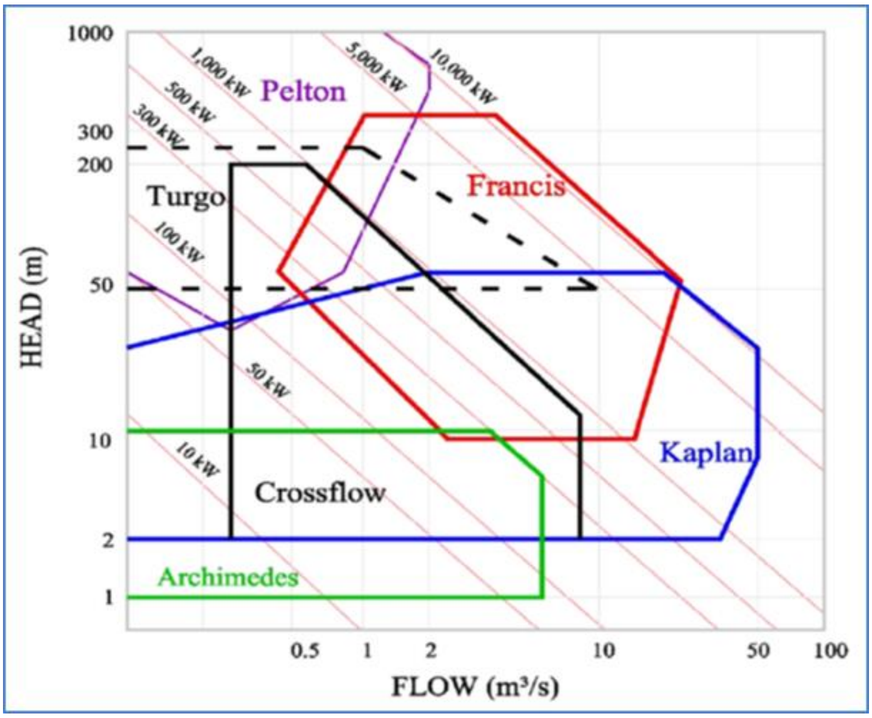


**Figure 3.4: Turbine selection chart in terms of flow and head (Fraenkel et al., 1991)**

Mümtaz et al., (2017) found in an evaluation of low-head hydropower technologies at a wastewater treatment plant in Turkey that the AST outperformed the Kaplan turbine at that specific site. Some of the advantages of AST is that it has a shorter construction duration, shorter payback period, higher energy generation performance, has aeration capacity, and it is fish friendly.

Power et al., (2014) also found the Kaplan and Francis turbines to be best suited for wastewater treatment plants. In another study, Loots *et al.*, (2015) found the Siphen turbine to be better suited at wastewater treatment plants, but the heads were much higher than that of the ZWWTW in this study.

From the information presented above, AST technology stands out as the most suitable for the outflow conditions at the ZWWTW. Hence, AST is going to be used for the design. Figure 3.5 shows a typical installation of multiple Archimedes screw turbines in a canal.

**Figure 3.5: Archimedes screw turbine (From HydroSmart, 2021)**

## 3.6 Description and features of the AST

The AST has many favourable attributes that make it the superior choice of hydropower turbine for the outlet of the ZWWTW. The following sections describe the various attributes.

- **Efficiency**

The overall efficiency of AST is typically between 60% and 80%, depending on the design, operating, and site conditions of the system (Lashofer et al., 2012). The hydraulic efficiency can even be higher if the optimum conditions are reached (Rorres, 2000).

- **Fish and debris friendly**

Although the fish-friendly feature of ASTs is not a major consideration at a wastewater outlet, the ability of this turbine to allow debris through, is a major plus point. This makes AST the better turbine option over its rivals in this instance (Boys et al., 2018).

## 3.7 Archimedes screw turbine design

In the previous sections, the AST is selected as the best-suited turbine to use at the outlet of the ZWWTW. It was further determined that a head of 1.5 m with an average flow of 66.34 million litres per day can be used to model the potential power at the site. To determine the potential hydropower of an AST for the above site conditions, this study considers commercial manufacturers' data, which covers a broad range of head and flow conditions and a few other specifications such as angle of inclination. They normally cater to a small selection of specific sizes which makes commercially produced turbines very unpredictable to use in different conditions. In the brochure of Spaans Babcock, the AST power chart in Figure 3.6 shows the power, head, and flow relation (Spaans Babcock, 2017). It can be noted that the lower head options, below 2 m, are not well defined. It would thus be advantageous to look closer at the design of the AST.

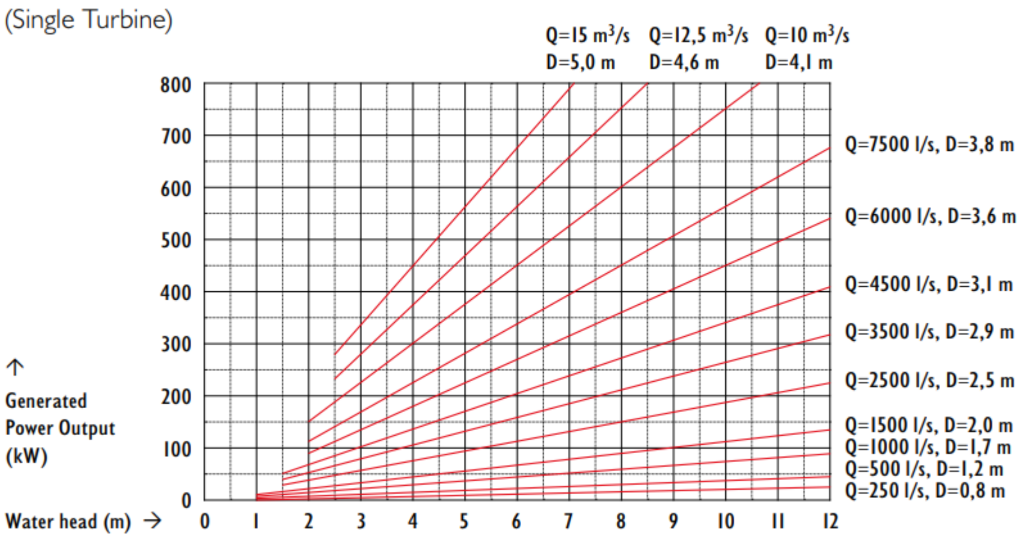


**Figure 3.6: Archimedes screw turbine power chart from Spaans Babcock, (2017)**

Presently, there is no perfect design (YoosefDoost & Lubitz, 2020) and mathematical modelling that describes the power generation using the AST method (Lyons, 2014). Furthermore, due to the complexity and varying approaches to a yet unfinalized AST design (Dellinger et al., 2016), this study investigates methods that can produce a functional design. The basic operation and factors that affect AST efficiency are discussed in the next section.

- **Operation of the Archimedes screw turbine**

An AST comprises of a screw that fits inside a trough that may be open on the top or it can be enclosed in a tube. The complete unit is installed at an incline to allow the flowing liquid to pass through it due to gravity. The screw blades vary in number as well as the angle of the blades. Water flows along the bottom of the screw blades that lie in the individual compartments called buckets. The potential energy of the water exerts pressure on the blades, causing the screw to turn and produce mechanical energy. The shaft is coupled via a gearbox to a generator that generates electrical energy. The general formula for hydropower produced by AST is given by (Rorres, 2000):

$$P = \eta . \rho . g . H . Q \qquad \text{Equation 3.1}$$

where $\eta$ is the efficiency of the complete turbine, $\rho$ is the density of the liquid in $kg/m^3$, $g$ is the gravitational acceleration, $H$ is the effective head, $Q$ is the mass flow rate in $m^3/s$, and $P$ is the mechanical power (Rorres, 2000), (Dellinger et al., 2016).
The potential hydraulic power of the site is given:

$$P = \rho . g . Q . H = \rho . g . Q . m . \Delta y \ \text{(Watt)} \qquad \text{Equation 3.2}$$

Where $m$ is the number of turns of the blades, $\Delta y$ is the height difference of the blades, $\rho$, $g$, and $Q$ is the density, gravity, and flow respectively.

The mechanical power of the screw ($P$) is the torque ($T$) times the angular velocity ($\omega$) of the screw, written as:

$$P = T . \omega \ \text{(Watt)} \qquad \text{Equation 3.3}$$

The efficiency of the screw is thus determined by the mechanical power as a percentage of the total hydraulic power (Saroinsong et al., 2015):

$$\eta = \frac{P}{Phyd} . 100\% \qquad \text{Equation 3.4}$$

The most significant parameters that affect the AST efficiency and output are the head (H), the flow rate (Q), and the rotational speed (n) of the screw. The geometrical features that define the AST are shown in Figure 3.7.

| | |
|---|---|
| Inner radius: | Ri |
| Outer radius: | Ra |
| Length: | L |
| Number of blades: | N |
| Pitch of the screw: | S |
| Screw angle: | β |
| Length of thread: | Lb |

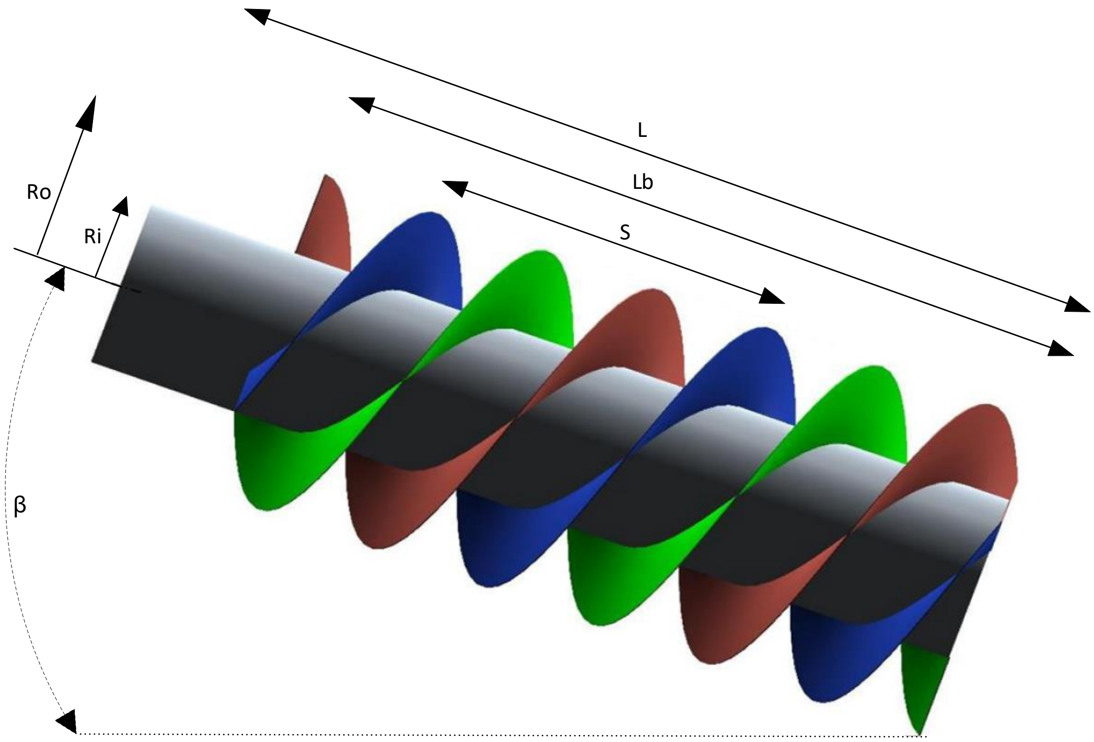


**Figure 3.7: Dimension diagram of the Archimedes screw turbine**

- **Efficiency of the Archimedes screw**

Various studies and simulation programs have been undertaken to determine the optimum specifications for the best efficiency of the AST. This research will selectively use a combination of these results from past literature to model the proposed AST for the highest efficiency. Some of the efficiencies that were found in research on various sizes of AST are shown in Table 3.2

**Table 3.2: Efficiency of AST from past literature**

| Research | AST Efficiency (%) |
|---|---|
| Rohmer *et al.*, 2016 | 72 |
| Dellinger *et al.*, 2016 | 80 |
| Abdullah *et al.*, 2020 | 81.4 |
| Saroinsong *et al.*, 2015 | 89 |
| Priyadi, 2017 | 80 |
| (Priyadi, 2017) | 81 |
| (Simmons & Lubitz, 2021) | 75 |

The efficiency of the AST is a collective result of the screw efficiency and the hydraulic losses. These losses are due to leakages and frictional losses that are influenced by the viscosity of the water.
The space between two blades that is occupied by water is called a bucket (Rorres, 2000). This bucket size is important to help determine the total flow through the screw, the turn speed, and ultimately its efficiency. Leakage in the screw gap between the blades and trough, and leakage during overfill are factors that influence efficiency. (Dellinger et al., 2016) used the formula in Equation 3.5 to describe the nominal flowrate as:

$$Q_{nom} = N.V_b \frac{n}{60} \qquad \text{Equation 3.5}$$

Where *Q* is the flow in m$^3$/s, *N* is the number of blades, *Vb* is the bucket volume in m$^3$, and *n* is the rotational speed in rpm. The rotational speed of the screw is thus:

$$Q_{nom} = 60 \frac{Q_{nom}}{NV_b} \qquad \text{Equation 3.6}$$

The total flowrate Q in the screw is the sum of the leakage and over spilling flow, plus the nominal flow through the screw, given by:

$$Q = Q_{nom} + Q_l + Q_{over} \qquad \text{Equation 3.7}$$

### 3.7.1 Design parameters

To achieve a flow rate of 500 to1000 litres per second downwards through the "buckets" of the screw and with a hydrostatic head of 1.5m, multiple geometric features should be considered to achieve maximum mechanical power. Most of the previous studies were experimenting with pre-built screws to determine their performances. In this study, a set of geometrical and flow conditions are needed to develop an Archimedes screw with matching dimensions. The following paragraphs put forward various design parameters and suggested values.

- **Number of blades (N)**

Three-blade screws are some of the most common blade types, used in prior research. Rorres (2000) tabulated the optimal ratio parameter of a screw from 1 to 25 blades. He found that a 3-blade screw has the highest volume-per-turn ratio. Lyons (2014) found that the efficiency of the screw decreases slightly when increasing the number of blades upwards from 3, and there is a bigger change when using less than 3 blades. Table 3.3 shows how Songin (2017) experimented with a 3-, 4-, and 5-blade screw of similar length and concluded that the power output and efficiency are within close range. This study will use a 3-blade screw for the reasons stated above.

**Table 3.3: Power and efficiency of three different screws (Songin, 2017)**

| Number of blades | Outside Diameter (mm) | Power (W) | Efficiency (%) |
|---|---|---|---|
| 5 | 31.69 | 30.20 +/- 1.39 | 65 +/- 3.1 |
| 4 | 31.66 | 30.42 +/- 1.37 | 65 +/- 3.0 |
| 3 | 31.62 | 30.17 +/- 1.39 | 66 +/- 3.1 |

- **Angle of inclination (β)**

Saroinsong *et al.*, (2015) experimented with different screw axis angles in a 3-blade AST. The highest efficiency (89%) was found to be at a 25° angle. Songin (2017) did an experimental analysis of the Archimedes screw turbines and found the highest output power occurred at an angle of 24.5°. There are various other researchers that used angles close to 25°. Simmons and Lubitz (2020) and Dellinger et al. (2016) used an angle of 24.5° and 24° respectively, while YoosefDoost and Lubitz (2020) recommended a slant of 22° for the AST. Lyons (2014), Rohmer *et al.* (2016), and Abdullah *et al.* (2020) found in their experiments that the inclination angle that produces maximum efficiency for the AST is 28°,30°, and 35° respectively. From the researched information presented above, this design will use an inclination angle of 25°.

- **Length of the screw (L)**

The length of the screw is restricted by the overall dimensions of the hydropower site. Taking the effective hydrostatic head as 1.5 m, and the inclination angle as 25", the screw length dimensions are shown in Figure 3.8.

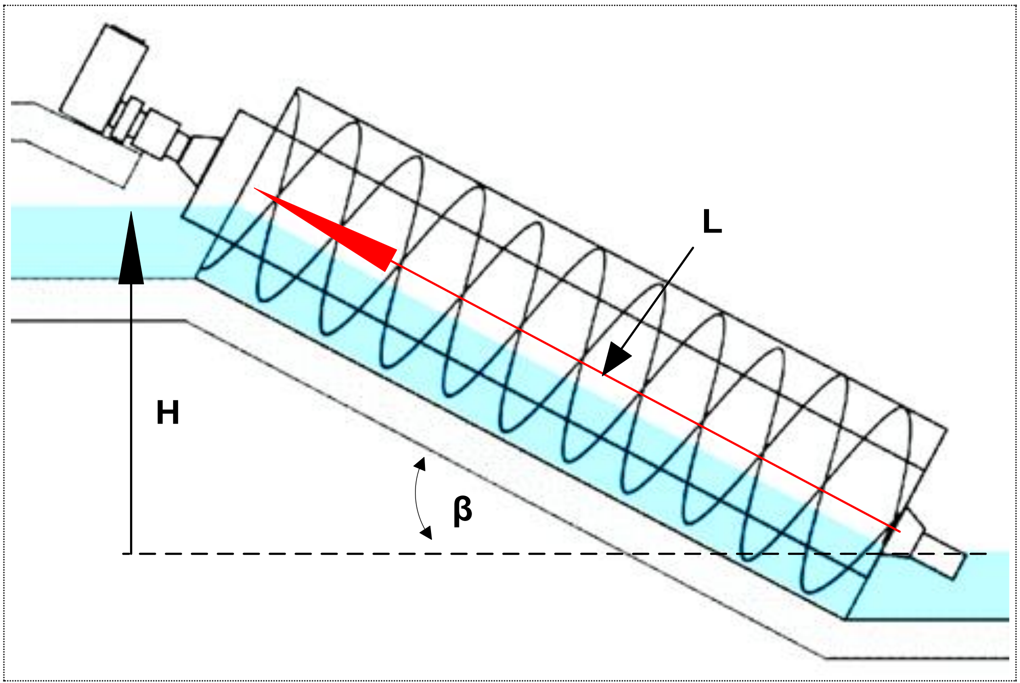


**Figure 3.8: Diagram of AST length and incline angle**

From the right-angled triangle in Figure 3.8 we can calculate the length of the screw with the formula:

$Sin\,\beta = H/L$ Equation 3.8

Hence, the length ($L$) of the screw will be 3.6 m.

- **Radius ratio (Di/Do)**

The ratio of the inner diameter over the outer diameter of the screw is another key parameter that influences the performance of the AST. Lisicki et al. (2016), found in a case study using Bayesian optimization techniques that 0.54 is the optimal value of the inner over outer diameter. To determine the optimal radius- and pitch ratio, Rorres

(2000) experimented with 25 different number of blade combinations. It was found that the optimal radius ratio is between 0.535 and 0.539. A marginally lower ratio of 0.5 is commonly used in practice (Simmons & Lubitz, 2020). Hence this study will use a Di/Do of 0.5.

From the recommendations of (YoosefDoost & Lubitz, 2020), the ratio of the length over the outer diameter of the screw (L/Do), should be less than 2 and greater than 1.25. This corresponds to the screw outer diameter (Do) ranging between 1.8 m and 2.8 m in this study.

- **Pitch ratio (S/Di)**

The pitch ratio (S/Do) is the relation between the pitch (S) (Figure 3.8), and the outside diameter (Do) of the screw. A pitch ratio of approximately one is the most commonly used value (Songin, 2017; Simmons & Lubitz, 2020). The pitch (S) will be made equal to the outer diameter (Do) when starting the design. A value of 2 m is used in this study. All the parameters found above are used in the next section to model the power and efficiency of the Archimedes screw turbine.

### 3.7.2 Summary of AST design parameter details

Table 3.4 shows a list of all the design parameters of the proposed AST for the ZWWTW. The head and mass flow rate are given while the rest are derived by considering existing research. Many assumptions had to be made which include: Bucket volume, inflow will be regulated to limit overfill, gap and flow leakages.

**Table 3.4: Dimensions of the designed AST**

| Symbol | Parameter | Derived | Value |
|---|---|---|---|
| H | Head | Given | 1.5 m |
| β | Inclination angle | Literature | 25 |
| L | Length of screw | L = sin β/H | 3.6 m |
| Do | Outside diameter | l/Do=1.25<>2 | 2 m |
| Di | Inside diameter | Di=Do*0.5 | 1 m |
| S | Pitch | S ~Do | 2 m |
| N | Number of blades | Literature | 3 |
| Q | Flow rate | $Q_{nom} = 60\frac{Q_{nom}}{NV_b}$ | tbd |
| η | Efficiency | $\eta = \frac{P}{P_{hyd}}.100\%$ | tbd |
| ρ | Density (est) | Sci law | 1000 $Kg/m^3$ |

| | | | |
|---|---|---|---|
| T | Torque of shaft | $P = T.\omega$ | tbd |
| ω | Angular velocity | $\omega = 60\frac{2\pi n}{60}$ | |
| n | RPM | Derived from *T, ω* | |

Table 3.5 lists the calculated value of the low and high efficiency mechanical power of the AST at the ZWWTW, on a monthly basis.

**Table 3.5 Monthly mechanical power at low and high efficiency**

| Month | Ml/d | l/s | Mechanical Power at Low efficiency | Mechanical Efficiency at high efficiency |
|---|---|---|---|---|
| January | 62,88 | 727,77 | 7496 | 9103 |
| February | 60,14 | 696,08 | 7170 | 8706 |
| March | 68,58 | 793,78 | 8176 | 9928 |
| April | 66,35 | 767,92 | 7910 | 9605 |
| May | 64,83 | 750,38 | 7729 | 9386 |
| June | 66,38 | 768,28 | 7914 | 9609 |
| July | 68,84 | 796,76 | 8207 | 9966 |
| August | 62,90 | 727,97 | 7498 | 9105 |
| September | 62,16 | 719,46 | 7411 | 8999 |
| October | 73,34 | 848,81 | 8743 | 10617 |
| November | 69,80 | 807,83 | 8321 | 10104 |
| December | 69,89 | 808,92 | 8332 | 10118 |
| Average | 66,34 | 767,83 | 7909,03 | 9603,82 |

## 3.8 Hydropower usage at a wastewater treatment plant

The hydropower that is generated at wastewater treatment plants is mainly used at the plant itself. The reason for this is that wastewater treatment plants are energy-intensive plants. The percentage of electricity produced by hydropower onsite is low compared to the total usage of the plant (Llácer-Iglesias et al., 2021a). There is thus no spare capacity to export power outside of the plant, but the connection to the internal grid will reduce the power that is drawn from the grid. Table 3.6 shows the self-sufficiency and hydropower share of few case studies that were obtained using various key performance indicators (KPIs). It is clear from the table that hydropower rarely caters for the full electricity demand of a wastewater treatment plant. The average contribution of hydropower in Table 3.6 is only 25.5%.

**Table 3.6: Case studies of wastewater treatment plants with hydropower generation, showing their self-sufficiency and the hydropower share of the total power consumption** (From Llácer-Iglesias et al., 2021a)

| Country | Name of WWTP | Self-sufficiency (%) | Hydropower (%) |
|---|---|---|---|
| Austria | Plobb-Seefeld | >100 | >100 |
| Austria | Ebswien | 11 | 2,6 |
| Switzerland | L'Asse | 66.1 | 33,9 |
| Switzerland | Engelberg | >100 | 65 |
| UK | Esholt | >100 | 5 |
| Spain | Sur | 91.2 | 2,1 |
| Belgium | Brussels-North | 30 | 18 |
| Jorda. | As Samra | 80 | 24 |
| USA | Deer Island | 26 | 4 |
| Canada | Clarkson | 30,8 | 1,3 |

However, hydropower is often implemented in conjunction with combined heat and power (CHP) engines that run on biogas that is generated at the same plant. Table 3.7 shows the self-sufficiency of a few plants that employ a combination of hydropower and CHP technology. The higher self-sufficiency percentage indicates that hydropower performs better when combined with other technologies at wastewater treatment plants.

**Table 3.7: The self-sufficiency percentage at plants where hydropower and CHP are combined** (Adapted from Llácer-Iglesias et al., 2021a)

| Country | Name of WWTP | Location | % Self sufficiency |
|---|---|---|---|
| Switzerland | Chaux-de- Fonds | La Chaux-de-Fonds | 65 |
| UK | Esholt | Bradford (Yorkshire) | >100 |
| Spain | Sur | Getafe (Madrid) | 91,2 |
| Australia | North Head | Sydney | 58 |
| Australia | Gippsland Water Factory | Maryvale (Gippsland, Victoria) | 40 |
| Jordan | As samra | Amman City | 80 |
| Korea | Nan Ji | Seoul | 51,6 |
| USA | Point Loma | San Diego | >100 |
| Canada | Clarkson | Mississauga | 30,8 |

### 3.9 River flow and turbine selection

In this section, the condition and hydropower potential of the Kuilsriver is investigated. The focus is at the point where the Zandvliet wastewater treatment plant is connected to the river. The suitable turbines for these conditions are evaluated in terms of power and efficiency. The selected turbine's specifications is designed to suit the site conditions and water flow.

- **Background**

The ZWWTW canal discharges recycled water into the Kuilsriver. The perennial river originates about 35 km upstream to the north, with an average flow rate of 4 $m^3/s$. The excerpt in Figure 3.9 indicates the location of the ZWWTW. The blue line is the discharge canal that links the ZWWTW to the river. From there the Kuilsriver runs about 7 km to the sea.

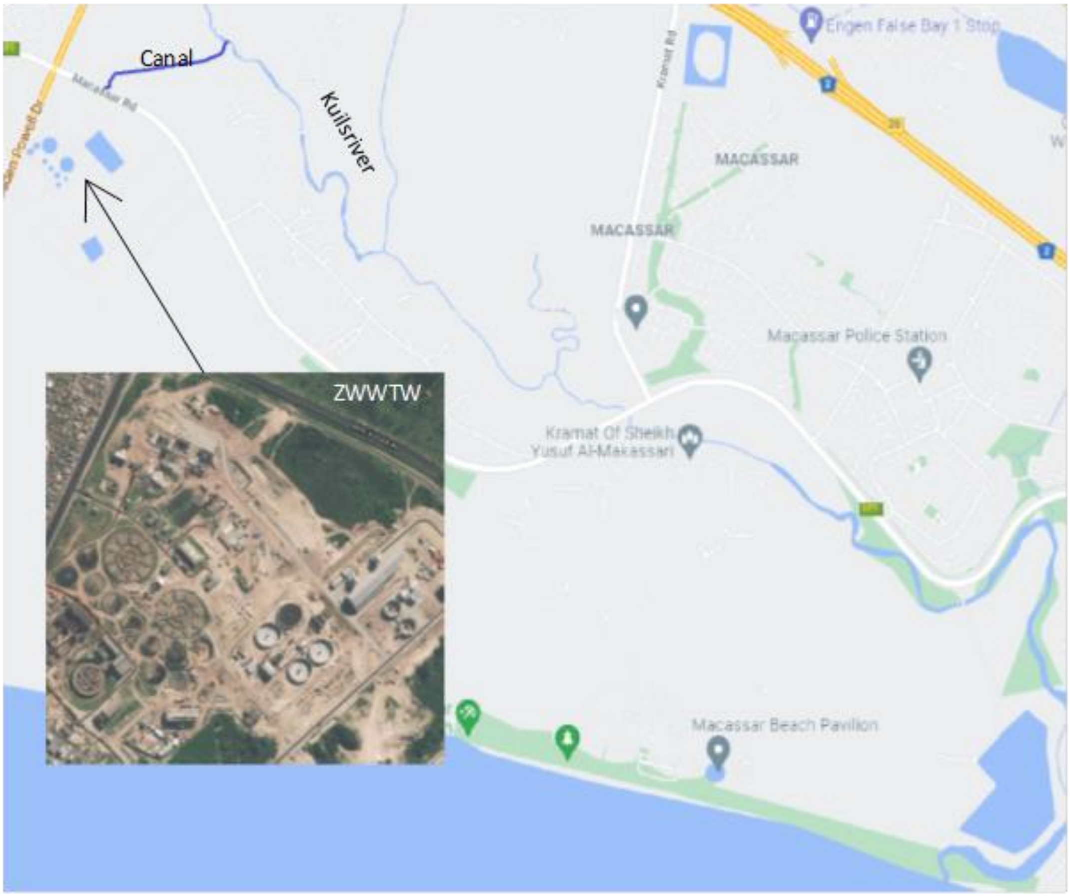


**Figure 3.9: The ZWWTW, Kuilsriver, and linking canal at location -34.049531, 18.719145 Adapted from (Google Maps, 2021), (SatellitesPro, 2021)**

Figure 3.10 shows two potential hydropower sites on the Kuilsriver. The site on the left is adjacent to the point where the ZWWTW canal joins the river. The site on the right is a typical view of the river downstream.

(a)

(b)

**Figure 3.10: Two potential sites on the Kuilsriver for Hydropower implementation: (a) the position just after the canal entry. (b) the site about 400 m downstream**

## 3.10 Calculation of river flow

The total flow of the Kuilsriver was manually recorded for four seasons (September 2020 to June 2021). Figure 3.11 shows an illustration of the basic method that was used to calculate the total flow of the river. The cross-sectional area of the river was obtained by multiplying the total width, with the average depth. The velocity was also obtained by placing a floating piece on the surface and timing it over a demarcated distance. The average flow was obtained by repeating the above step several times across the width of the river.

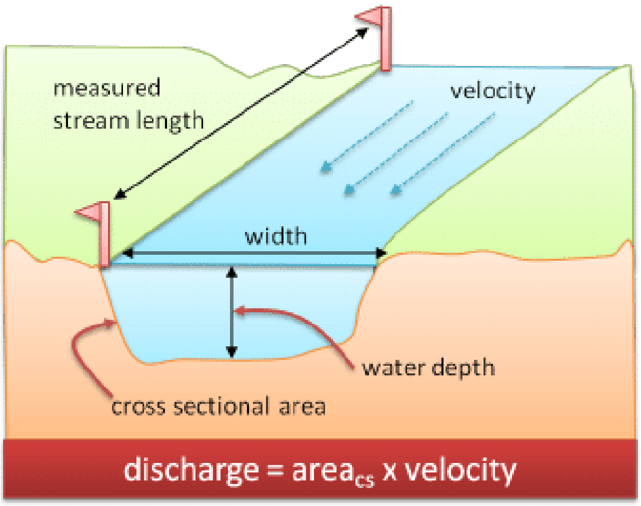


**Figure 3.11: Calculation method of river volume flow (Scheider et al., 2011)**

Table 3.8 lists the recorded values of the river total flow for four seasons. Figure 3.12 shows the converted monthly flow data of Kuilsriver at the evaluation site.

**Table 3.8: Recorded seasonal flow data of Kuilsriver**

| Month | Width | Height (ave) | Area $m^2$ | Velocity m/s | Flow $m^3/s$ |
|---|---|---|---|---|---|
| Mar | 6 | 0,25 | 1,5 | 0,9 | 1,35 |
| Jun | 6 | 0,6 | 3,6 | 1,4 | 5,04 |
| Sep | 6 | 0,45 | 2,7 | 1,2 | 3,24 |
| Dec | 6 | 0,3 | 1,8 | 1 | 1,8 |
| Average | 6 | 0,4 | 2,4 | 1,125 | 2,8575 |

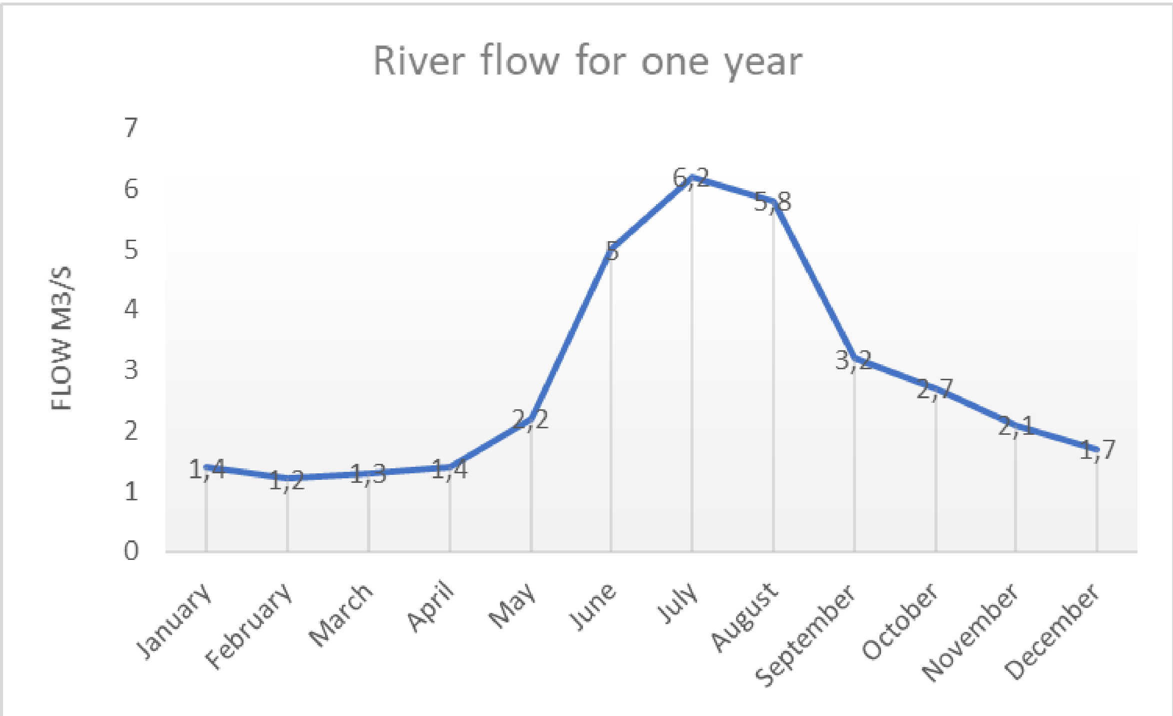


**Figure 3.12: Monthly flow rate of the Kuilsriver**

This lower coarse of the Kuilsriver has a very small, almost unnoticeable slope that is sometimes referred to as "zero head" (Masud et al., 2019). According to the topographical snippet in Figure 3.9, the river has an estimated slope of less than one meter over the 1 km section of discharge. This small head or zero-head flow limits the types of hydro turbines that can be implemented for hydropower.

### 3.11 River flow improvement

To maximise the hydropower generation from the river, the water flow through the turbine should be enhanced. One of the means to achieve increased flow is to construct a funnelling barrier across the river, hence this research will implement a weir for this purpose. Figure 3.13 demonstrates how a weir will be constructed across the widths of the river with a gap to funnel the water (Kirke, 2020).


**Figure 3.13: Diagram of weir positioning in a stream**

**(Kirke, 2020)**

#### 3.11.1 Weir design

The weir height and width concerning the total width of the river, the gap of the turbine, and the turbine type determine the new increased flow rate. The average flow of the river is 2.85 $m^3$/s, with a cross-sectional area of 2,4 $m^2$. Moreover, the river flows at a velocity of 1,25 m/s. These values are used to determine the optimum size of the weir with more in-depth analysis. Figure 3.14 shows an example of an existing weir that is in use in a canal.

**Figure 3.14: Example of a river weir (Rickard et al., 2003)**

For the present study, a simplified weir plan is developed to achieve a plausible model. The area of the river where this hydropower scheme is proposed, has varying widths from 5 m to 10 m. The width of the HPW can thus be increased as much as needed. To maximise the water kinetic and potential energy, a weir is designed to funnel the maximum water flow onto the wheel. Figure 3.15 shows a cross-sectional illustration of a weir constructed in the river. The turbine gap will be constructed in the lowest part of the river bed to ensure maximum depth. After some iteration, the average weir height is chosen as 300 mm and the gap width is 2 m. We will assume the river bed to be level for this exercise which results in a gap area of 2 m x 0.3 = 0,6 $m^2$.

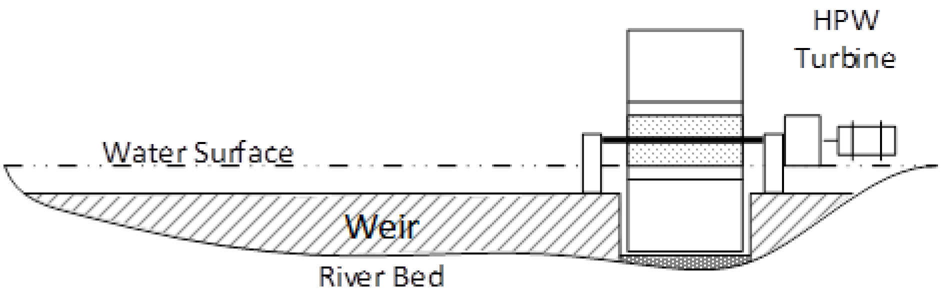


**Figure 3.15: Cross-sectional sketch of weir in the river**

The lowest flow of the river (1,2$m^3$/s) was achieved in February. The cross-sectional area of the water is 1,5 $m^2$. If the gap size is removed, the resultant height above the weir during the lowest flow is,

Height (above weir) = total cross section area – gap area / width

From the above equation, the height of water above the weir is, Low flow – 150 mm

High flow – 550 mm

These calculations do not take into account the accelerated flow such as to produce ample head during the low flow season and allow enough flow during high flow season and flooding (Dehdar-Behbahani & Parsaie, 2016). Table 3.9 list the respective weir and water values at low and high flow.

**Table 3.9: Water height calculation for the lowest and highest level**

| Flow (m3) | Month | Cross-section area ($m^2$) | Gap area ($m^2$) | Height above weir (mm) | Weir height (mm) | Total height (mm) |
|---|---|---|---|---|---|---|
| 1,2 (lowest) | February | 1.5 | 0,6 | 150 | 300 | 450 |
| 6,2 (highest) | July | 3.6 | 0,6 | 550 | 300 | 850 |

## 3.12 Turbine options for the river

### 3.12.1 Stream wheels

Without any flow enhancement techniques to extract maximum hydropower energy from the river, the only usable turbine is the conventional undershot waterwheel or stream wheel in Figure 3.16. The Sagebien and Zuppinger water wheels are the most efficient of the undershot waterwheels (Quaranta & Revelli, 2018). The efficiency of low entry stream wheels in low flow conditions is however low (Denny, 2004), making it unfeasible.

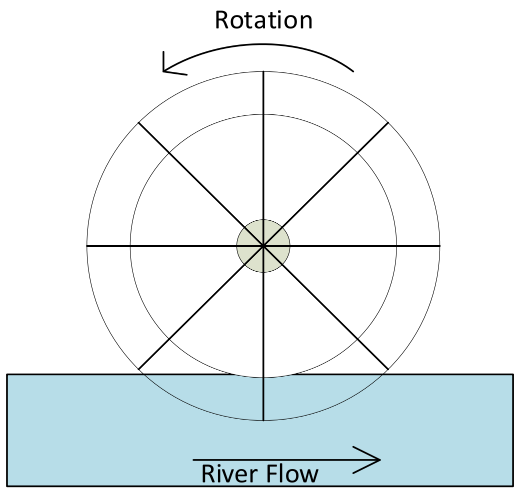


**Figure 3.16: Illustration of a stream wheel or undershot waterwheel**

From the literature, it was found that very few commercial turbines are available for in-stream run-of-river applications. Amongst those in-stream types of turbine, very few units are suitable for streams with a combined volume flow of 5 $m^3/s$ and a velocity of less than 2 m/s. In a summary of published literature on the topic of turbine investigations by Jawahar & Michael, (2017), all the studies of turbines for small heads are listed in Table 3.10. Although these are all the smallest types that were investigated, all of them are specified for a head of over 1m and are not suitable for our application.

**Table 3.10: Table of turbines for heads under 1.5m (Jawahar & Michael, 2017)**

| Author | Turbine | Net Head (m) | Discharge (l/s) | Output (kW) | Efficiency (%) |
|---|---|---|---|---|---|
| (Date et al., 2013) | Reaction Turbine | 1.45 | 30 | 0.28 | 65-70 |
| (Ikeda et al., 2010) | Nano Hydraulic Turbine | 1.2 | 1-3 | 0.1-0.2 | 20 |
| (Girma and Dribssa, 2014) | Cross Flow Turbine | 3 | 420 | 2.5 | 83 |
| (Date et al., 2012) | Simple Reaction Turbine | 1-4 | 1-8 | 0.15 | 50 |
| (Williamson et al., 2013) | Turgo Turbine | 1-3.5 | 10 | 0.25 | 87-91 |
| (Denny, 2004) | Undershot waterwheel | 1-3 | 1-5000 | | ~30 |

In the research on ultra-low-head (ULH) turbines by Zhou & Deng (2017), only one turbine was listed in Table 3.10 that can work with a head of less than 0.5 m, but that unit also needs a flow velocity above 2 m/s. This means that none of the turbines in Table 3.11 is suited for this study's river application.

**Table 3.11: List of ultra-low-head turbines (Zhou & Deng, 2017)**

| | | |
|---|---|---|
| Open flume Francis turbine | $H > 2.0$ m | $N > 100$ kW |
| Kaplan turbine | $H > 1.5$ m | $N > 100$ kW |
| Propeller turbine | $H > 1.5$ m | $N > 10$ kW |
| Tubular turbine (double-regulated) | $H > 1.0$ m | $N > 100$ kW |
| Tubular turbine (single-regulated) | $H > 1.0$ m | $N > 50$ kW |
| Tubular turbine (non-regulated) | $H > 1.0$ m | $N > 10$ kW |
| Cross-flow turbine | $H > 0.5$ m or $V > 2.0$ m/s | $N > 1$ kW |
| Archimedes turbine | $H > 1.5$ m | $N > 10$ kW |
| Hydro-kinetic turbine | $V > 0.5$ m/s | $N > 10$ W |

### 3.12.2 Hydrokinetic turbines

Khan et al (2009) classifies the different types of hydro-kinetic (HK) turbines in their research on river current turbines. Figure 3.17 arranges the different HK turbines in groups of axial flow and cross-flow. This study compares one of each of these types of turbines to determine the most suitable type for the river specifications. Niebuhr *et al.*, (2019) further investigates HK turbine options and lists multiple commercially available options. The Smart Freestream HK turbine was found to be the best turbine for their canal application.

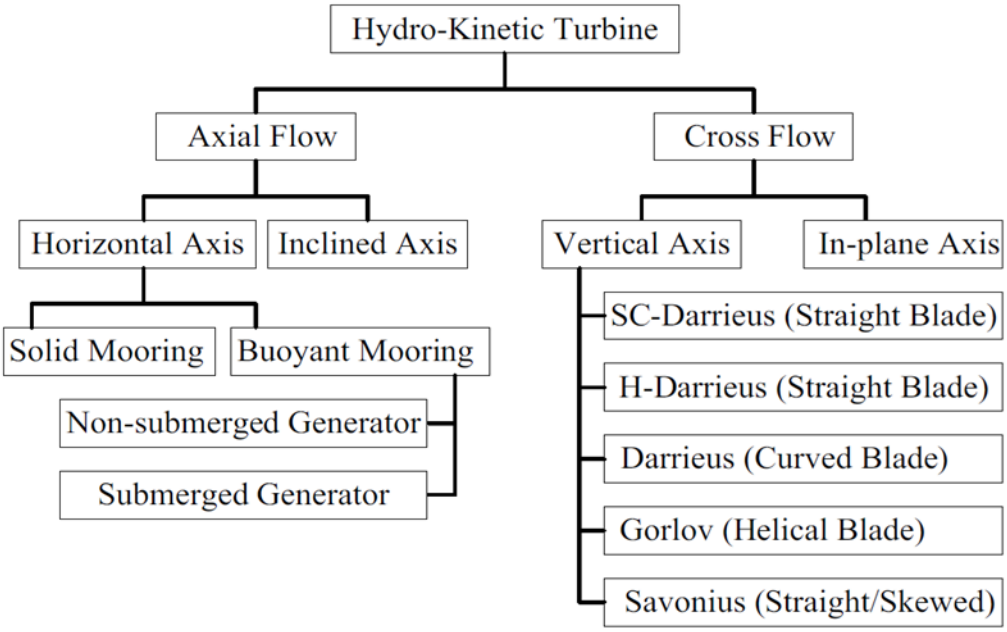


**Figure 3.17: Hydrokinetic turbine types** (Khan et al., 2009)

### 3.12.3 Hydrostatic pressure wheels

The hydrostatic pressure wheel (HPW) and hydrostatic pressure machine (HPM) are a redesign or upgrade of the conventional waterwheel. This turbine makes use not only of the kinetic energy of flowing water, but it dams up the water on the upstream side to create a head, thereby utilising the potential energy of the water as well. Figure 3.18 gives an illustration of this.

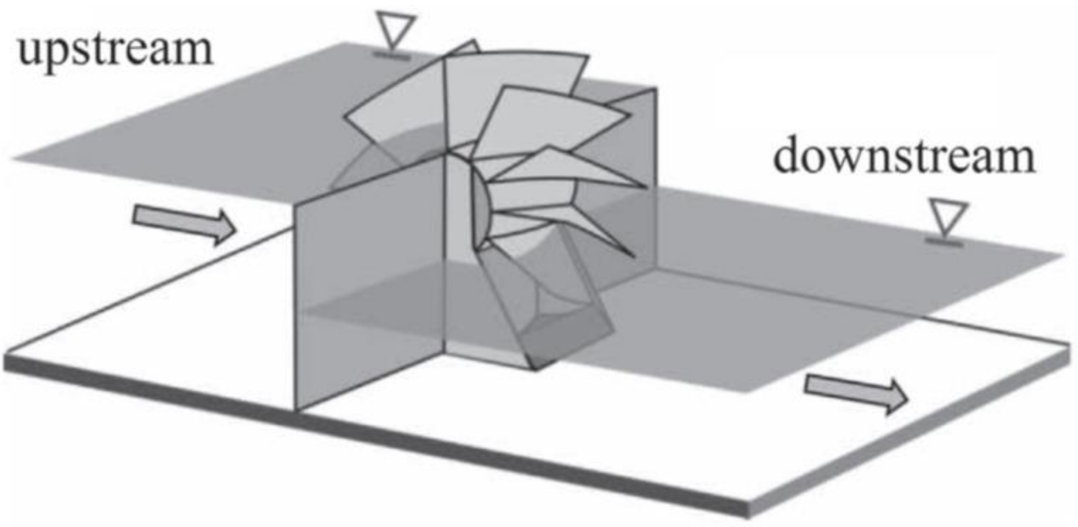


**Figure 3.18: Illustration of the hydrostatic pressure wheel** (Senior et al., 2010)

Hydrostatic pressure wheels work with a head of between 0.3 m and 1.0 m and discharge up to 1.5 $m^2/s$ (Müller et al., 2007). Hydrostatic pressure machines work with a head of between 1.0 m and 2.5 m (Senior et al., 2008). Figure 3.19 shows the chart of multiple turbines with their HPM position (Quaranta, 2018).

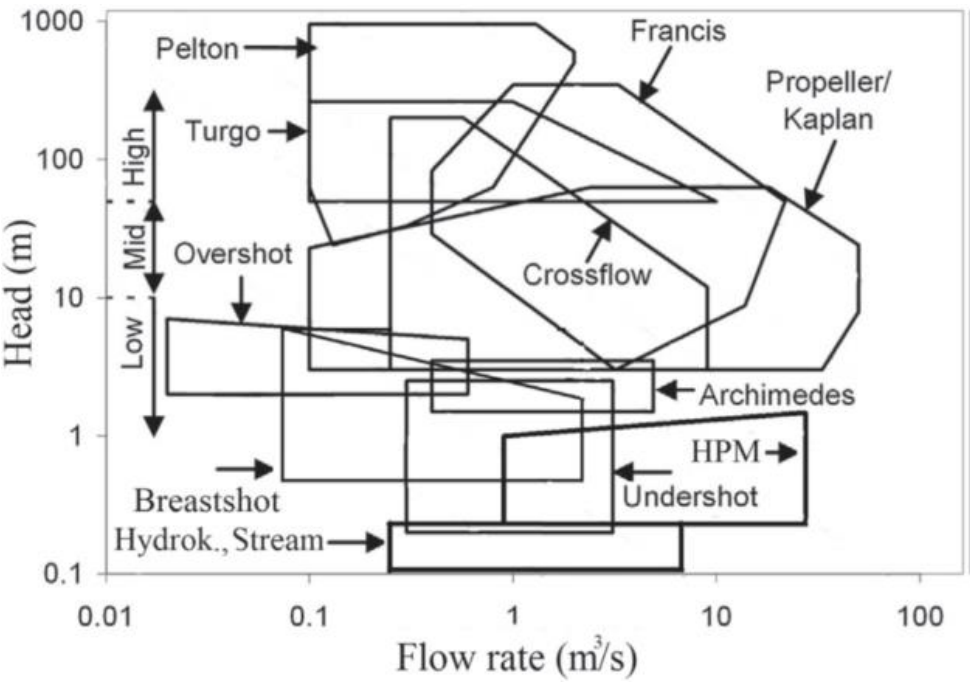


**Figure 3.19: Multiple turbine chart to show the HPM position** (Quaranta, 2018)

**Table 3.12: Comparison table of all the prospective turbines for the river application**

| Turbine type | Minimum head and flow required | Efficiency (η), Power (W) | Features | Sample image |
|---|---|---|---|---|
| Hydrokinetic Smart Freestream<br><br>https://www.smart-hydro.de/renewable-energy-systems/hydrokinetic-turbines-river-canal/ | Min height: 1.1m<br>Flow: 1m/s | η: not specified<br>P: 200 W at 1.2 m/s | Advantages<br>Easy install<br>Submersible<br>Small space<br><br>Disadvantages<br>Costly<br>Need high water<br>Full power only at 3m/s | 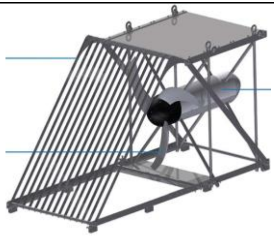 |
| Hydrokinetic Waterotor<br>https://waterotor.com/ | Min height: 1.12 m<br>Min flow: 0.9 m/s | η: 50%<br>P: ~250 W at 1.2 m/s | Advantages<br>Easy install<br>Submersible<br>Compact<br>Quiet<br><br>Disadvantages<br>Need high water<br>Limited power output |  |
| Waterwheel<br>Stream wheel<br>https://en.wikipedia.org/wiki/Water_wheel | Min height: 0.4m<br>Min flow: 0.9m/s | η: 29%<br>P: 300 W at 1.2 m/s (depending on size) | Disadvantages<br>Large<br>Low Efficiency<br>Low power | 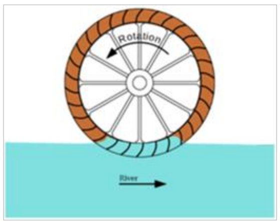 |
| Hydrostatic pressure wheel (HPW)<br>Marco Licari e al (2019) | Min height: 0.3m<br>Min flow: 1m/s | η: 80%<br>P: >3000 W at the head of 0.5 m (depending on diameter and width) | Advantages<br>High efficiency<br>Use potential energy (head)<br>Smaller than conventional wheel<br><br>Disadvantages<br>Relatively new technology.<br>Limited research | 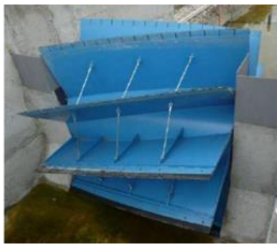 |

From the comparisons in Figure 3.19, the HPM stands out as the most suitable turbine to use in low-head rivers in terms of power and efficiency. Hydrostatic pressure wheels have received a lot of interest in the past decade. Several studies have been undertaken to reach an optimized model for hydrostatic pressure wheels (Senior et al., 2008; Müller et al., 2007; Linton, 2013; Quaranta, 2018; Cassan et al., 2021; Bhatti, 2018; Schwyzer, 2016). The term hydrostatic pressure wheels is sometimes used as a collective category, but other research draws a definite distinction between HPW and HPM. Other researchers refer to it as hydrostatic pressure converters.

This research will make use of a combination of these research approaches to simplify the process of finding the power potential of the best-suited turbine for this site. This is because there are few real-world installations of HPM. There are no installations of HPM in South Africa known to the author. Figure 3.20 shows two field trial installations in Northern Bavaria and Bulgaria that were experimented with by Linton (2013) and Licari et al. (2020) respectively.

(a) (b)

**Figure 3.20: Two installations of the hydrostatic pressure machine (HPM): (a) in Bavaria (Linton, 2013). (b) in Bulgaria (Licari et al., 2020)**

Various concept designs of small hydraulic turbines are under research. According to Licari et al., (2020), the HPM is best suited for ultra-low head sites between 0.5 m and 2 m. Senior et al., (2008) classifies the HPW for head differences of 0.2 m to 1 m, and the HPM for heads of 1 m to 2.5 m. Figure 3.21 shows an example of the HPM turbine.

## 3.13 Hydrostatic Pressure Machine (HPM)

The HPM technology is relatively new, although several experimental and simulation studies were carried out already. There is also no clear guideline when it comes to the geometry and dimensions of these systems (Licari et al., 2020). In this study, the simplest available methods in prior research is used to determine the physically possible maximum hydropower of the site.

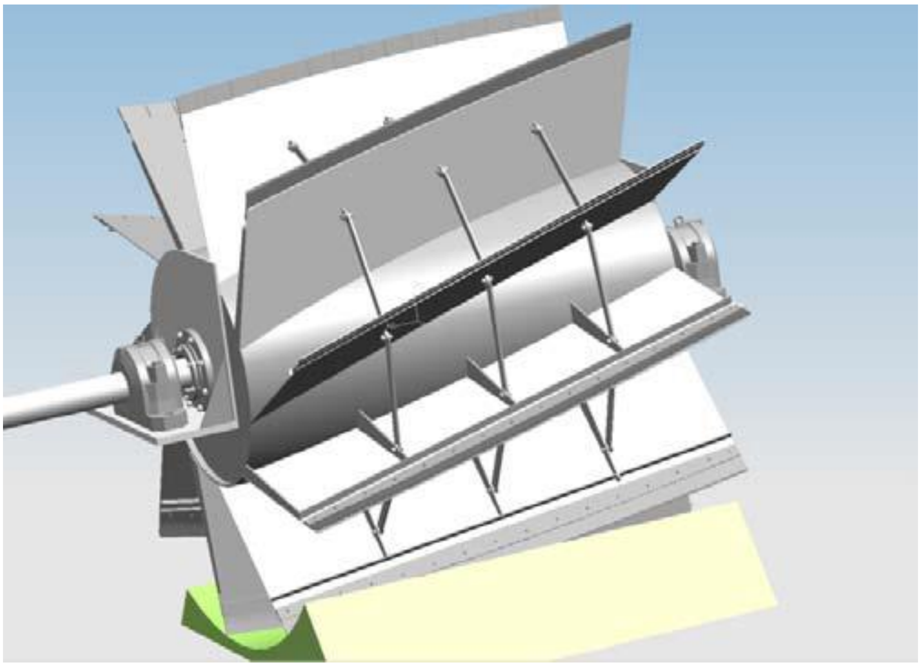

**Figure 3.21: Hydrostatic pressure machine with base** (Azmanov et al., 2011)

### 3.13.1 Description of HPM assembly

Figure 3.22 shows an image of the HPW or HPW which consists of a wheel hub with flat blades that are longer than the height of the upstream water. The length and shape of the blades, the outer diameter, and hub diameter, and width all contribute to the output power and efficiency of the wheel.

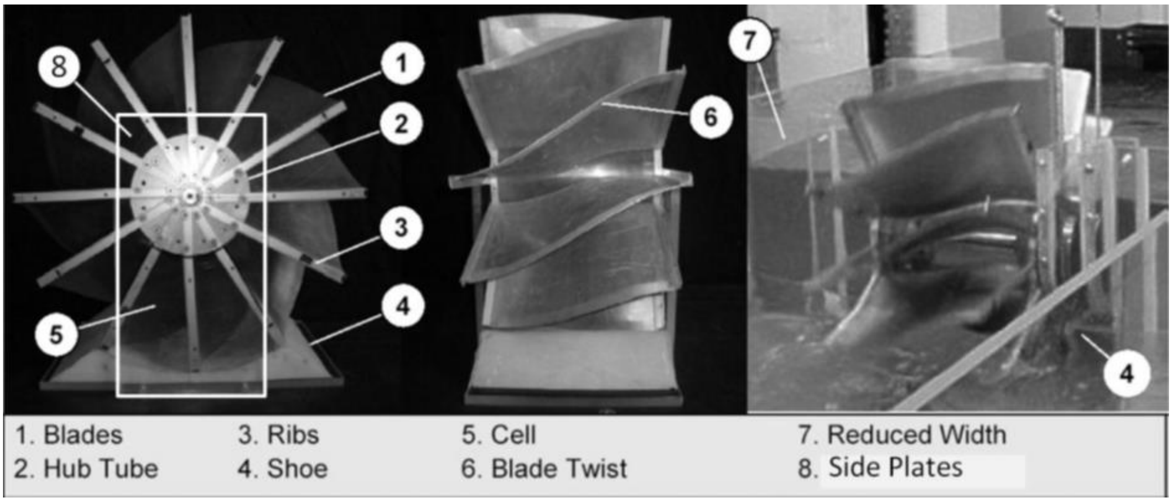


**Figure 3.22: Graphical illustration of the hydrostatic pressure machine** (Linton, 2013)

The rotor consists of a hub tube (2), to which 12 blades (1), supported by ribs (3), are attached, forming an assembly free to spin about its axis. The hub tube acts as a weir, separating up and downstream water levels to maintain a head difference acting across the device. The segment of the rotor formed between adjacent blades is termed a ‘cell’

(5). This is the working chamber of the device into which fluid enters and leaves and from which power is extracted, during rotation. The blade twist or in the case of flat blades inclination (6), aids efficient filling and emptying of the cells, encourage water to enter from the sides of the machine as it resides in a channel significantly wider than the machine itself (7). A shoe (4) is shaped to seal off the bottom of the rotor, preventing leakage of flow along the channel bed, and together with the side plates (8).

### 3.13.2 Theory of operation

The HPM is installed in a gap of a flume or weir in a river or canal where it blocks or backs up the water. The resultant difference between the upstream and downstream water levels causes a hydraulic pressure difference that causes the wheel to turn (Senior et al., 2008).

- **Static condition**

Linton (2013) describes the working of the HPM by looking at its static condition. In Figure 3.23, the upstream water level ($d_1$) is in line with the upper curve of the hub radius ($r_0$). The downstream water level ($d_2$) is in line with the bottom curve of the hub. The difference of the head (H) is thus 2 x ($r_0$). The bed of the river is the same throughout.

In the static condition, the difference in the upstream and downstream water level causes hydrostatic pressure on the bottom blade of the resulting force given by,

$$FQ_{nom} = N.V_b \frac{n}{60},$$ Equation 4.1

And the force that is exerted on the hub is given,

$$F_{blade} = \frac{pg}{2}\ d_2(d_1{-}d_2)\ ,$$ Equation 4.2

Where *p* is the water density, *g* is gravity. The force acting on the hub is,

$$F_{hub} = \frac{pg}{2}\ (d_1{-}d_2)^2\ ,$$ Equation 4.3

But the force on the hub does not produce any torque.

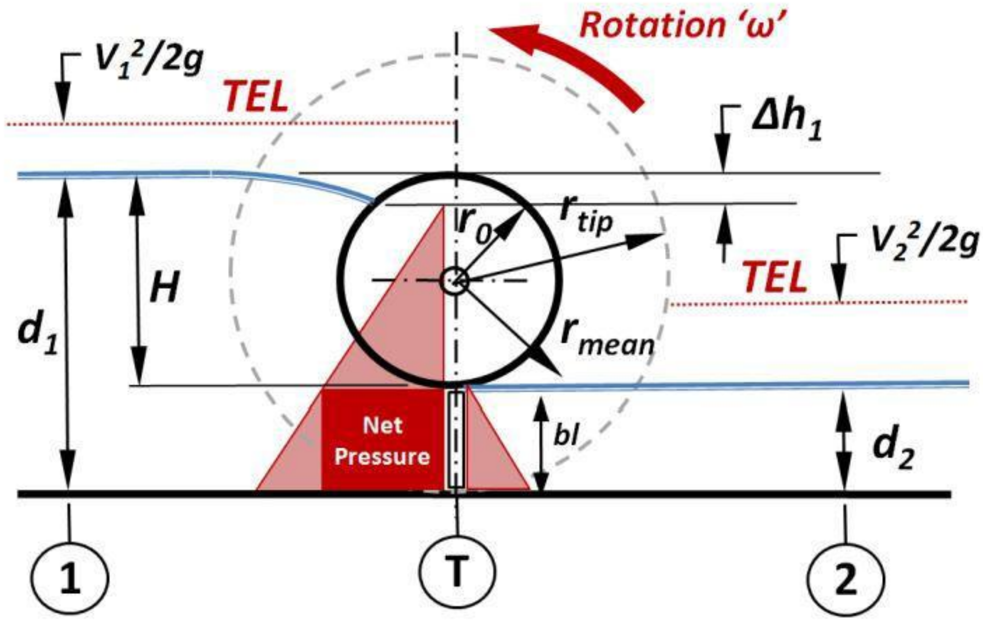


**Figure 3.23: Hydrostatic pressure machine in-river diagram for static condition** (Linton, 2013)

- **Running condition**

When the RPM is moving, the wheel has an angular velocity (*w*) that produces a flow rate of (Q). the velocity (V2) at the centre of the blade is taken to be the same as the downstream water velocity. The blade with length (bl) is fixed to the hub radius.

The energy equations from the up and downside are,

$$\frac{v1^2}{2g} + d1 = \frac{v2^2}{2g} + d2 \ , \qquad \text{Equation 4.4}$$

From continuity,

$$Q = v_1 d_1 = v_2 d_2 \ , \qquad \text{Equation 4.5}$$

From this we derive that,

$$v1 = v2\frac{d2}{d1} , \qquad \text{Equation 4.6}$$

The flow through the turbine causes a drop in the head of,

$$\Delta h_1 = \frac{v2^2 - v1^2}{2g} \ , \qquad \text{Equation 4.7}$$

This results in a static force of,

$$Fp = \rho gbl(d_1 - d_2 - \Delta h_1) \ , \qquad \text{Equation 4.8}$$

If we disregard any losses, the up-and downstream equate as,

$$Q = \omega r_{mean} bl = d_2 v_2 \ , \qquad \text{Equation 4.9}$$

Power output of the ideal machine without losses is thus,

$$P_{ideal} = F_p v_2 \ , \qquad \text{Equation 4.10}$$

Which may be written as,

$$P_{ideal} = \rho g d_2 v_2 \left[d_1 - d_2 - \frac{{v_2}^2}{2g}\left(1 - \left(\frac{d_2}{d_1}\right)^2\right)\right] \ , \qquad \text{Equation 4.11}$$

The hydraulic power available from the flow passing through the machine is,

$$P_{ideal} = Q\rho gH \ , \qquad \text{Equation 4.12}$$

Which for this installation may also be written as,

$$P_{flow} = \rho g d_2 v_2 (d_1 - d_2), \qquad \text{Equation 4.13}$$

Enabling the ideal Efficiency of the machine to be calculated as,

$$\eta_{ideal} = \frac{d_1 - d_2 - \frac{{v_2}^2}{2g}\left(1 - \left(\frac{d_2}{d_1}\right)^2\right)}{d_1 - d_2} \ , \qquad \text{Equation 4.14}$$

To normalise the power and flow, the value at a given moment is divided by the maximum power and flow respectively. The maximum theoretical power and flow are given by,

$$v_{max} = \sqrt{2g(d_1 - d_2) + {v_1}^2} \ , \qquad \text{Equation 4.15}$$

When applying the above velocity to the full blade area, the maximum theoretical flow is given by,

$$Q_{max} = d_2 v_{max} \quad , \qquad \text{Equation 4.16}$$

The resultant power and hydraulic efficiency of the ideal machine is given in Figure 3.24

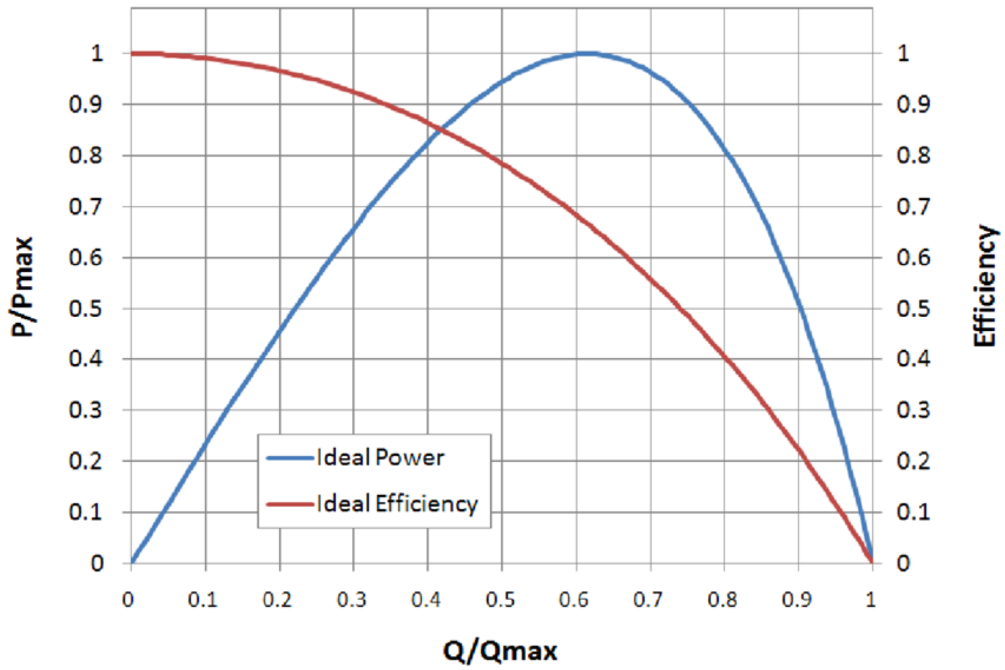


**Figure 3.24: Power and efficiency graph for the ideal HPM** (Linton, 2013)

### 3.13.3 Theoretical model and design specifications

- **Blade length (L)**

The upstream water depth varies between 0,25 m and 0,6 m during low and high seasons. With the weir installed, depending on weir size and gap width, this height will vary between 450 mm and 850 mm. The blade length will be made 800 mm to accommodate the high flow.

- **Hub size (h)**

Quaranta (2018) suggests that the blade length should be made the same size as the head difference and three times larger than the downstream water depth, and the central hub should be the same size as the downstream water depth. With the two blades totalling 1,6 m in size, the hub will be made 400 mm. this gives the wheel a total blocking height to the upstream side of 1,2 m. This top level of the hub is just above the river banks and just above the highest recorded flood level which makes it suitable.

- **Wheel diameter (D)**

The wheel diameter is the sum of the two blades and the hub. With the uncertainty of many dimensions, an estimated wheel diameter of 2 m is chosen. This outside diameter and width size is a trade-off between the river width, the rotational speed of $V_2$ = ND/2 (Quaranta, 2018), drag losses, and even engineering work.

- **Number of blades (N)**

The number of blades is a choice between six and twelve and it affects the speed of the wheel, cell emptying, and blade force amongst others. The installation type, water depth, or critical flow affects the blade number. Linton (2013) found in an experiment of a stream wheel that the power increased from 6 to 10 blades. Senior et al. (2008) randomly chose 12 blades with many researchers following suit. Linton (2013) also found that the 6-blade wheel outperformed the 12-blade wheels. Notwithstanding the above, we will choose 10 blades, spacing the cells 36° apart.

- **Unit width (W)**

The width of the blades is chosen to maximise the power potential and available flow while considering the channel width. With a channel of 6 - 7 m, the weir is constructed to leave a 2m wheel gap.

- **River flow**

From the river bed characteristics, a height difference of at least 0.5 m between the low and high flow was observed. The cross-sectional area of the average flow value is 2.97 $m^2$. In the absence of clear guidance of the wheel diameter design, the rotational speed of the wheel can be derived from $V_2$ = ND/2, Table 3.13

**Table 3.13: Turbine parameters formulae comparison (Quaranta, 2018)**

| Wheel type | Flow regime | Max. $\eta$, $C_p$ | kW/m | Speed | $\frac{n_{min}}{n}$ |
|---|---|---|---|---|---|
| HPW | Sub. shallow | $\eta = 0.8–0.9, C_p = 0.4$ | $< 20$ | $\frac{v_2}{\sqrt{2g\Delta H}} = 0.20$ | 1 |
| HPM | Sub. shallow | $\eta = 0.60–0.65$ | $> 10$ | $\frac{v_2}{\sqrt{2g\Delta H}} = (0.25–0.3)$ | 1 |
| Kinetic wheel | Sup. shallow | $\eta = 0.4, C_p = 0.4$ | 10–13 | $\frac{v_2}{v_1} = 0.3–0.55$ | – |
| Floating wheel | Deep flow | $C_p = 0.4$ | 0.5–2 | $\frac{v_2}{v_1} = 0.4–0.55$ | $7.76\frac{l}{D} - 0.$ |
| Floating HPW | Deep flow | $C_p = 0.7–0.8$ | 5 | $\frac{v_2}{v_1} = 0.6–0.8$ | 1 |

Comparison of experimental results of different wheels' maximum performance. For HPM, $\eta$ is the efficiency, v2 is the velocity before the wheel, $g$ the gravity and $\Delta H$ the head difference.

### 3.13.4 Flow calculations

As stated in section 4.3, the weir has a height of 0.3 m and a gap width of 2 m. This means that if the water is lower than the weir height, all the water will theoretically flow through the turbine. The flow rate however is specified as the total volume flow, without a weir present. To calculate the flow and head difference, the cross-sectional area of the river is depicted in a simplified square diagram (Figure 3.25). Table 4.7 presents the cross-sectional area and flow rate per month. The flow through the gap is determined through iteration.

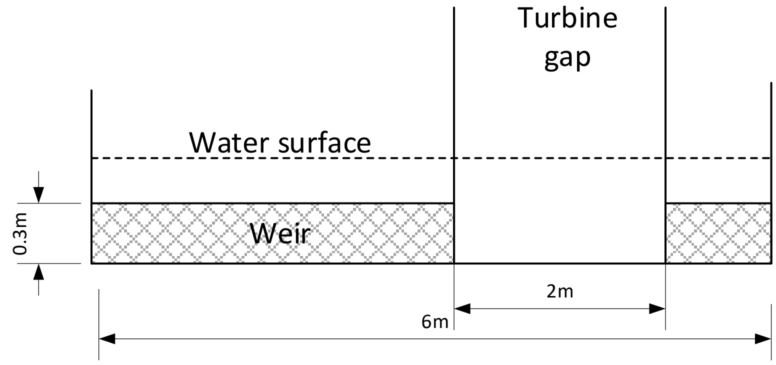


**Figure 3.25: Simplified weir size calculation diagram**

To determine the water height at the turbine gap:

Water cross-sectional area (width x height) without weir.

- Minus gap weir area (2 m x 0.3 m =0.6 $m^2$)
- New area /width (6 m) = height above gap
- Height at gap = height above gap + height of weir gap (0.3)

The resultant weir size is used in Table 3.14 to calculate the potential flow through the weir. The normalised flow ($Q/Q_{max}$) is the respective monthly average flow rate(Q) in relation to the maximum flow rate ($Q_{max}$). This normalised flow rate is used in conjunction with the ideal HPM curve (Figure 3.24) to determine the final efficiency of the turbine.

**Table 3.14: HPM monthly flow rate with derived efficiency data**

| Month | Width (ave) | Flow rate | River Height | Total Area | Flow | Turbine gap Total -weir gap | Height at Gap | Flow Normalised Q/Qm | Efficiency Ideal value | Final Efficiency |
|---|---|---|---|---|---|---|---|---|---|---|
| | m | m³/s | m | m² | m³/s | m² | m | 6,8m =1 | | η |
| Jan | 6 | 1,4 | 0,28 | 1,68 | 1,4 | 1,08 | 0,48 | 0,21 | 0,96 | **0,77** |
| Feb | 6 | 1,2 | 0,2 | 1,2 | 1,2 | 0,6 | 0,4 | 0,18 | 0,98 | **0,78** |
| Mar | 6 | 1,3 | 0,25 | 1,5 | 1,35 | 0,9 | 0,45 | 0,19 | 0,97 | **0,78** |
| Apr | 6 | 1,4 | 0,28 | 1,68 | 1,4 | 1,08 | 0,48 | 0,21 | 0,96 | **0,77** |
| May | 6 | 2,2 | 0,32 | 1,92 | 2,2 | 1,32 | 0,52 | 0,32 | 0,92 | **0,74** |
| Jun | 6 | 5,1 | 0,6 | 3,6 | 5,04 | 3 | 0,8 | 0,75 | 0,5 | **0,40** |
| Jul | 6 | 6,8 | 0,7 | 4,2 | 6,8 | 3,6 | 0,9 | 1,00 | 0,2 | **0,16** |
| Aug | 6 | 6,9 | 0,7 | 4,2 | 6,9 | 3,6 | 0,9 | 1,01 | 0,2 | **0,16** |
| Sep | 6 | 3,5 | 0,45 | 2,7 | 3,24 | 2,1 | 0,65 | 0,51 | 0,77 | **0,62** |
| Oct | 6 | 3,1 | 0,4 | 2,4 | 3,1 | 1,8 | 0,6 | 0,46 | 0,84 | **0,67** |
| Nov | 6 | 2,5 | 0,35 | 2,1 | 2,5 | 1,5 | 0,55 | 0,37 | 0,87 | **0,70** |
| Dec | 6 | 1,8 | 0,3 | 1,8 | 1,8 | 1,2 | 0,5 | 0,26 | 0,94 | **0,75** |
| Ave | 6 | 3,1 | 0,4025 | 2,415 | 3,0775 | 1,815 | 0,6025 | 0,46 | 0,76 | 0,61 |

## 3.14 Summary

In this chapter, the Zandvliet wastewater treatment works site and the Kuilsriver have been selected to evaluate hydropower potential. The volume of the ZWWTW discharge outflow and the site specifications were obtained. The various turbine options were investigated and assessed. Thereafter, the Archimedes screw turbine was found to be the best suited for this site. A realistic workable model of the AST was also designed and all its geometric specifications were determined.

The recorded flow of the Kuilsriver and how it was obtained are presented. The initial investigation revealed that it is not feasible to use the river for hydropower without improving the river flow. Hence, a weir was designed to optimise the flow over the turbine. Turbines that can be used in the river flow conditions were evaluated. The top-rated turbine for the river conditions in terms of maximum energy generation was found to be the hydrostatic pressure machine (HPM). A description as well as the operation theory of the HPM turbine was discussed. The geometric dimensions of the full-scale model were calculated and tabulated. Finally, the efficiency of the turbine was calculated according to the ideal model and the value for each month was obtained. The next chapter focusses on the modelling of the turbine output power.

# CHAPTER FOUR

# MODELLING AND SIMULATION



## 4.1 Introduction

In this chapter, the AST turbine at the ZWWTW and the HPM turbine at the Kuilsriver sites are modelled according to the values that were established in Chapter 3. For both sites, it was anticipated that the power of each turbine would be calculated using formulae that consider velocity, torque, speed, and head. However, these values have to be measured using special equipment that are not available in this research. The mechanical power of both these turbines is modelled by using the hydraulic power multiplied by the efficiency (Equation 3.2).

## 4.2 Archimedes screw at the ZWWTW

In the modelling of the selected turbines, the leakage losses are not considered. It is assumed that the leakages on both the AST and HPM turbines are the same and thus negligible for a comparison. Only the mechanical power of the two turbines is used to compare the respective power outputs of the two sites.

Figure 4.1 shows a MATLAB Simulink layout of the various elements used to determine the power output of the AST at the ZWWTW. The top section depicts the formula to calculate the hydraulic power given in Equation 3.2.

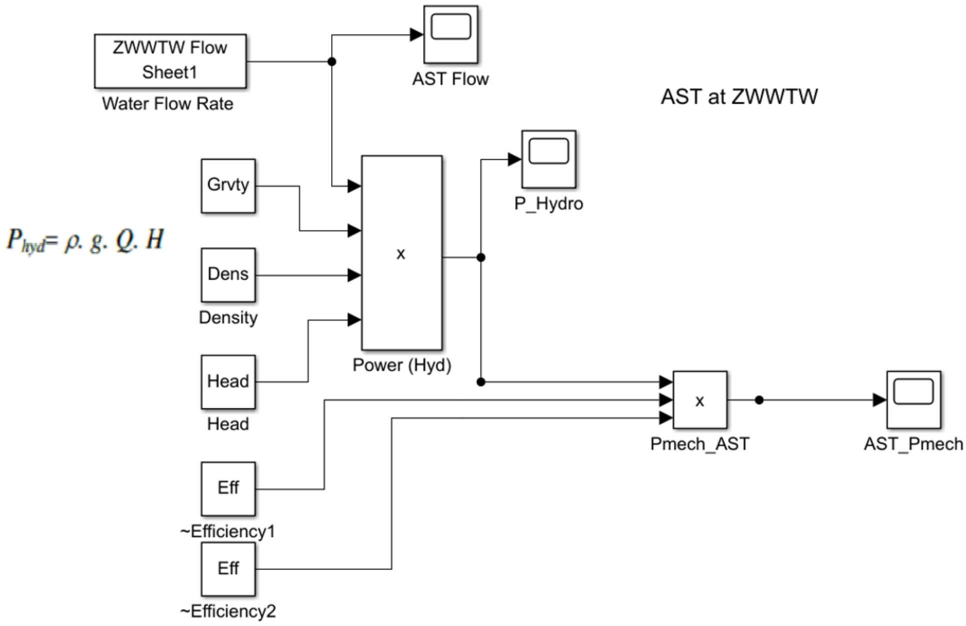


**Figure 4.1: Simulink layout of the AST model**

The gravity ($g$) is represented by the "Grvty'' box with a value of 9.81m/s. The density ($\rho$) of the water is represented by the "Dens" box. A value of 1000kg/m$^3$ is used. The Head (H) was determined in Chapter 3 to be 1.5 m. The flow (Q) is imported from the MS Excel spreadsheet that was obtained from the municipal authority. The monthly flow figures are fed to the multiplier block, together with the gravity, density, and head. The resultant output represents the maximum potential hydropower of the water.

To determine the mechanical power output, the hydraulic power of the hydropower site is multiplied by the turbine's efficiency given in Equation 3.1.

In the case of the AST at the ZWWTW site, the efficiency of a typical turbine is given in the literature to vary over a range of values. For this research, we will use a low and a high-efficiency factor to indicate the prospective power range. The efficiency of 70% and 85% is used for the low and high values respectively. Both efficiency inputs are depicted in Figure 4.1 although only one efficiency input is used at any given time.

## 4.3 Modelling of the Hydrostatic pressure machine at the river

The mechanical power of the HPM at the river is calculated using the total hydraulic power at the site, multiplied by the efficiency of the turbine. The HPM's efficiency was calculated using the ideal model discussed in paragraph 3.13.2. The resultant flow calculations in Table 3.14, are fed into the MATLAB simulation. Figure 4.2 gives the MATLAB Simulink presentation of the different elements that make up the mechanical power calculation of the HPM at the river. Figure 4.3 shows the combined diagram of the comparison of the two turbines.

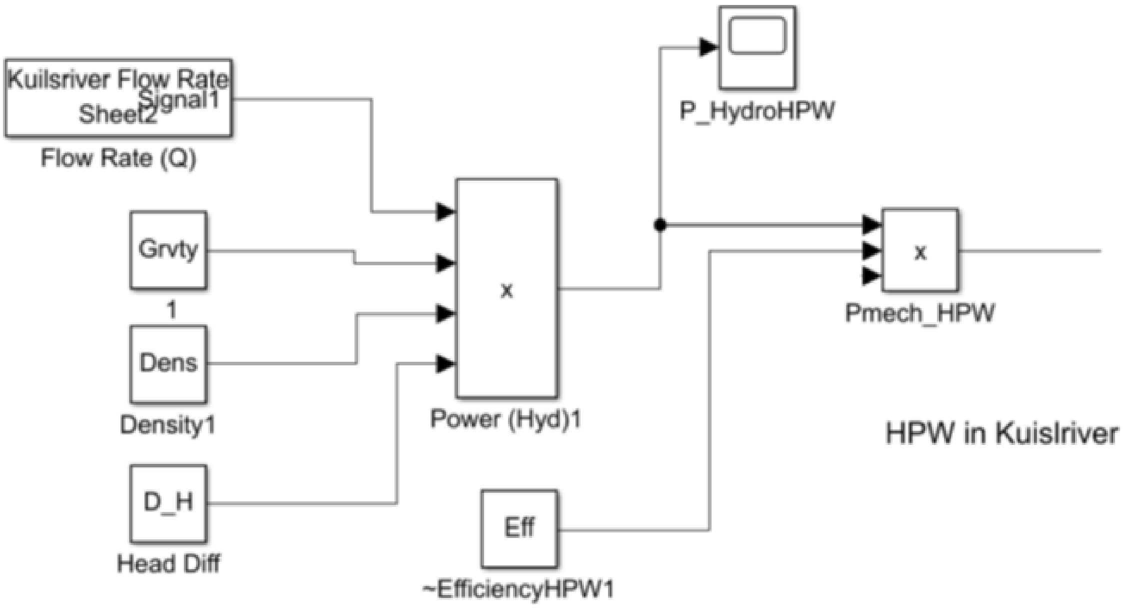


**Figure 4.2: Simulink layout of the HPM model**

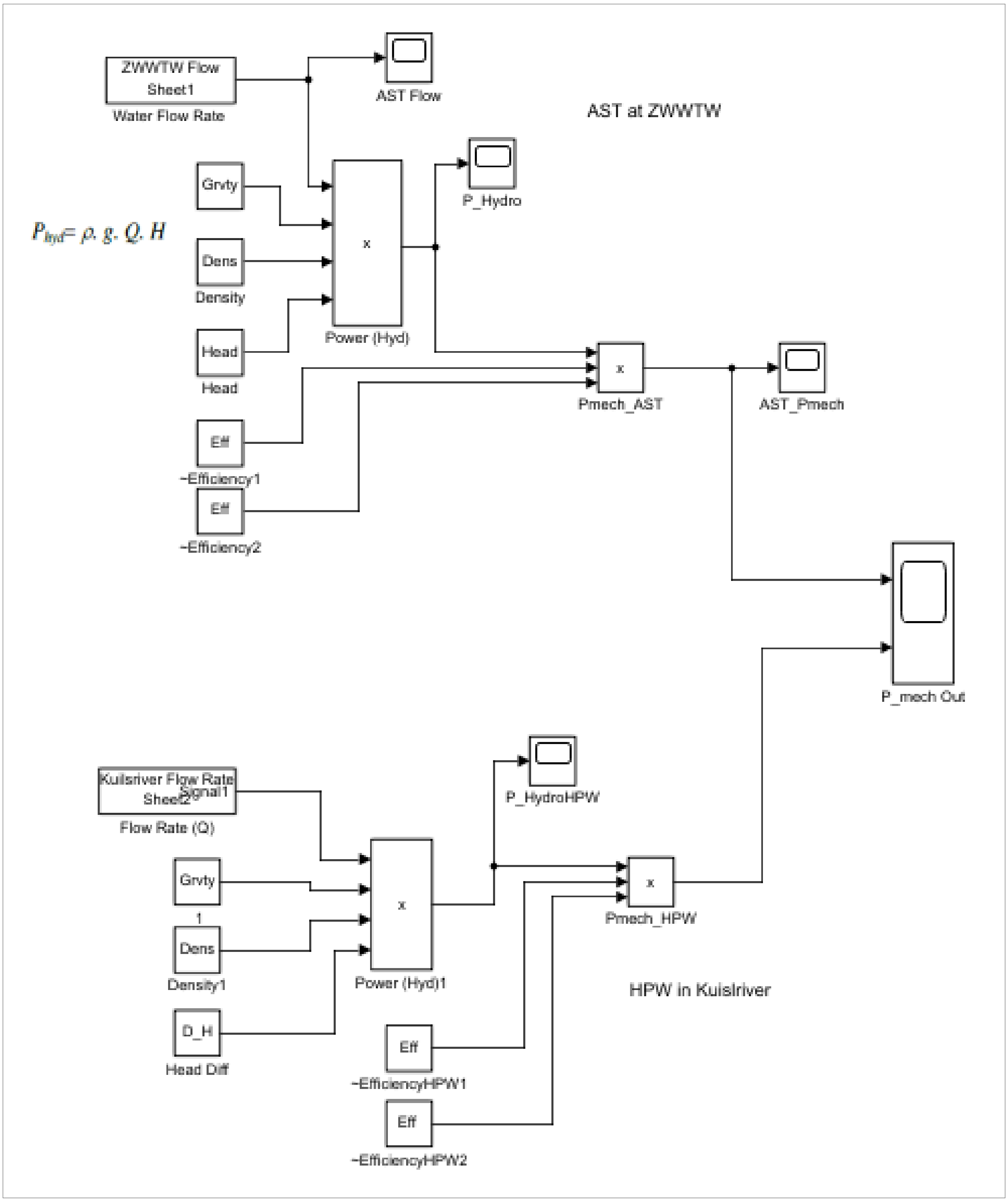


**Figure 4.3: Archimedes screw turbine and Hydrostatic pressure machine models**

The following section presents the ZWWTW outflow quantities of the wastewater treatment plant as well as the river.

## 4.4 Zandvliet Wastewater Treatment Works daily flow

The discharge outflow data of the ZWWTW is plotted in Figure 4.4. The daily flow in million liters is shown for each of the 365 days. From the graph, we can observe a fairly constant average flow of about 65 million liters per day. Five distinct peak flows can be observed in the months of March, July, October and November. The highest daily flow over this period was recorded in July, at about 88 Ml/d. The lowest daily flow rate was recorded in August at about 50 Ml/d. To obtain the instantaneous flow rate per second, the daily flow rate is divided by the number of seconds in a day, namely 86400. Alternatively, the daily flow rate is divided by 24 hours to get the hourly flow rate. This is divided by 60 minutes to get the flow rate per minute, and further divided by 60 seconds to get the flow rate per second on a specific day.

The difference between the highest and lowest daily flow rate is 40 Ml/d. The calculated per second discharge flowrate is thus between 578 l/s and 1041 l/s with an average of 775 l/s.

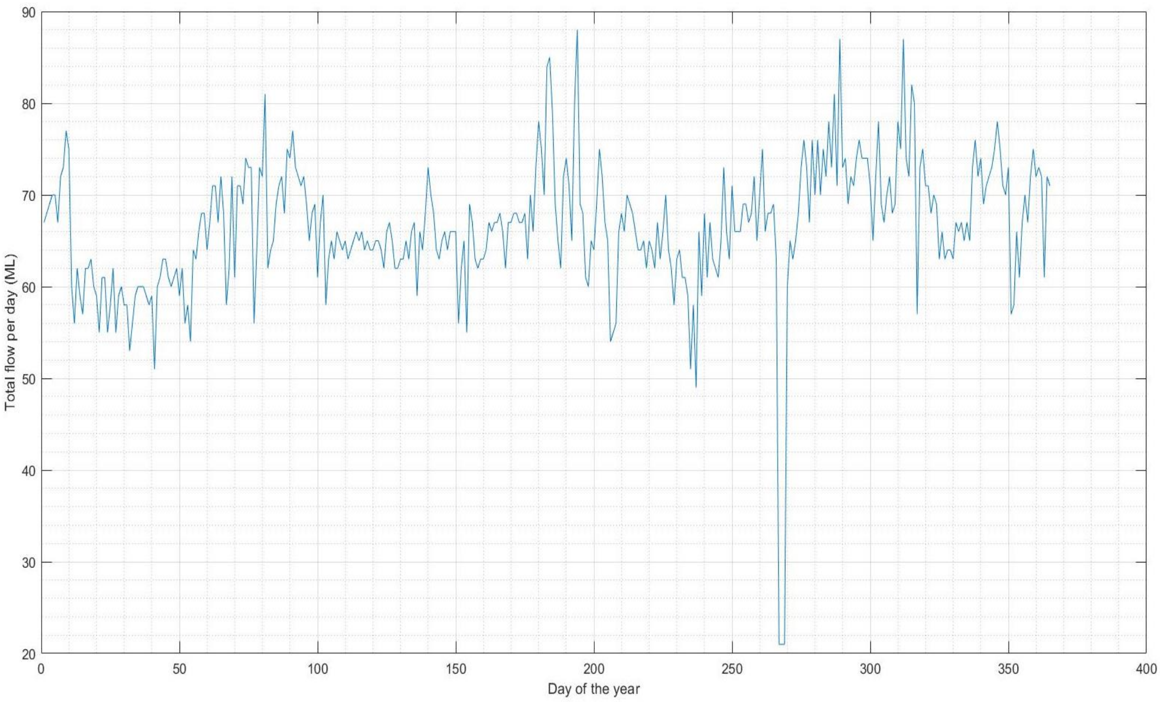


**Figure 4.4: Daily outflow from the Zandvliet wastewater treatment works**

The per-second monthly discharge flowrate is listed in the third column of Table 4.1. These values were converted from the daily figures in Figure 4.4. This flow rate will be used to calculate the potential power of the turbine.

**Table 4.1: Wastewater treatment plant monthly flow and power**

| Month | Average Flow Ml/d | Flowrate l/s | Power Low Flow (W) | Power High flow (W) |
|---|---|---|---|---|
| January | 62,88 | 727,77 | 7496 | 9103 |
| February | 60,14 | 696,08 | 7170 | 8706 |
| March | 68,58 | 793,78 | 8176 | 9928 |
| April | 66,35 | 767,92 | 7910 | 9605 |
| May | 64,83 | 750,38 | 7729 | 9386 |
| June | 66,38 | 768,28 | 7914 | 9609 |
| July | 68,84 | 796,76 | 8207 | 9966 |
| August | 62,90 | 727,97 | 7498 | 9105 |
| September | 62,16 | 719,46 | 7411 | 8999 |
| October | 73,34 | 848,81 | 8743 | 10617 |
| November | 69,80 | 807,83 | 8321 | 10104 |
| December | 69,89 | 808,92 | 8332 | 10118 |
| Average | 66,34 | 767,83 | 7909,03 | 9603,82 |

### 4.5 Archimedes screw turbine power at the Zandvliet wastewater treatment works

The simulation results of the Archimedes screw turbine at the ZWWTW outlet discharge is depicted in Figure 4.5. The output power of the turbine is calculated using Equation 3.1. Realistic turbine low and high-efficiency values that were calculated in prior research of the selected turbine are used in this research to calculate the resultant daily power output. The obtained results show that the output power curve resembles the water discharge flowrate pattern closely. At 70% overall efficiency, the mechanical power output of the scheme is averagely 7909 W. At 85% efficiency, the mechanical power generated is about 9603 W.

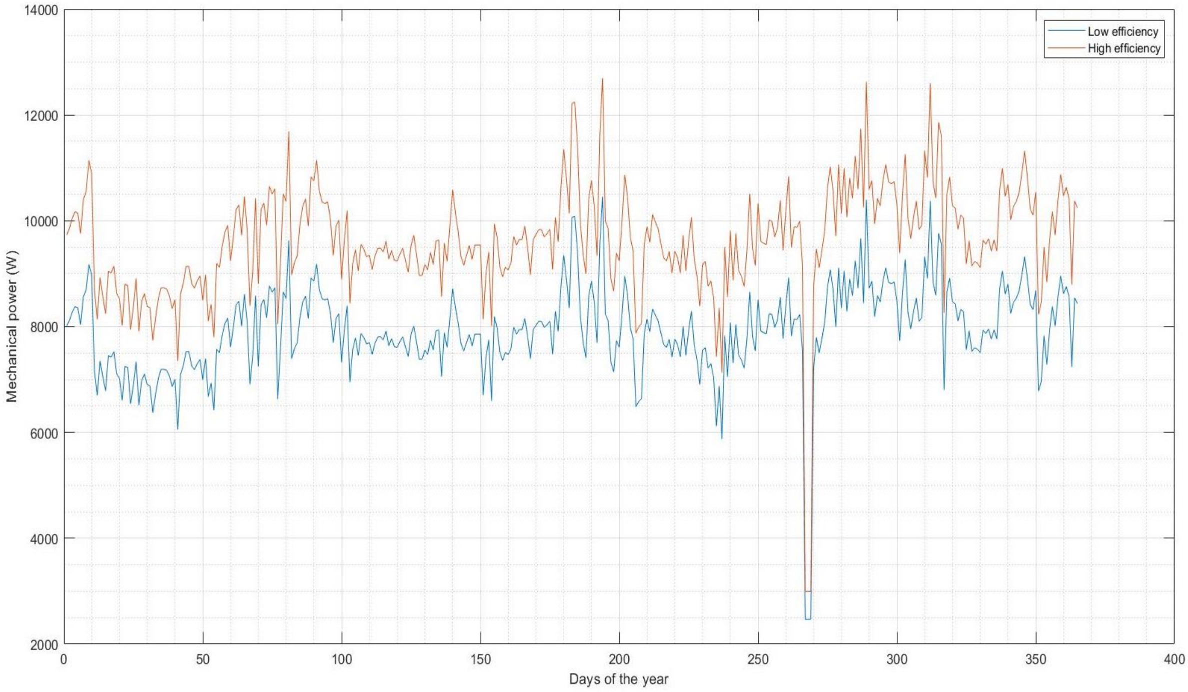


**Figure 4.5: Output power of the Archimedes screw turbine at the Zandvliet wastewater treatment works for low and high-water efficiencies**

## 4.6 Flow versus hydraulic power at the Kuilsriver

The monthly flow rate of the water in the Kuilsriver and the potential hydraulic energy are shown in Figure 4.6. The identical shapes of the graphs show that the relationship between the two is very similar. The flow rate of the water is directly proportional to the potential hydraulic power. A definite peak can be observed around months 6, 7, and 8, which is the winter rainfall season of the region.

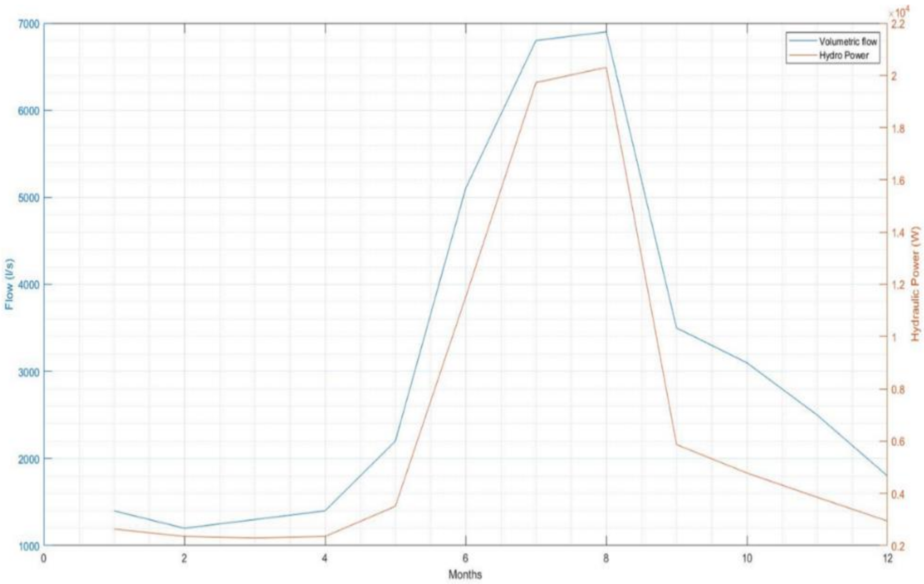


**Figure 4.6: Flow vs power at Kuilsriver**

## 4.7 Mechanical power versus flow at the river

The potential hydraulic power is compared to the mechanical power of the HPM turbine, installed in the weir at the Kuilsriver. The mechanical power output shows a relatively flat curve, as shown in Figure 4.7. The highest mechanical power of the HPM is 4 kW in August, while the maximum hydraulic power in that same month is 20 kW. The reason for this discrepancy is the characteristics of the HPM turbine. The turbine design is optimised to an average water level. When the maximum water level goes higher than the hub-height, the efficiency decreases.

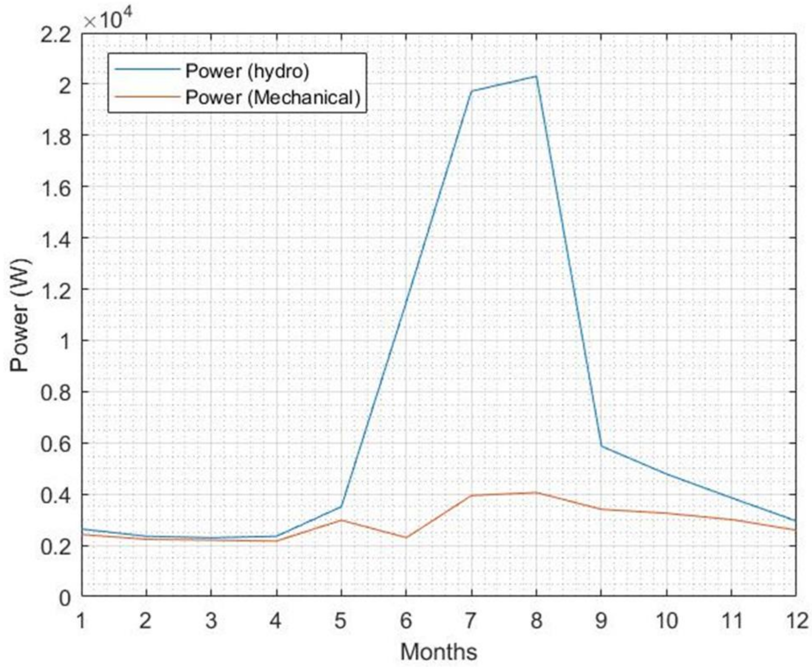


**Figure 4.7: Mechanical power of the hydrostatic machine in the Kuilsriver**

## 4.8 Power generation at the ZWWTW compared to the Kuilsriver site.

The mechanical output power of the Archimedes screw turbine (AST) system at the ZWWTW and the power output of the HPM at the Kuilsriver are plotted in Figure 4.8. The AST delivers 7.8 kW power at 70% efficiency and a monthly average of 9.7 kW at 85% efficiency. The HPM turbine (blue line) has an average of 2.9 kW, with a maximum of 4 kW and a minimum of about 2.2 kW. The top two lines represent the power of the AST at the plant.

The results show the potential hydropower of one specific wastewater treatment plant, with one set of conditions. These conditions such as volumetric flow and head vary greatly from site to site. The observed differences mean that several turbines may be more suitable to other site conditions. It also means that the potential power would vary as well. Although this research looks at a site with a head of lower than two meters, it would be useful to compare it to other sites. However, only a few wastewater treatment plants are found in South Africa where hydropower is generated. The next section compares the ZWWTW to other sites in South Africa.

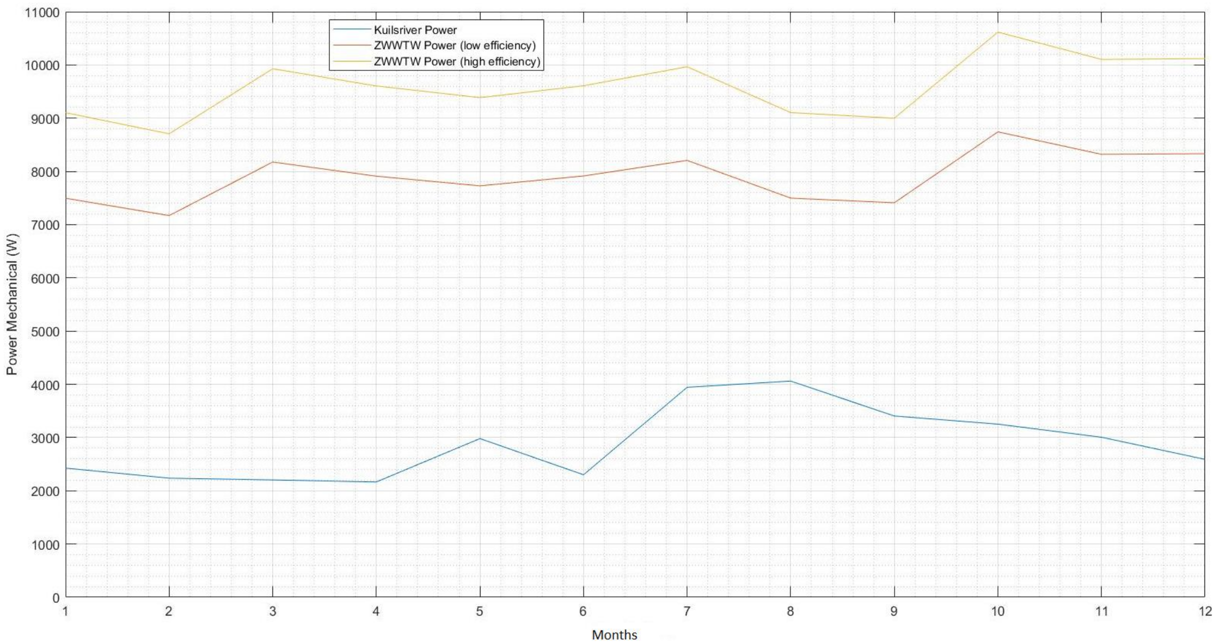


**Figure 4.8: Mechanical output power of the hydropower turbine at the wastewater treatment plant and the river.**

## 4.9 Comparison of the ZWWTW to other sites

Hydropower schemes at wastewater treatment plants are not common to have a head of lower than 3 m. However, in a comprehensive research of working plants that use wastewater treatment plants for energy generation, Llácer-Iglesias et al. (2021) found that there is a need to reduce the minimum cut-off for hydropower capacity in new plants to as low as 100 W. The ZWWTW with head of 1.5 m is shown to have an output power of 9.6 kW. In terms of generation capacity versus the site conditions, the plant compares well with the three working plants in South Africa. These plants are listed in Table 4.2 namely, Rooiwal WWTW with a potential power of 109 kW at eight-meter head. The turbine at the Zeekoegat plant with a head of 3.6m has a capacity of 6.9 kW which are planned to be tripled (SJ van Vuuren, M van Dijk & B Barta & BG Scharfetter, 2014). The international plants listed in Table 4.2, namely the Tatlar WWTP in Turkey, North Head in Australia, and Mid Halton in Canada, also compare well with the ZWWTW if we consider the respective flow and head available.

To compare the output performance of the above sites, a power output factor is calculated in the last column of Table 4.2. The produced power is expressed as a percentage of the available hydraulic power. The ZWWTW has a predicted efficiency of about 63% compared with Zeekoegat and Rooiwal with figures of 56.3% and 48.8% respectively. Wemmershoek and Temba WWTW were not considered due to the varying range of input figures.

**Table 4.2: Wastewater treatment plants with hydropower options**

| Plant name | Country | Province | City | Year installed | Scheme type | Flow Ml/d | Flow l/s | Head | Turbine type | Produced power kW | Power output factor |
|---|---|---|---|---|---|---|---|---|---|---|---|
| | | | | | **South African Plants** | | | | | | |
| Northern WWTW | RSA | Gauteng | | 2012 | CHP | 450 | 5208,3 | | | 1100 | |
| Driefontein WWTW | RSA | Gauteng | | 2012 | CHP | 35 | 405,1 | | | 750 | |
| Neuberg | RSA | Northern Cape | | 2015 | ROR | | | | | 10000 | |
| Stortemelk | RSA | Freestate | | 2016 | ROR | | | | | 4300 | |
| Kruisvallei | RSA | Freestate | | 2021 | ROR | | | | | 4000 | |
| Wemmershoek WWTW | RSA | Gauteng | Tswane | 2022 | | 40-250 | 462,9 | 24-28 | Francis | 208 | 183,2 |
| Zantvliet WWTW | RSA | Western Cape | Cape Town | 2022 | WWTP Outlet | 66 | 767 | 1,5 | AST | 7,2 | 63,8 |
| Zeekoegat WWTW | RSA | Gauteng | Tshwane | 2015 | WWTP Outlet | 30 | 347 | 3,6 | Siphon | 6,9 | 56,3 |
| Rooiwal WWTW | RSA | Gauteng | Tshwane | 2022 | | 245 | 2847 | 8 | | *109* | 48,8 |
| Temba WCW | RSA | Gauteng | Tshwane | 2022 | | 120 | 1388,9 | 3,6 | | *40* | 81,5 |
| | | | | | **International Plants** | | | | | | |
| Tatlar WWTP | Turkey | | Ankara | 2013 | | 765 | 8854 | 9,2 | AST & Kaplan | 965 | |
| North Head Sewage Treatment Plant | Australia | NS Wales | Sydney | 2010 | WWTP Outlet | 300 | 3472 | 60 | | 4500 | |
| Mid Halton WWTP | Canada | Ontario | | 2021 | | 125 | 1447 | 40 | Osberger | 700 | |

## 4.10 Summary

In this chapter, the results of the modelling of the turbines at the outlet of the ZWWTW and the Kuilsriver are plotted and discussed. The water flow conditions at both sites are shown with the potential hydraulic power. The mechanical power of both sites that were determined considering the specific site turbine and conditions, are also clearly represented. The graphs give a clear comparative view of the energy generation at the two sites. The chapter concludes by comparing the results to existing real cases of wastewater treatment plants where hydropower is generated, specifically in South Africa.

# CHAPTER FIVE

# CONCLUSIONS AND RECOMMENDATIONS

This dissertation investigated the hydropower potential at a wastewater treatment plant. It further investigated whether implementing the scheme at the outlet of the plant can yield more energy in comparison to installing it at the river in which the plant discharges. A comprehensive literature review was done on hydropower implementation at wastewater treatment plants. The review extended to the current renewable energy landscape in South Africa with emphasis on the current Renewable Energy Independent Power Producer Procurement Programme (REIPPPP) to show the share of hydropower in relation to the total renewable energy supply. The various turbine types and applications were explored.

## 5.1 Wastewater treatment plant and the generated hydroelectric power

The Zandvliet Wastewater treatment works in Cape Town, South Africa was selected for evaluation. The randomly selected plant was found to have a head of about 1.5m to implement a hydropower scheme. The outflow discharge data of the plant was obtained from the local authority. The conditions at the outflow of the plant such as the volume of flow, water quality, head, purity of the water, and consistency of the flow, was used to determine the best suited turbine. The Archimedes screw turbine (AST) was found to be the best suited one for the conditions. After the best turbines were selected for the respective sites, the schemes were modelled using MATLAB. The energy yield for each site was determined using the universal hydropower formula. The results show that the AST turbine at the Zandvliet wastewater treatment works produces 7.9 kW average power, or 69.2 MWh per annum, excluding downtime.

The point in the river at which the plant discharges its water was also evaluated for its hydropower potential. The river flow was measured over a yearly period. The recorded data were converted to a monthly figure for ease of comparison with the plant outlet. A weir was designed to improve the flow conditions of the river water to maximise hydropower potential. Various turbines were evaluated for the site. The best suited turbine for the resultant conditions was found to be the hydrostatic pressure machine (HPM). The HPM model at the river produces an average of 2.9 kW

In conclusion, the hydropower scheme at the Zandvliet Wastewater Treatment Works' outlet was found to produce more than double the average power at the river site. Although, the river has pre-existing water flow besides the plant discharge that is channelled into the river. The profile of the river bed was also altered to optimise the energy potential. Despite these conditions, the plant site yielded more power.

The results of this research give municipal authorities and other related entities an early indication of the viability of a hydropower scheme, in terms of energy yield. The uncertainty on whether to install the hydropower scheme at the plant versus at the discharging canal was clearly answered.

## 5.2 Recommendations and possible future work

- Future studies would focus on the development of the actual Archimedes screw and hydrostatic pressure machine turbines for plant and river sites, respectively.
- A positive outcome of the research above could lead to a successful local manufacturing market.
- A hydropower feature should be considered during every plant design process.
- The design specifications on the AST and HPM need to be formulated.
- A set of specifications should be researched that draws a comparison when hydropower would be preferred over CHP at a wastewater treatment plant.
- With the current 853 wastewater plants in SA, a more comprehensive survey should be done on all plants. If only 20% are found to have a low head similar to the one in this research, it will mean that 170 plants can deliver 7 kW of power. This equates to a possible annual energy yield of 10.4 GWh.

# REFERENCES


Abdullah, O.S., Khalil, W.H., Kamel, A.H. & Shareef, A.J. 2020. Investigation of Physical and Numerical Model of Archimedes Screw Turbine. *Journal of Power and Energy Engineering*, 08(10): 26–42.

ANDRITZ. 2021. Small hydropower plants. https://www.andritz.com/products-en/hydro/markets/small-mini-hydropower-plants 28 October 2021.

Angelakis, A.N., Asano, T., Bahri, A., Jimenez, B.E. & Tchobanoglous, G. 2018. Water reuse: From ancient to modern times and the future. *Frontiers in Environmental Science*, 6(MAY).

Ansar, A., Flyvbjerg, B., Budzier, A. & Lunn, D. 2014. Should we build more large dams? The actual costs of hydropower megaproject development. *Energy Policy*, 69.

Apostoleris, H., Sgouridis, S., Stefancich, M. & Chiesa, M. 2018. Evaluating the factors that led to low-priced solar electricity projects in the Middle East. *Nature Energy*, 3(12): 1109–1114. http://dx.doi.org/10.1038/s41560-018-0256-3.

Ashley Theron. 2015. Timber IPP to build 25MW biomass plant - ESI-Africa.com. *ESI Africa*. https://www.esi-africa.com/top-stories/timber-ipp-to-build-25mw-biomass-plant/ 17 December 2021.

Azmanov, K., Bozhinova, S. & Andreev, I. 2011. Design and construction of a novel low head hydropower convertor at River Iskar–Bulgaria. *Dresdener Wasserbauliche Mitteilungen*: 301–306.

Bank, W. 2020. World Bank, W., 2020. Operation And Maintenance Strategies For Hydropower. [online] Openknowledge.worldbank.org. Available at: https://openknowledge.worldbank.org/handle/10986/33313> - Google Search. https://www.google.com/search?q=World+Bank%2C+W.%2C+2020.+Operation+And+Maintenance+Strategies+For+Hydropower.+%5Bonline%5D+Openknowledge.worldbank.org.+Available+at%3A+https%3A%2F%2Fopenknowledge.worldbank.org%2Fhandle%2F10986%2F33313%3E+&rlz=1C1GCEA_enZ 26 October 2021.

Barta, B. 2018. The contribution of pumped storage schemes to energy generation in South Africa.

Barta, B. & Rask Grøn, H. 2002. Evaluation of potential for small (<10 mw) hydropower in south africa. www.weathersa.co.za 27 October 2021.

Basar, M.F., Sapiee, R., Rahman, S., Hamdan, Z., Borhan, S. & Sopian, K. 2014. Cost analysis of pico hydro turbine for power production. *Advances in Environmental Biology*, 8(14).

Basso, S. & Botter, G. 2012. Streamflow variability and optimal capacity of run-of-river hydropower plants. *Water Resources Research*, 48(10).

Bhatti, A.A. 2018. Investigation and Design of Undershot Hydrostatic Pressure Converter for the Exploitation of Very Low Head Hydropower Potential in Pakistan. , 22(January): 44–50.

Bousquet, C., Samora, I., Manso, P., Rossi, L., Heller, P. & Schleiss, A.J. 2017. Assessment of hydropower potential in wastewater systems and application to Switzerland. *Renewable Energy*, 113: 64–73.

Boys, C.A., Pflugrath, B.D., Mueller, M., Pander, J., Deng, Z.D. & Geist, J. 2018. Physical and hydraulic forces experienced by fish passing through three different low-head hydropower turbines. *Marine and Freshwater Research*.

Breeze, P. 2019. Power generation technologies. *Power Generation Technologies*: 1–449.

Cassan, L., Dellinger, G., Maussion, P. & Dellinger, N. 2021. Hydrostatic pressure wheel for regulation of open channel networks and for the energy supply of isolated sites. *Sustainability (Switzerland)*, 13(17): 1–18.

Corcoran, L., McNabola, A. & Coughlan, P. 2015. Optimization of Water Distribution Networks for Combined Hydropower Energy Recovery and Leakage Reduction. *Journal of Water Resources Planning and Management*, 142(2): 04015045. https://ascelibrary.org/doi/abs/10.1061/%28ASCE%29WR.1943-5452.0000566 26 October 2021.

Couto, T.B.A. & Olden, J.D. 2018. Global proliferation of small hydropower plants – science and policy. *Frontiers in Ecology and the Environment*, 16(2): 91–100.

Covert, T., Greenstone, M. & Knittel, C.R. 2016. Will We Ever Stop Using Fossil Fuels? *Journal of Economic Perspectives*, 30(1): 117–38. http://dx.doi.org/10.1257/jep.30.1.117 26 October 2021.

Date, Abhijit, Date, Ashwin & Akbarzadeh, A. 2013. Investigating the potential for using a simple water reaction turbine for power production from low head hydro resources. *Energy Conversion and Management*, 66: 257–270.

Date, Abhijit, Date, Ashwin, Akbarzadeh, A. & Alam, F. 2012. Examining the Potential of Split Reaction Water Turbine for Ultra-Low Head Hydro Resources. *Procedia Engineering*, 49: 197–204.

Davis, S. & Graham, S. 2004. Micro-Hydropower Systems: A Buyer's Guide.

Dehdar-Behbahani, S. & Parsaie, A. 2016. Numerical modeling of flow pattern in dam spillway's guide wall. Case study: Balaroud dam, Iran. *Alexandria Engineering Journal*, 55(1): 467–473. http://dx.doi.org/10.1016/j.aej.2016.01.006.

Dellinger, G., Garambois, P.A., Dufresne, M., Terfous, A., Vazquez, J. & Ghenaim, A. 2016. Numerical and experimental study of an Archimedean Screw Generator. *IOP Conference Series: Earth and Environmental Science*, 49(10).

Denny, M. 2004. The efficiency of overshot and undershot waterwheels. *European Journal of Physics*, 25(2).

Department of Energy. 2016. 2016/17 Annual Performance Plan. : 1–147.

DMRE. 2019. Integrated Resource Plan | Department: Energy | REPUBLIC OF SOUTH AFRICA.

DMRE, S. 2021. Media Statement DEPARTMENT OF MINERAL RESOURCES & ENERGY.

DOE. 2013. Integrated Resource Plan for Electrity. , (November): 114. http://www.doe-irp.co.za/content/IRP2010_updatea.pdf.

DOE. 2019. *The South African Energy Sector Report-2019*. http://dx.doi.org/10.1016/j.powtec.2017.06.008%0Ahttps://doi.org/10.1016/j.jwpe.2017.08.012%0Ahttps://doi.org/10.1016/j.jhazmat.2021.125853%0Ahttps://doi.org/10.1080/10962247.2018.1521349%0Ahttp://www.energy.gov.za.

Eberhard, A; Naude, R. 2017. The South African Renewable Energy Ipp Procurement Programme Review, Lessons Learned & Proposals to Reduce Transaction Costs. https://www.gsb.uct.ac.za/files/EberhardNaude_REIPPPPReview_2017_1_1.pdf.

Eberhard, A. 2014. South Africa's Renewable Energy IPP Procurement Program: Success Factors and Lessons. www.ppiaf.org 2 December 2021.

Eberhard, A. & Naude, R. 2016. The South African renewable energy independent power producer Procurement programme: A review and lessons learned. *Journal of Energy in Southern Africa*, 27(4): 1–14.

Edirisinghe, D.S., Yang, H., Kim, M., Kim, B., Gunawardane, S.P. & Lee, Y. 2021. Computational Flow Analysis on a Real Scale Run-of-River Archimedes Screw Turbine with a High Incline Angle. : 1–18.

Eme, L.C., Ulasi, J.A., Alade Tunde, A.I. & Odunze, A.C. 2019. Hydrokinetic turbines for power generation in Nigerian river basins. *Water Practice and Technology*, 14(1).

EPA. 2020. Environmental Protection Agency, Ireland. https://www.epa.ie/ 27 October 2021.

ESHA. 2004. Guide on How to Develop a Small Hydropower Plant ESHA 2004.

Fajar, B., Winoto, S.H. & Facta, M. 2018. Early Analysis of Jumping Water Effect on Breastshot Waterwheel for Microhydro Power Plant Early Analysis of Jumping Water Effect on Breastshot Waterwheel for Microhydro Power Plant. : 0–7.

Fraenkel, P., Parish, O., Bolkalders, V. & Harvey, A. 1991. Micro-hydro Power. *Micro-hydro Power*: 1–160.

Franks, L., Euston-Brown, M., Ferry, A. & Giljova, S. 2013. Municipal wastewater treatment works - biogas to energy. http://www.cityenergy.org.za/uploads/resource_336.pdf.

Gielen, D., Boshell, F., Saygin, D., Bazilian, M.D., Wagner, N. & Gorini, R. 2019. The role of renewable energy in the global energy transformation. *Energy Strategy Reviews*, 24(June 2018): 38–50. https://doi.org/10.1016/j.esr.2019.01.006.

Girma, M. & And, E.D. 2014. Flow simulation and performance prediction of cross flow turbine using CFD tool. *Citeseer*, 2(6). https://citeseerx.ist.psu.edu/viewdoc/download?doi=10.1.1.677.5744&rep=rep1&type=pdf 30 October 2021.

Google Maps. 2021a. Google Maps. https://www.google.com/maps/@-34.0660729,18.7463704,5787m/data=!3m1!1e3 1 November 2021.

Google Maps. 2021b. Neusberg Hydro Power Station - Google Maps. https://www.google.co.za/maps/place/Neusberg+Hydro+Power+Station/@-28.7668014,20.7267988,315m/data=!3m1!1e3!4m5!3m4!1s0x1c2413387be15555:0xca71d58f15654dc5!8m2!3d-28.7666853!4d20.7266784 17 December 2021.

Green, M. 2012. Hydropower generation opportunities in South Africa -. *ESI*. https://www.esi-africa.com/features-analysis/status-and-possibilities-for-micro-hydro-generation-in-south-africa/ 26 March 2021.

Hatata, A.Y., El-Saadawi, M.M. & Saad, S. 2019. A feasibility study of small hydro power for selected locations in Egypt. *Energy Strategy Reviews*, 24.

Hijdra, A., Arts, J. & Woltjer, J. 2014. Do We Need to Rethink Our Waterways? Values of Ageing Waterways in Current and Future Society. *Water Resources Management*, 28(9).

HydroSmart. 2021. HydroSmart Srl | Impianti idroelettrici | Efficienza energetica. https://www.hydrosmart.it/energia-rinnovabile 28 October 2021.

IEA. 2018. World Energy Outlook 2018 – Analysis - IEA. https://www.iea.org/reports/world-energy-outlook-2018 26 October 2021.

IHA. 2019. IHA releases 2019 Hydropower Status Report charting growth in renewable hydro. https://www.hydropower.org/news/iha-releases-2019-hydropower-status-report-charting-growth-in-renewable-hydro 26 October 2021.

Ikeda, T., Iio, S. & Tatsuno, K. 2010. Performance of nano-hydraulic turbine utilizing waterfalls. *Renewable Energy*, 35(1): 293–300.

IOL. 2019. R1.7bn upgrade underway at Zandvliet Wastewater Treatment Works in Cape Townhttps://www.iol.co.za/news/south-africa/western-cape/r17bn-upgrade-underway-at-zandvliet-wastewater-treatment-works-in-cape-town-28818192. https://www.iol.co.za/news/south-africa/western-cape/r17bn-upgrade-underway-at-zandvliet-wastewater-treatment-works-in-cape-town-28818192 27 October 2021.

IPCC. 2018. IPCC Climate Report 2018. https://www.ipcc.ch/sr15/ 27 October 2021.

IPP. 2021. IPP Renewables. https://www.ipp-renewables.co.za/ 9 December 2021.

IRENA. 2018. Renewable Power Generation Costs in 2017. *International Renewable Energy Agency*.

IRENA. 2021. Solar energy data. https://www.irena.org/solar 28 November 2021.

IRENA. 2020. South Africa ENERGY PROFILE. https://www.irena.org/IRENADocuments/Statistical_Profiles/Africa/South Africa_Africa_RE_SP.pdf.

Jawahar, C.P. & Michael, P.A. 2017. A review on turbines for micro hydro power plant. *Renewable and Sustainable Energy Reviews*, 72.

Khan, M.J., Bhuyan, G., Iqbal, M.T. & Quaicoe, J.E. 2009. Hydrokinetic energy conversion systems and assessment of horizontal and vertical axis turbines for river and tidal applications: A technology status review. *Applied Energy*, 86(10): 1823–1835. http://dx.doi.org/10.1016/j.apenergy.2009.02.017.

Kirke, B. 2020. Hydrokinetic turbines for moderate sized rivers. , (January).

Kumar, D. & Katoch, S.S. 2014. Sustainability indicators for run of the river (RoR) hydropower projects in hydro rich regions of India. *Renewable and Sustainable Energy Reviews*, 35: 101–108.

Lahimer, A.A., Alghoul, M.A., Sopian, K., Amin, N., Asim, N. & Fadhel, M.I. 2012. Research and development aspects of pico-hydro power. *Renewable and Sustainable Energy Reviews*, 16(8): 5861–5878.

Lashofer, A., Hawle, W. & Pelikan, B. 2012. State of technology and design guidelines for the Archimedes screw turbine. *The international Journal on Hydropower & Dams, Hydro 2012 - Proceedings*, (October).

Letcher, T.M. 2018. Why Solar Energy? *A Comprehensive Guide to Solar Energy Systems*: 3–16.

Licari, M., Benoit, M., Anselmet, F., Kocher, V., Faucheux, P. Le, Licari, M., Benoit, M., Anselmet, F., Kocher, V. & Clément, S. 2020. Study of low-head hydrostatic pressure water wheels for harnessing hydropower on small streams To cite this version : HAL Id : hal-02568541 Study of low-head hydrostatic pressure water wheels for harnessing hydropower on small streams. *CongrèsFrançais de Mécanique2019*. https://hal.archives-ouvertes.fr/hal-02568541/document.

Linton, N.P. 2013. *Field Trials and Development of a Hydrostatic Pressure Machine*. University of Southampton, Engineering and the Environment, Doctoral Thesis, 360pp

Lisicki, M., Lubitz, W. & Taylor, G.W. 2016. Optimal design and operation of Archimedes screw turbines using Bayesian optimization. *Applied Energy*, 183.

LIU, D., LIU, H., WANG, X., and Kremere, E. 2019. World Small Hydropower Development Report 2019: Case Studies. United Nations Industrial Development Organization; International Center on Small Hydro Power. Available from www. smallhydroworld.org. https://www.unido.org/our-focus-safeguarding-environment-clean-energy-access-productive-use-renewable-energy-focus-areas-small-hydro-power/world-small-hydropower-development-report 26 October 2021.

LIU, D. et. a. 2019. (PDF) World Small Hydropower Development Report 2019- Case Studies. https://www.researchgate.net/publication/339528484_World_Small_Hydropower_Development_Report_2019-_Europe_Region_Spain 26 October 2021.

Llácer-Iglesias, R.M., López-Jiménez, P.A. & Pérez-Sánchez, M. 2021a. Energy self-sufficiency aiming for sustainable wastewater systems: Are all options being explored? *Sustainability (Switzerland)*, 13(10).

Llácer-Iglesias, R.M., López-Jiménez, P.A. & Pérez-Sánchez, M. 2021b. Hydropower technology for sustainable energy generation in wastewater systems: Learning from the experience. *Water (Switzerland)*, 13(22).

Loots, I., Van Dijk, M., Barta, B., Van Vuuren, S.J. & Bhagwan, J.N. 2015. A review of low head hydropower technologies and applications in a South African context. *Renewable and Sustainable Energy Reviews*, 50(2015): 1254–1268. http://dx.doi.org/10.1016/j.rser.2015.05.064.

Lyons, M.W.K. 2014. *Lab Testing and Modeling of Archimedes Screw Turbines*.

Masud, I.A., Yusuke, S. & Suwa, Y. 2019. Performance prediction of zero head turbine at different water levels. In *IOP Conference Series: Earth and Environmental Science*.

Mejbel Ali, A., Saadoon Algburi, S. & Abdelmajed Aljaradin, r. M. 2018. DESIGN OPTIMIZATION OF A HYBRID HYDRO-WIND MICROPOWER SYSTEM FOR RURAL COMMUNITIES. *Journal of Engineering and Sustainable Development*, 22(02): 1–10.

Müller, F. & Claar, S. 2021. Auctioning a 'just energy transition'? South Africa's renewable energy procurement programme and its implications for transition strategies. *Review of African Political Economy*, 0(0): 1–19. https://doi.org/10.1080/03056244.2021.1932790.

Müller, G., Denchfield, S., Marth, R. & Shelmerdine, B. 2007. Stream wheels for applications in shallow and deep water. *32nd IAHR Conference*, (1): 1–9. https://eprints.soton.ac.uk/53060/.

Mümtaz Aka, Elçin Kentela, S.K. 2017. A fuzzy logic tool to evaluate low-head hydropower technologies at the outlet of wastewater treatment plants. *Renewable and Sustainable Energy Reviews*, 68(September 2016): 727–737. http://dx.doi.org/10.1016/j.rser.2016.10.010.

Niebuhr, C.M., van Dijk, M. & Bhagwan, J.N. 2019. Development of a design and implementation process for the integration of hydrokinetic devices into existing infrastructure in South Africa. *Water SA*, 45(3).

Niebuhr, C.M., van Dijk, M., Neary, V.S. & Bhagwan, J.N. 2019. A review of hydrokinetic turbines and enhancement techniques for canal installations: Technology, applicability and potential. *Renewable and Sustainable Energy Reviews*, 113(April): 109240. https://doi.org/10.1016/j.rser.2019.06.047.

NS ENERGY. 2018. Redstone Concentrated Solar Project, South Africa. https://www.nsenergybusiness.com/projects/redstone-concentrated-solar-project/ 9 December 2021.

NWS. 2016. Chief Joseph Dam. https://www.nws.usace.army.mil/Missions/Civil-Works/Locks-and-Dams/Chief-Joseph-Dam/ 18 November 2021.

Orsted. 2021. Offshore Wind Energy **|** Ørsted. https://orsted.co.uk/energy-solutions/offshore-wind 17 December 2021.

Paish, O. 2002. Small hydro power: Technology and current status. *Renewable and Sustainable Energy Reviews*, 6(6): 537–556.

Piccinini, A. 2018. The South African market. *ESI Africa*.

Power, C., McNabola, A. & Coughlan, P. 2014. Development of an evaluation method for hydropower energy recovery in wastewater treatment plants: Case studies in Ireland and the UK. *Sustainable Energy Technologies and Assessments*, 7.

Priyadi, B. 2017. Design of Turbine Screw Model for Pico-Hydro. *American Journal of Engineering Research (AJER)*, (6): 130–140. www.ajer.org.

Quaranta, E. 2018. Stream water wheels as renewable energy supply in flowing water: Theoretical considerations, performance assessment and design recommendations. *Energy for Sustainable Development*, 45: 96–109. https://doi.org/10.1016/j.esd.2018.05.002.

Quaranta, E. & Revelli, R. 2018. Gravity water wheels as a micro hydropower energy source: A review based on historic data, design methods, efficiencies and modern optimizations. *Renewable and Sustainable Energy Reviews*, 97(September): 414–427. https://doi.org/10.1016/j.rser.2018.08.033.

Rae, G. & Erfort, G. 2020. Offshore wind energy - South Africa's untapped resource. *Journal of Energy in Southern Africa*, 31(4): 26–42.

Red Rocket. 2021. News – Red Rocket. https://redrocket.energy/media/photos/ 20 December 2021.

REH. 2016. Stortemelk Hydro – REH Group. https://www.rehgroup.co.za/project/stortemelk-hydro/ 20 December 2021.

Rehman, S., Al-Hadhrami, L.M. & Alam, M.M. 2015. Pumped hydro energy storage system: A technological review. *Renewable and Sustainable Energy Reviews*, 44.

Rickard, C., Day, R. & Purseglove, J. 2003. *River Weirs-Good Practice Guide* Guide-Section B2. R&D Publication W5B-023/HQP. Mott MacDonald Ltd and University of Hertfordshire

Rohmer, J., Knittel, D., Sturtzer, G., Flieller, D. & Renaud, J. 2016. Modeling and experimental results of an Archimedes screw turbine. *Renewable Energy*, 94: 136–146. http://dx.doi.org/10.1016/j.renene.2016.03.044.

Roodbol, A. 2020. Biomass beneficiation has huge potential for South Africa. *ESI Africa*. https://www.esi-africa.com/renewable-energy/biomass-beneficiation-has-huge-potential-for-south-africa/ 17 December 2021.

Rorres, C. 2000. The Turn of the Screw: Optimal Design of an Archimedes Screw. *Journal of Hydraulic Engineering*, 126(1).

SA Mitchell, MP de Wit, JN Blignaut, D.C. 2014. *WASTE WATER TREATMENT PLANTS: THE FINANCING MECHANISMS ASSOCIATED WITH ACHIEVING GREEN DROP RATING Report to the Water Research Commission by SA Mitchell, MP de Wit, JN Blignaut, D Crookes ASSET*

*Research*. www.wrc.org.za 10 December 2021.

Sari, M.A., Badruzzaman, M., Cherchi, C., Swindle, M., Ajami, N. & Jacangelo, J.G. 2018a. Recent innovations and trends in in-conduit hydropower technologies and their applications in water distribution systems. *Journal of Environmental Management*, 228.

Sari, M.A., Badruzzaman, M., Cherchi, C., Swindle, M., Ajami, N. & Jacangelo, J.G. 2018b. Recent innovations and trends in in-conduit hydropower technologies and their applications in water distribution systems. *Journal of Environmental Management*, 228(August): 416–428. https://doi.org/10.1016/j.jenvman.2018.08.078.

Saroinsong, T., Soenoko, R., Wahyudi, S. & Sasongko, M.N. 2015. The effect of head inflow and turbine axis angle towards the three row bladed screw turbine efficiency. *International Journal of Applied Engineering Research*, 10(7): 16977–16984.

SatellitesPro. 2021. Satellites.pro. 2021; https://satellites.pro/South_Africa_map#-34.053744,18.723975,16> [Accessed 11 November 2021].

Scheider, S., Keßler, C., Ortmann, J., Devaraju, A., Trame, J., Kauppinen, T. & Kuhn, W. 2011. Semantic Referencing of Geosensor Data and Volunteered Geographic Information. : 27–59.

Schwyzer, O. 2016. DigitalCommons @ USU International Junior Researcher and Engineer Analysis of clearance gap losses on the hydraulic pressure machine.

Senior, J., Saenger, N. & Müller, G. 2010. New hydropower converters for very low-head differences. *Journal of Hydraulic Research*, 48(6): 703–714.

Senior, J., Wieman, P. & Muller, G. 2008. The Rotary Hydraulic Pressure Machine for Very Low Head Hydropower sites. *Hidroenergia conference*: 1–8.

Simmons, S.C. & Lubitz, W.D. 2020. Analysis of internal fluid motion in an Archimedes screw using computational fluid mechanics. *Journal of Hydraulic Research*.

Simmons, S.C. & Lubitz, W.D. 2021. Archimedes screw generators for sustainable micro-hydropower production. *International Journal of Energy Research*, 45(12).

Singh, V.K. & Singal, S.K. 2017. Operation of hydro power plants-a review. *Renewable and Sustainable Energy Reviews*, 69: 610–619.

SJ van Vuuren, M van Dijk, I.L. & B Barta & BG Scharfetter. 2014. Conduit hydropower development guide : report to the Water Research Commission.

Smith, T. 2021. Preferred energy bidder for Bid Window 5 to be revealed soon -. *ESI Africa*. https://www.esi-africa.com/industry-sectors/generation/preferred-bidder-for-bid-window-5-to-be-revealed-end-october/ 17 December 2021.

Songin, K. 2017. Experimental Analysis of Archimedes Screw Turbines. , (August): 1–151.

Spaans Babcock. 2017. Archimedean Screw Turbine.

Springmann, M., Mason-D'Croz, D., Robinson, S., Garnett, T., Godfray, H.C.J., Gollin, D., Rayner, M., Ballon, P. & Scarborough, P. 2016. Global and regional health effects of future food production under climate change: A modelling study. *The Lancet*, 387(10031).

Steffanutti Stocks. 2020. Zandvliet's mega expansion showcases excellence | IMIESA. *Sabinet IMIESA*. www.stefanuttistocks.com 27 October 2021.

Swilling, M. & Annecke, E. 2012. Just Transitions Explorations of sustainability in an unfair world.

Technology, R. 2016. Jasper Solar Power Plant, Northern Cape, Kimberley - Renewable Technology. https://www.renewable-technology.com/projects/jasper-solar-power-plant-northern-cape-kimberley/ 9 December 2021.

topographicmap.com. 2021. Cape Town topographic map, elevation, relief. https://en-gb.topographic-map.com/maps/lp3p/Cape-Town/ 28 October 2021.

UNFCC. 2021. What is the Kyoto Protocol? | UNFCCC. https://unfccc.int/kyoto_protocol 26 October 2021.

UNIDO. 2015. LCET Programme Low Carbon Low emission CLean energy TeChnoLogy TransFer Programme.

Viadero, Roger, Rehbein, Michele, Singh, A. 2017. Hydropower on the Mississippi River (PDF). https://www.researchgate.net/publication/318469208_Hydropower_on_the_Mississippi_River 27 October 2021.

Van Vuuren, S.J., van Dijk, M., Loots, I., Barta, B. & Scharfetter, B.G. 2014. *Conduit Hydropower Development Guide WRC Report No. TT 597/14*.

Wikimedia. 2007. Cahorra_bassa.jpg (500×333). https://upload.wikimedia.org/wikipedia/commons/7/71/Cahorra_bassa.jpg 10 December 2021.

Wikimedia. 2015. File:Geothermal-energy.png - Wikimedia Commons. https://commons.wikimedia.org/wiki/File:Geothermal-energy.png 17 December 2021.

Williamson, S.J., Stark, B.H. & Booker, J.D. 2013. Performance of a low-head pico-hydro Turgo turbine. *Applied Energy*, 102: 1114–1126.

Wisatesajja, W., Roynarin, W. & Intholo, D. 2019. Comparing the Effect of Rotor Tilt Angle on Performance of Floating Offshore and Fixed Tower Wind Turbines. *Journal of Sustainable Development*, 12(5): 84.

YoosefDoost, A. & Lubitz, W.D. 2020. Archimedes screw turbines: A sustainable development solution for green and renewable energy generation-a review of potential and design procedures. *Sustainability (Switzerland)*, 12(18).

Zhou, D. & Deng, Z. (Daniel). 2017. Ultra-low-head hydroelectric technology: A review. *Renewable and Sustainable Energy Reviews*, 78.

## APPENDICES

**APPENDIX A**: MATLAB Simulation diagrams

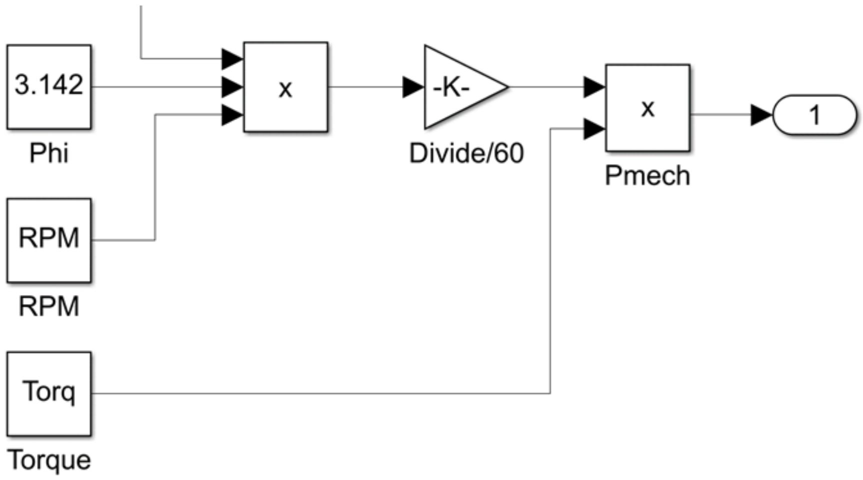


**Figure A.1: Diagram for AST power calculation using torque and rotational speed**

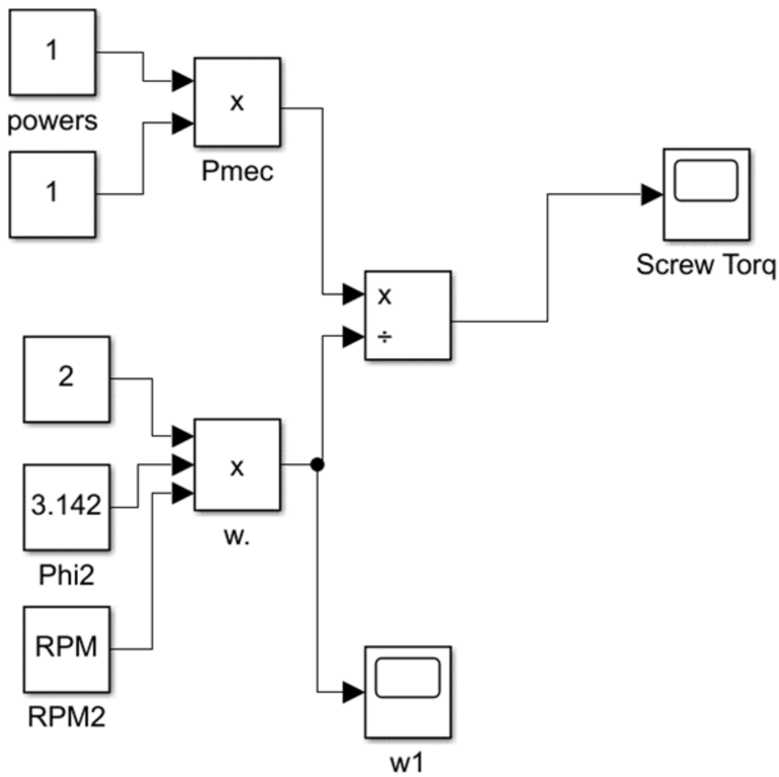


**Figure A.2: Diagram for calculation of torque using power and RPM**

**APPENDIX B**: Hydrostatic pressure machine

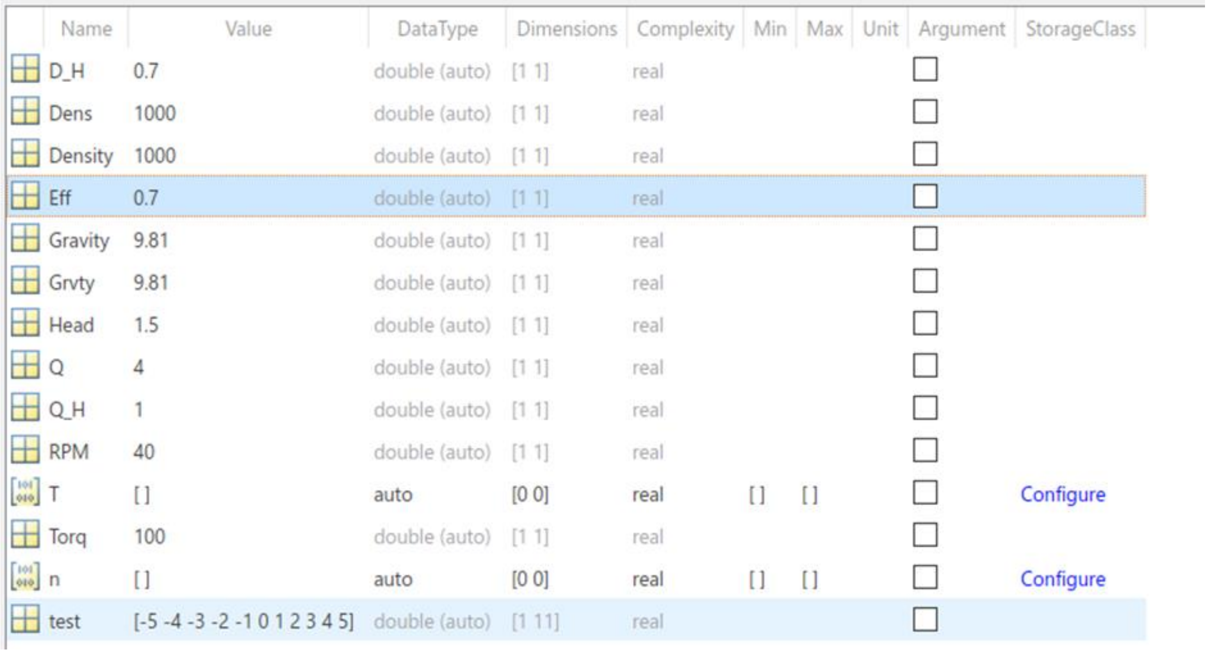

| Name | Value | DataType | Dimensions | Complexity | Min | Max | Unit | Argument | StorageClass |
|---|---|---|---|---|---|---|---|---|---|
| D_H | 0.7 | double (auto) | [1 1] | real | | | | ☐ | |
| Dens | 1000 | double (auto) | [1 1] | real | | | | ☐ | |
| Density | 1000 | double (auto) | [1 1] | real | | | | ☐ | |
| Eff | 0.7 | double (auto) | [1 1] | real | | | | ☐ | |
| Gravity | 9.81 | double (auto) | [1 1] | real | | | | ☐ | |
| Grvty | 9.81 | double (auto) | [1 1] | real | | | | ☐ | |
| Head | 1.5 | double (auto) | [1 1] | real | | | | ☐ | |
| Q | 4 | double (auto) | [1 1] | real | | | | ☐ | |
| Q_H | 1 | double (auto) | [1 1] | real | | | | ☐ | |
| RPM | 40 | double (auto) | [1 1] | real | | | | ☐ | |
| T | [] | auto | [0 0] | real | [] | [] | | ☐ | Configure |
| Torq | 100 | double (auto) | [1 1] | real | | | | ☐ | |
| n | [] | auto | [0 0] | real | [] | [] | | ☐ | Configure |
| test | [-5 -4 -3 -2 -1 0 1 2 3 4 5] | double (auto) | [1 11] | real | | | | ☐ | |

**Figure B.1: MATLAB variable list created for HPM calculations**

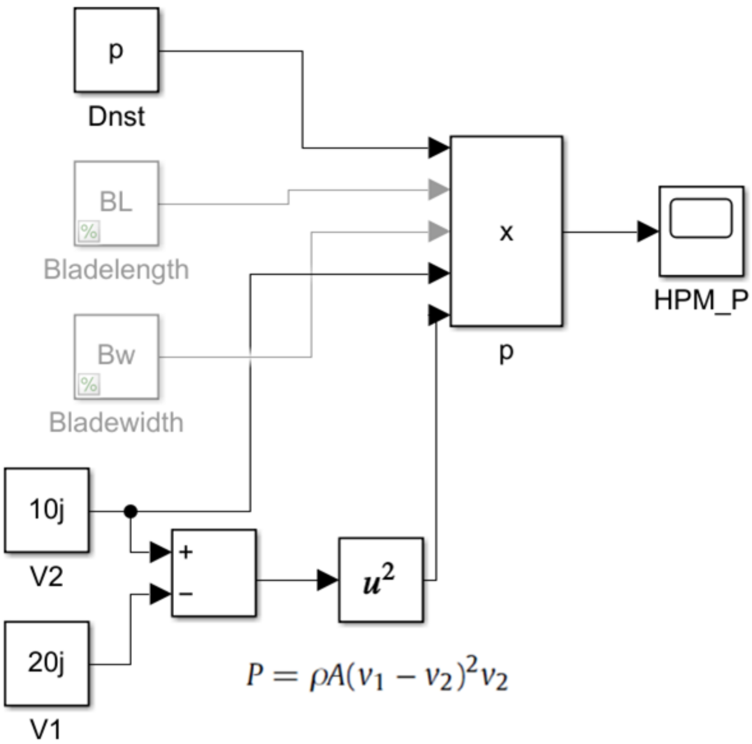


**Figure B.2: Diagram for power calculation on HPM**

**APPENDIX C:** River depth measurements of the Kuilsriver close to the ZWWTW canal entry point.


**Figure C.1: Measurement close to the river bank**


**Figure C.2: Measurement close to the centre of the river**

**APPENDIX D: Images at different points between the Zantvliet Wastewater Treatment Works and the Kuilsriver, to illustrate the visible slope**

**Figure D.1: ZWWTW canal from the road to the river**

**Figure D.2: View of the ZWWTW from the road**

**APPENDIX E: Measurement of the Kuilsriver water velocity using the method of a floating object between a set distance**


**APPENDIX E: Confluence of the Kuilsriver and ZWWTW canal**